INL/EXT-18-51359
Revision 0

Case Study: Nuclear-Renewable-Water Integration in Arizona

Aaron Epiney
Cristian Rabiti
Paul Talbot
Jong Suk Kim
James Richards
Shannon Bragg-Sitton

September 2018

The INL is a
U.S. Department of Energy
National Laboratory
operated by
Battelle Energy Alliance

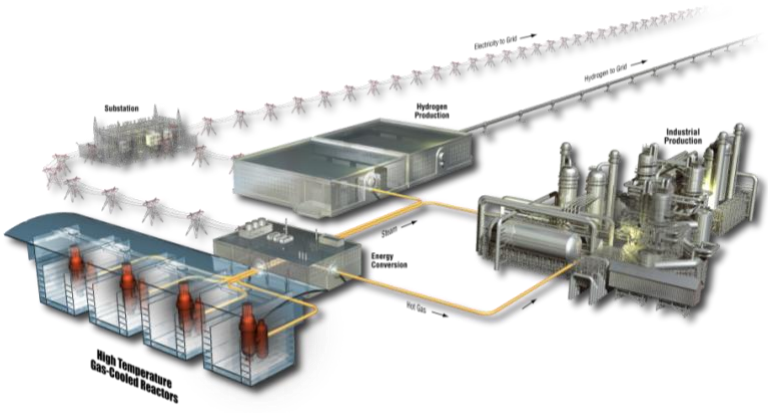

INL/EXT-18-51359
Revision 0

Case Study: Nuclear-Renewable-Water Integration in Arizona

Aaron Epiney
Cristian Rabiti
Paul Talbot
Jong Suk Kim
James Richards
Shannon Bragg-Sitton

September 2018

Idaho National Laboratory
Idaho Falls, Idaho 83415

http://www.inl.gov

Prepared for the
U.S. Department of Energy
Office of Nuclear Energy
Under DOE Idaho Operations Office
Contract DE-AC07-05ID14517

ABSTRACT

This document reports the application of the Nuclear-Renewable Hybrid Energy System (N-R HES) software framework to a case study conducted in collaboration with Arizona Public Service (APS). The study is a work in progress; this report presents a detailed description of the current model inputs and the corresponding results.

APS is currently anticipating several operational challenges: First, APS is coping with the rapid growth of Variable Renewable Energy (VRE) sources on the grid in the APS service region. To mitigate the resulting demand volatility, APS is seeking to add more baseload. The second challenge to APS is that the cooling water acquisition contract with the Sub Regional Operating Group (SROG) will expire soon and a renewal is only available for a significantly higher price of water. An opportunity for less expensive water may be to pump brackish water from the regional ground water. One caveat is that the salinity of the brackish water is so high that it could, depending on the percentage used, need additional treatment via an on-site Reverse Osmosis (RO) desalination plant. The RO plant would help resolve both problems APS is facing, i.e. increasing the baseload to help mitigate VRE-induced demand volatility and, in addition, the clean water produced can be used by APS for plant cooling to lower their water acquisition cost.

The analysis in this report considers three scenarios: (1) The status quo, where all cooling water is purchased from the SROG and no RO is built (CASE 0); (2) A case in which one RO is built on-site to treat the blend of SROG and brackish water (CASE 1); and (3) A case in which two ROs are built, one on-site and another one close to the brackish water well (CASE 2). The second RO could produce clean (potable) water that can be sold to generate additional revenue for APS. The analysis evaluates the differential Net Present Value (NPV) between the scenarios.

To model the three APS cases, additional functionality for the N-R HES software framework was needed. In particular, the RAVEN CashFlow plugin was updated to add more flexibility in project and component definitions and the synthetic time history generator was updated to include the possibility to correlate the noise portion of different signals after Fourier de-trending. The report also includes description of how the reduced order RO model was derived from a high fidelity Modelica model. Furthermore, the physical models used for water flows and chemistry, as well as the economic models detailing the assumptions made and data used, are described.

The report shows that the recently implemented correlated Auto-Regressive, Moving Average model (FVARMA) capability is working as intended. However, after removing the long-term trends and correlations by Fourier de-trending, no correlation could be found between the demand and the rooftop solar photovoltaics (rPV) or between the demand and the hub price in the stochastic portion of the signal, although it is suspected that such correlations exist and are important drivers for the economic analysis. It is worth mentioning that no industrial solar is considered in the evaluation, since per APS policy industrial solar is considered curtailable. The main conclusions concerning the input data are that, with regard to the rPV, higher resolution data is needed to perform a meaningful correlation analysis; for the hub price it is assumed that there actually is no (or only weak) correlation. Furthermore, the report shows that further work is needed to understand which net demand and hub price forecast models are right for this type of analysis.

The future projection of the net demand and the hub prices show that APS could curtail its internal production to take advantage of negative electricity prices at the Palo Verde Hub. This could add up to an additional 10% of the APS revenue. While in principle adding more internal baseload (i.e. RO electricity consumption) enhances such capability, the size of the RO in this study is such that the effect is negligible. With regard to the overall economics of purifying brackish water, the study shows that no RO is needed up to ~8000 acre-foot of brackish water per year if one allows for variable chloride content in the cooling water. However, considering a hard limit of 450 ppm Cl^-, an RO of ~500 kg/s capacity is necessary. In the latter case the delta NPV is negative, i.e. it is economically beneficial to continue buying all effluent water

rather than build the RO plant. For CASE 2, the size of RO needed is comparable to CASE 1. The resulting Levelized Cost of Water (LCOW) is ~1.5$/m^3. A sensitivity study for the amount of brackish water purchased shows that the delta NPV is approximately constant, indicating that the savings associated with buying brackish water versus effluent purchased from SROG are roughly offset by the increased RO cost. However, when scaling the ROs for the volume weighted yearly average chloride concentration (instead of the maximum), the CASE 1 becomes economically viable while the LCOW for CASE 2 becomes ~1$/m^3. This would suggest that using the reservoir ponds to mitigate salinity peaks could lead to an economically viable project.

CONTENTS

ABSTRACT vii

ACRONYMS xvii

1. INTRODUCTION 1

2. APS CASE DESCRIPTION 2
   2.1 Status quo (CASE 0) 2
   2.2 One RO is built on site (CASE 1) 3
   2.3 Tow ROs are built (CASE 2) 4

3. MODEL DESCRIPTION 5
   3.1 N-R HES framework developments 5
      3.1.1 Reverse Osmosis model development 5
      3.1.2 CashFlow developments 13
      3.1.3 FVARMA developments 15
   3.2 APS case model within N-R HES framework 20
      3.2.1 Nomenclature 20
      3.2.2 Overall data flow 22
      3.2.3 FVARMA and “ARMA PostP” 24
      3.2.4 APS model 25
      3.2.5 Economics (“NPV PreP” and “NPV”) 29

4. SIMULATIONS 36
   4.1 Input data and assumptions 36
      4.1.1 Non-stochastic input data 36
      4.1.2 Stochastic input data 38
   4.2 APS case simulations 49
      4.2.1 Reference case 49
      4.2.2 Sensitivity studies 65

5. CONCLUSIONS AND FUTURE WORK 77
   5.1 Conclusion 77
   5.2 Future Work 79

6. REFERENCES 80

FIGURES

Figure 1: CASE 0. All water is purchased from the SROG and the RO is not built. 3

Figure 2: CASE 1. Effluent water is purchased from the SROG and brackish water is pumped from the ground. This blended water needs to be treated in an on-site RO in addition to the WRF. 4

Figure 3: CASE 2. Effluent water is purchased from the SROG and brackish water is pumped from the ground. The brackish water is purified and sold, while the waste is blended with the effluent. This mix needs to be treated in an on-site RO in addition to the WRF. 5

Figure 4: RO desalination: (a) process flow diagram for a two-stage BWRO plant and (b) schematic of an RO vessel, which consists of six membrane modules in series [12]. 7

Figure 5: Top-level model for the BWRO plant implemented in Modelica. 9

Figure 6: FWP power consumption (P_{FWP}) predicted by the high-fidelity (blue points) and surrogate (red dashed line) models. 9

Figure 7: Permeate flow rate (m_p) versus feed flow rate (m_f) simulated for a range of feed salinity (S_f) by the high-fidelity model. 10

Figure 8: Permeate salinity (S_p) versus feed flow rate (m_f) simulated for a range of feed salinity (S_f) by the high-fidelity model. 10

Figure 9: Permeate flow rate (m_p) predicted by the high-fidelity (points) and surrogate (lines) models. 11

Figure 10: Permeate salinity (S_p) predicted by the high-fidelity (points) and surrogate (lines) models. 12

Figure 11: Correlated VARMA demonstration. Upper right: training data. Upper left: training versus synthetic for “A”. Lower left: training versus synthetic for “B”. Lower right: synthetic data. 16

Figure 12: Wind Speed for a Week-Long Period in ERCOT North-Central Region, June 2007. Black and white background indicates day and night for better visibility of daily trends in the signal. 17

Figure 13: Energy Demand for a Week-Long Period in ERCOT North-Central Region, June 2007. Black and white background indicates day and night for better visibility of daily trends in the signal. 18

Figure 14: Global Horizontal Irradiance (GHI): Original and Unfiltered Synthetic Data, 3 days. 19

Figure 15: Global Horizontal Irradiance (GHI): Original and Zero-Filtered Synthetic Data, 3 days. 19

Figure 16: Data flow of the APS case model inside the N-R HES software framework. 26

Figure 17: Synthetic demand and input demand over three representative days. 40

Figure 18: rPV actual generation vs. synthetic generation over three representative days. The plot on the left is direct output from the FVARMA model. The plot on the right is with postprocessing to ensure that the generation is zero at night. 40

Figure 19: Output of correlated FVARMA with adjustment for demand and rPV for three representative days. 42

Figure 20: One-year synthetic demand vs actual demand. The plot on the left is data sampled from the one-year FVARMA and the right is data sampled from the six, two-month FVARMAs. 43

Figure 21: Output of two-month correlated FVARMA with zeroFilter demand and rPV for three representative days. 43

Figure 22: Results of 10^4 runs: Mean and variance for synthetic demand. 44

Figure 23: Results of 10^4 runs: Mean and variance for synthetic rPV production. 44

Figure 24: Results for 10^4 runs: Mean and variance for synthetic hub price production. 44

Figure 25: Two-week period of demand and rPV generation: a) demand, uncorrelated FVARMA, b) rPV, uncorrelated FVARMA, c) demand, correlated FVARMA and d) rPV, correlated FVARMA. 45

Figure 26: Left) Three-day training data for demand and rPV; Right) Synthetic data with correlated FVARMA where lowest Fourier frequency is 1-week (for demonstration purposes only). 46

Figure 27: 2-week period of demand and hub price: correlated FVARMA. 46

Figure 28: Exponential demand growth at 3.3%/year. 47

Figure 29: rPV growth: Left) linear at 200MW/year; Right) exponential at 3.3%/year. 48

Figure 30: Net demand growth: Left) using rPV linear at 200MW/year; Right) using rPV exponential at 3.3%/year. 48

Figure 31: Reference CASE 0, monthly water flows through the system for one year. Top) RO1_split 20%; Bottom) RO1_split 80%. 51

Figure 32: Reference CASE 1, monthly water flows through the system for one year. Top) RO1_split 20%; Bottom) RO1_split 80%. 52

Figure 33: Reference CASE 2, monthly water flows through the system for one year. Top) RO1_split 20%; Bottom) RO1_split 80%. 53

Figure 34: Reference CASE 1, monthly recovery ratio for RO1 for one year. Top) RO1_split 20%; Bottom) RO1_split 80%. 54

Figure 35: Reference CASE 0, monthly water flows to the reservoir ponds for one year. 55

Figure 36: Reference CASE 1, monthly water flows to the reservoir ponds for one year. Top) RO1_split 20%; Bottom) RO1_split 80%. 55

Figure 37: Reference CASE 1, monthly water chemistry (6 tracked chemicals) through the system for one year; RO1_split 20%. 56

Figure 38: Reference cases, yearly number of hours when electricity is sold at the PV hub and the average hub price at which electricity has been sold for each year of the project lifetime. 59

Figure 39: Results for 10^4 runs: Mean and standard deviation for number of hours during a year when electricity has to be sold at the APS hub. 60

Figure 40: Results for 10^4 runs: Mean and standard deviation for yearly average hub price when electricity has to be sold at the APS hub. 61

Figure 41: Results for 10^4 runs: Mean and standard deviation for yearly number of hours when EDNet > PowAPScor and the hub price is negative at the same time. 62

Figure 42: Results for 10^4 runs: Mean and standard deviation for yearly possible opportunity revenue during hours when EDNet > PowAPScor and the hub price is negative at the same time. 63
Figure 43: Reference case: Delta NPV for CASE 1 and LCOW for CASE 2 as a function of RO1 capacity. 64
Figure 44: Reference case: Maximum chloride concentration in the reservoir ponds for CASE 1 and CASE 2 as a function of RO1 capacity. 65
Figure 45: Reference case: Maximum water flow to the evaporation ponds for CASE 1 and CASE 2 as a function of RO1 capacity. 65
Figure 46: Sensitivity study: Discount rate. Optimum RO and pump capacities. 67
Figure 47: Sensitivity study: Discount rate. Maximum water flows to evaporation ponds. 67
Figure 48: Sensitivity study: Discount rate. Delta NPV (CASE 1) and LCOW (CASE 2). 68
Figure 49: Sensitivity study: Wholesale electricity price. Optimum RO and pump capacities. 68
Figure 50: Sensitivity study: Wholesale electricity price. Maximum water flows to evaporation ponds. 69
Figure 51: Sensitivity study: Wholesale electricity price. Delta NPV (CASE 1) and LCOW (CASE 2). 69
Figure 52: Sensitivity study: Project lifetime. Optimum RO and pump capacities. 70
Figure 53: Sensitivity study: Project lifetime. Maximum water flows to evaporation ponds. 70
Figure 54: Sensitivity study: Project lifetime. Delta NPV (CASE 1) and LCOW (CASE 2). 71
Figure 55: Sensitivity study: Net demand projection model. Optimum RO and pump capacities. 71
Figure 56: Sensitivity study: Net demand projection model. Maximum water flows to evaporation ponds. 72
Figure 57: Sensitivity study: Net demand projection model. Delta NPV (CASE 1) and LCOW (CASE 2). 72
Figure 58: Sensitivity study: Brackish water, max Cl^- 450 ppm. Optimum RO and pump capacities. 73
Figure 59: Sensitivity study: Brackish water, max Cl^- 450 ppm. Maximum water flows to evaporation ponds 74
Figure 60: Sensitivity study: Brackish water, max Cl^- 450 ppm. Delta NPV (CASE 1) and LCOW (CASE 2). 74
Figure 61: Sensitivity study: Brackish water, max Cl^- 500 ppm. Optimum RO and pump capacities. 75
Figure 62: Sensitivity study: Brackish water, max Cl^- 500 ppm. Maximum water flows to evaporation ponds 75
Figure 63: Sensitivity study: Brackish water, max Cl^- 500 ppm. Delta NPV (CASE 1) and LCOW (CASE 2). 76
Figure 64: Sensitivity study: Brackish water, average Cl^- 450 ppm. Optimum RO and pump capacities. 76

Figure 65: Sensitivity study: Brackish water, average Cl^- 450 ppm. Delta NPV (CASE 1) and LCOW (CASE 2). 77

TABLES

Table 1: BWRO plant specifications. 7
Table 2: Model parameters for the FilmTech 8" BW30-400 membrane [12]. 8
Table 3: Model parameter estimates for Eq. (1). 10
Table 4: Model parameter estimates for Eqs. (3) and (6). 12
Table 5: Example cash flows for NPV calculation. 14
Table 6: Model inputs provided by the RAVEN "sampler". 23
Table 7: Statistical properties of training and synthetic demand. 39
Table 8: Statistical properties for training, synthetic, and smoothed rPV Generation. 41
Table 9: Statistical properties of training data and synthetic demand for correlated FVARMA with adjustment. 41
Table 10: Statistical properties for real and synthetic rPV Generation for correlated FVARMA with adjustment. 42
Table 11: Reference input values for APS cases. 49
Table 12: Reference CASE 0, cash flow breakdown. Values shown for the first year of the project lifetime. RO1_split 20% and 80% (in million $). 57
Table 13: Reference CASE 1, cash flow breakdown. Values shown for the first year of the project lifetime. RO1_split 20% and 80% (in million $). 58
Table 14: Reference CASE 2, cash flow breakdown. Values shown for the first year of the project lifetime. RO1_split 20% and 80% (in million $). 58
Table 15: Sensitivity studies performed (reference in **red**). 66

ACRONYMS

APS	Arizona Public Service
ARMA	Auto-Regressive Moving Average
BWRO	Brackish Water Reverse Osmosis
CAPEX	Capital expenditure
CDF	Cumulative Distribution Function
FARMA	Fourier plus ARMA
FCO	Fuel Cycle Option campaign
FVARMA	Fourier plus VARMA
FWP	Feedwater Pump
GHI	Global Horizontal Irradiance
HP	High-pressure
HPS	Hassayampa Pump Station
INL	Idaho National Laboratory
IRR	Internal Rate of Return
LCM	Least Common Multiple
LCOW	Levelized Cost of Water
N-R HES	Nuclear-Renewable Hybrid Energy System
NPP	Nuclear Power Plant
NPV	Net Present Value
O&M	Operation and Maintenance
PI	Profitability index
PV	Palo Verde
PVGS	Palo Verde Generating Station
RAVEN	Risk Analysis Virtue Environment
RO	Reverse Osmosis
rPV	Rooftop Photovoltaic (Solar)
SROG	Sub Regional Operating Group
TDS	Total Dissolved Solids
VARMA	Vector ARMA
VRE	Variable Renewable Energy
WACC	Weighted Average Cost of Capital
WRF	Water Reclamation Facility
WRSS	Palo Verde Water Reclamation Supply System
WWTP	Waste-Water Treatment Plant

Case Study: Nuclear-Renewable-Water Integration in Arizona

1. INTRODUCTION

This document reports the application of the Nuclear-Renewable Hybrid Energy System (N-R HES) software framework to a case study conducted in collaboration with Arizona Public Service (APS), the operating owner of the Palo Verde Generating Station (PVGS) Nuclear Power Plant (NPP). The case study is a work in progress; this report presents a detailed description of the current model input data, assumptions, and the corresponding results produced by the developed software framework. The goal of the report is to identify where more detailed data is required and more accurate model assumptions are necessary to reproduce all of the driving physical and economic phenomena in order to capture sufficient complexity to allow APS to apply the results to inform strategic decisions.

Development of the N-R HES software framework was initiated at Idaho National Laboratory (INL) in 2016 [1-7]. The framework has reached some level of maturity such that it can be applied to more than simple demonstration cases, e.g. real industry problems. Nevertheless, more capabilities are constantly added to accommodate the special needs of these challenging real-life problems. The N-R HES framework is built on top of the Risk Analysis Virtual Environment (RAVEN) code [8-10], which it uses as a driver and workflow manager for all calculations. The framework has specifically been developed for the economic assessment of N-R HESs. There are four main cornerstones of the N-R HES simulation framework: 1) generation of stochastic time series, 2) a probabilistic analysis and optimization set of algorithms available in RAVEN, 3) a set of models for representation of the physical behavior of N-R HES, and 4) a RAVEN plug-in called CashFlow [4] that maps physical performance into economic performance. Within this framework, a broad spectrum of questions related to N-R HES can be addressed. One of the challenges currently of high interest is that the increasing penetration of variable renewables is altering the profile of the net demand (demand after removing all non-curtailable renewable energy sources), with which the other generators on the grid have to cope. The N-R HES software framework is capable of analyzing the potential feasibility of mitigating the resultant volatility in the net electricity demand. One possible solution to manage net demand volatility that is being intensively studied by the energy industry is adding stabilizing loads to the grid. These loads can be external industrial processes that are able to ramp production up and down quickly or for regulated markets, adding variable internal loads that will effectively increase the baseload of the power plant and therefore reduce the risk of internal demand that is lower than the capacity of the power plant. The latter is a possible solution currently being considered by APS.

APS is currently anticipating several operational challenges in the near future. One of these challenges is coping with the rapid growth of Variable Renewable Energy (VRE) sources on the grid. Although APS can sell its electricity for a fixed retail price (on a cost recovery base) to cover the local demand first, it also trades electricity at the local Palo Verde (PV) energy hub. Due to the growing VRE penetration, the PV Hub electricity spot price is negative more and more frequently, therefore APS can either sell excess electricity in moment of peak price or curtail its internal production to benefit from negative prices. To mitigate the demand volatility. APS is seeking to add more baseload, so that the quantity of excess energy to be sold for prices potentially less than the internal retail price or even negative prices at the hub is reduced. A second challenge APS is facing is that their cooling water acquisition contract with the Sub Regional Operating Group (SROG) will expire soon and a renewal can only be done for a significantly higher price of the water. Therefore, APS is also seeking alternative sources for their cooling water. An opportunity currently under investigation is to pump a limited quantity of brackish water from the regional ground water. Although much less expensive than the water from the new SROG contract, the salinity of the brackish water is so high that a blend of brackish and SROG water could need additional treatment to

improve its quality for use in the PVGS cooling towers. An on-site Reverse Osmosis (RO) desalination plant is envisaged to reduce the salinity to an acceptable level.

This report investigates the economic impact of such an RO plant. The RO plant would help with both problems APS is facing. First, it would raise the APS baseload demand, helping to mitigate VRE-induced demand volatility. From this perspective the RO plant can be seen as a stabilizing load on the grid as would be any other industrial process. Second, the RO's goods, e.g. the clean water produced, can be used by APS for a (hopefully) lower cost than the cost of 100% SROG water.

The report first describes the detailed APS water procurement strategy and lays out the possible alternative scenarios studied in this document (Chapter 2). Next, in Chapter 3, the APS case model developed within the N-R HES software framework is described. This chapter also includes a description of the necessary framework developments to accommodate the APS study. Chapter 4 presents all the model input data and assumptions and discusses the simulation results. Finally, Chapter 5 includes the conclusions as well as suggestions for further studies.

2. APS CASE DESCRIPTION

As mentioned in the introduction, APS is trying to simultaneously address two challenges by considering on-site installation of an RO plant. First, operation of the RO will increase the APS internal load so that less electricity needs to be sold for potentially low (lower than retail) or even negative prices at the PV energy hub. This will mitigate some of the demand volatility introduced by increasing amounts of VRE. Second, the RO could allow production of lower cost clean (but not potable) water as needed in the PVGS cooling towers by blending brackish ground water with SROG water, which would then be processed through the RO, compared to buying 100% of the water from the more expensive SROG that would not require processing though RO. The analysis in this report considers 3 scenarios presented in the following sections: CASE 0) The status quo, where all cooling water is purchased from the SROG and the RO is not built. In CASE 1 one RO plant would be built on-site to treat the blend of SROG and brackish water. CASE 2 would require two RO plants, one on site like for CASE 1 and another one close to the brackish water well. This second RO could produce potable water that can be sold to the regional municipality to generate additional revenue for APS. The analysis evaluates the differential Net Present Value (NPV) between the scenarios. This method only considers the cash flows that actually change between the scenarios to determine the change in the NPV (ΔNPV) (see Chapter 3.2.5).

2.1 Status quo (CASE 0)

The current APS water procurement strategy is as follows: Pre-treated effluent water is purchased from five local municipalities (the SROG) and is delivered to the PVGS Water Reclamation Supply System (WRSS) piping from the City of Phoenix 91st Avenue Waste-Water Treatment Plant (WWTP). The treated effluent is conveyed through the 36-mile WRSS piping system and arrives at the PVGS Water Reclamation Facility (WRF) where tertiary treatment is performed to achieve the water quality needed for the steam cycle cooling through large mechanical draft evaporative cooling towers. This scenario is shown in Figure 1. In CASE 0 it is assumed that all water is purchased from the SROG (with the new contract and anticipated future pricing) and no RO is built.

The effluent water that arrives at the WRF has a certain chemical composition that changes slightly during the year. The cooling towers have an established limit for the quantity of dissolved solids in the cooling water. Therefore, the WRF reduces the concentrations of some dissolved solids (softens the water) in the effluent water to an acceptable value through chemical means (mainly lime and soda ash). The most important impurities treated by the WRF are calcium, magnesium, sodium, sulfates as well as the total alkalinity.

The WRF is not well equipped to reduce the chloride content in the water, but the effluent water's chloride content is below the cooling tower limit of 450 ppm most of the time. In addition, PVGS can use water with a higher chloride concentration, but in this case the amount of water needed to cool the plant increases linearly with the chloride content. There is no additional performance benefit in further reducing the chloride content below 450 ppm, i.e. the cooling water need is not reduced for Cl^- <450 ppm. To illustrate this: for a chloride concentration <450 ppm, the nominal amount (100%) of cooling water is needed; it is possible to allow, for example, a chloride content of 475 ppm, but the cooling water required would increase to 100/450*475 = 105.5% of the nominal amount of cooling water.

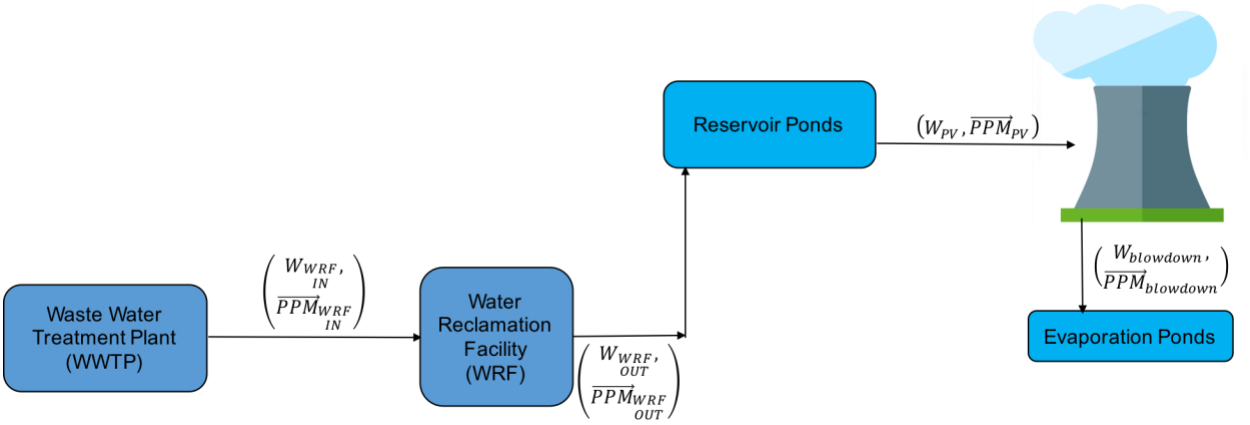

Figure 1: CASE 0. All water is purchased from the SROG and the RO is not built.

2.2 One RO is built on site (CASE 1)

The first case (CASE 1) considered in this study is shown in Figure 2. Abundant regional brackish groundwater is available and actively pumped to dewater local agricultural lands, thereby lowering the water table below the crop root zone (note that the salinity of the brackish groundwater is sufficiently high as to adversely affect agriculture). The brackish water is diverted and discharged downstream. Some portion of the brackish water may be diverted to the WRSS piping to blend with and offset the SROG effluent. Treatment (desalinization) would be required to improve the water quality to the level needed for plant steam cycle cooling. An RO plant design could be coordinated with the PVGS WRF. Note that this strategy will consider RO as baseline desalination technology, while other technologies may also be available. As one can see in Figure 2, the effluent and brackish water blend is first treated by the already existing WRF and then only a fraction (α) of the WRF outlet water is treated by the RO. The rest of the water is directly diverted to the reservoir ponds where it mixes with the treated water from the RO. The RO is capable of treating the water to a much cleaner level than needed by the PVGS cooling system. α, and, therefore, the capacity of the RO, is determined such that the quality of the mixed water in the reservoir pond is above the threshold for the PVGS cooling towers.

As mentioned under CASE 0, the WRF can reduce almost all major dissolved solids in the effluent water with the exception of chloride. The brackish water contains a much higher amount of chloride than the effluent water; hence, the resulting blend of effluent and brackish water may have a chloride concentration above the cooling tower limit depending on the amount of brackish water purchased. This case assumes that it is not possible to procure enough brackish water to cover the entire APS water need. Therefore, the APS cooling water will always be a blend of effluent and brackish.

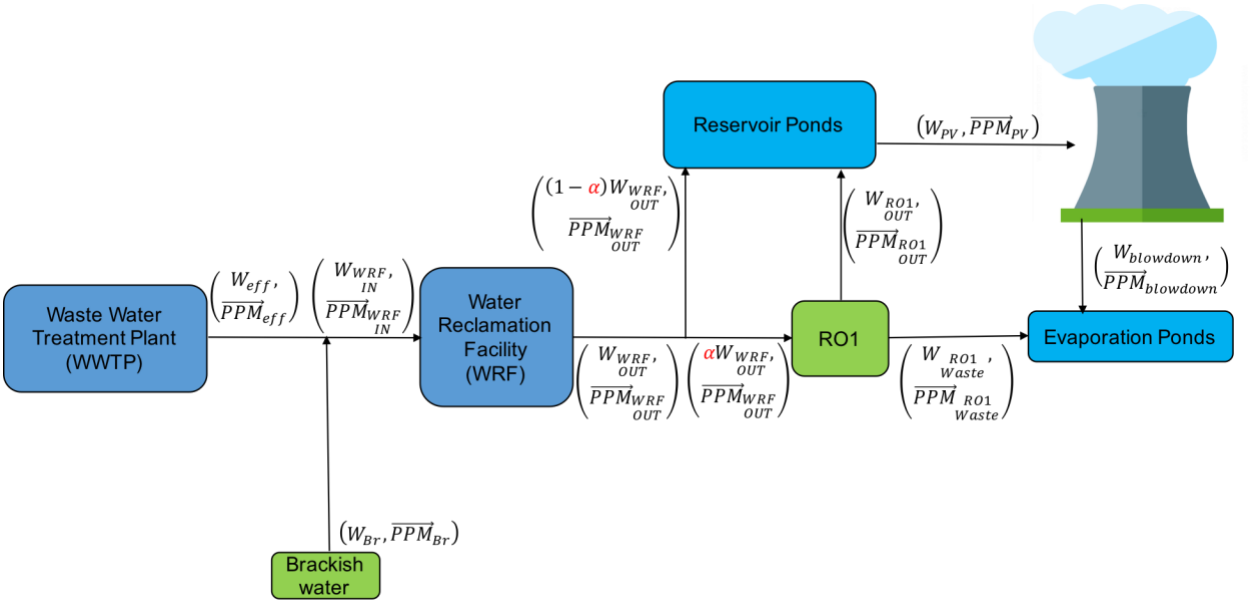

Figure 2: CASE 1. Effluent water is purchased from the SROG and brackish water is pumped from the ground. This blended water needs to be treated in an on-site RO in addition to the WRF.

2.3 Tow ROs are built (CASE 2)

One might argue that, *a priori*, it is not clear if the RO should be built near the SROG and brackish water pump rather than on-site as considered in CASE 1. In addition, APS could, for example, decide to enter the water supply business and sell part of the purified water from the RO. This scenario would even be more relevant in the spirit of hybridization, as the RO would be used as a more flexible load (compared to CASE 1) to satisfy not only the internal water need, but to also produce a variable excess amount of water that could be sold for profit. It should also be mentioned that treated effluent water can only be sold with restrictions, while desalinated brackish water could be sold as potable water.

There are two considerations to keep in mind for CASE 2:

- Building only one RO at the SROG bears the problem that there are no evaporation ponds at the SROG to accommodate the waste stream from the RO.
- The SROG and the brackish water acquisition site are ~40 miles from the PVGS site. Therefore, CASE 1 considers injecting the brackish water in the existing WRSS piping and transporting the blend of effluent and brackish water to the WRF and on-site RO. If APS would like to sell some of the purified water it has to consider that treated effluent water can only be sold with restrictions. In practice, to be able to sell water, only the brackish water should be treated in the RO, which would require separate piping from the SROG and brackish water pump location to the PVGS site.

There are many locations on which the RO could be built. In the framework of this project, a second case (see Figure 3) has been selected for illustration purposes. Other cases may be studied in the future.

The second case considers building two ROs, one at the SROG (RO2) and one at the PVGS site (RO1) like in CASE 1. CASE 2 takes CASE 1 as a base, but adds the second RO (RO2) at the SROG to treat the brackish water. The idea is that APS can sell the purified brackish water from RO2 (see the second consideration above) and inject the waste stream from that RO into the WRSS piping. This configuration avoids the need for evaporation ponds at the location of RO2 (see the first consideration above). APS can still reduce the amount of effluent water they need to buy by using the RO2 waste water, but the salinity of

the blended effluent and waste from the brackish water RO2 will likely be too high for the cooling system and would need treatment (like in CASE 1). Therefore, to reduce the salinity to a limit that the water can be used at the cooling towers, a second RO is needed. This second RO1 can be built at the PVGS site (as in CASE 1), where evaporation ponds are available.

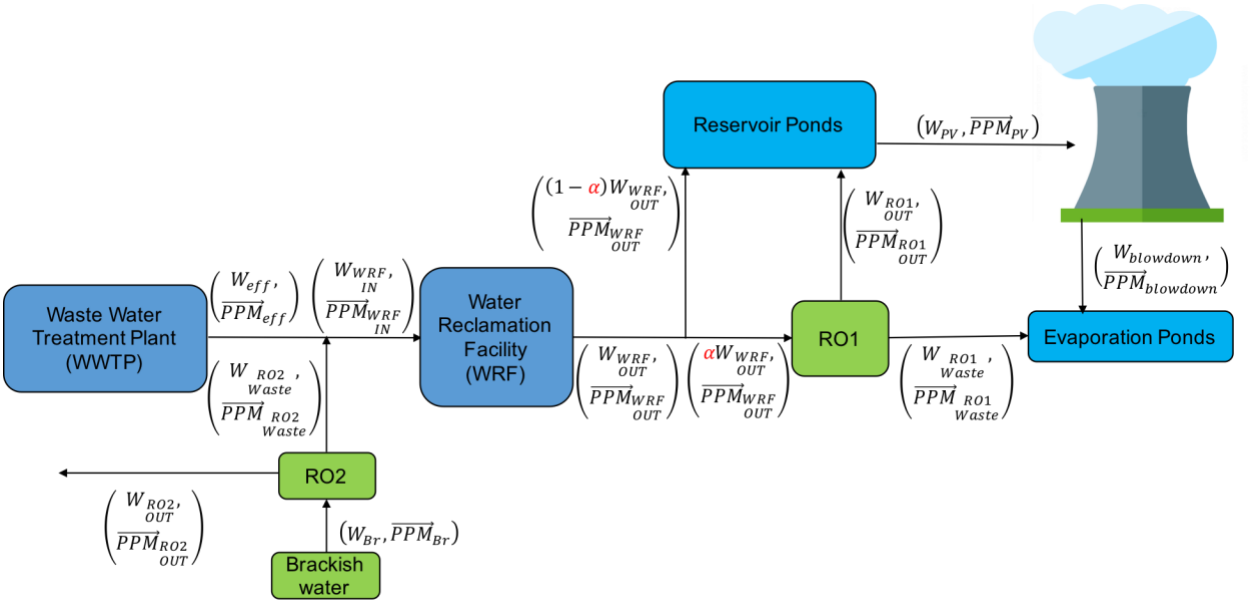

Figure 3: CASE 2. Effluent water is purchased from the SROG and brackish water is pumped from the ground. The brackish water is purified and sold, while the waste is blended with the effluent. This mix needs to be treated in an on-site RO in addition to the WRF.

3. MODEL DESCRIPTION

This section describes how the three APS cases described in Section 2 are modeled. In general, cases are modeled within the N-R HES software framework, where the framework provides some generic capabilities that can be used to build the case-specific models. To model the three APS cases, several additional framework developments are needed to provide all the generic functionalities needed. The first section of this chapter describes the added N-R HES framework functionalities. In the second section of this chapter, the APS models (for the three considered cases) within the N-R HES framework are described in detail. This chapter also includes a description of how the reduced order RO model used in the APS case models has been derived from a high fidelity Modelica model.

3.1 N-R HES framework developments

As mentioned, this section reports the N-R HES framework developments that are needed to model the APS cases.

3.1.1 Reverse Osmosis model development

This section is dedicated to the model development for an RO desalination plant (or simply referred to as an “RO plant”), in particular a low-fidelity representation of the physical behavior of the plant that is

based on a high-fidelity model developed previously [11-13]. A system overview of the proposed RO plant for the APS case study is also provided.

RO desalination utilizes a semi-permeable membrane that allows water to pass through but not salts, thus separating the fresh water from the saline feed water. A typical Brackish Water RO (BWRO) plant (see Figure 4(a)) consists of four main components: feedwater pretreatment, High-Pressure (HP) pumping, membrane separation, and permeate (fresh water) post-treatment. Figure 4(b) depicts the configuration of an RO vessel (a multi-element module) used in RO desalination, which is typically comprised of six to eight membrane modules connected in series. The concentrate water rejected by the first membrane module plays a role as the feed water for the second membrane module by the successive order, and so on. These pressure vessels are arranged in rows in each membrane stage, with two-stage membrane separation being typical in BWRO. Each stage has a recovery of 50–60%, achieving overall system recovery of 70–85% [14].

Recently, INL proposed the detailed dynamic modeling and control design of a two-stage BWRO plant, in which the modeling efforts were focused on the two main components: HP pumping and membrane separation units (enclosed in the dashed rectangle shown in Figure 4(a)) [11-13, 15, 16]. In this report, this high-fidelity model served as a starting point for deriving a low-fidelity representation of the proposed BWRO plant; additional assumptions and simplifications made for the APS case study are as follows:

- HP pumping accounts for 90.4% of the total energy consumption in the BWRO facility, i.e., an RO pretreatment system accounts for 9.6% of the total energy consumption in the BWRO facility.
- The system dynamics are, relatively speaking, much faster than the sampling rate (i.e., one hour); thus, steady-state assumption is valid.
- Feed water may contain up to six solids (solutes): bicarbonate (HCO_3^-), calcium (Ca^{2+}), magnesium (Mg^{2+}), sodium (Na^+), chloride (Cl^-), and sulfate ($SO4^{2-}$).

The plant was sized for 698 $m^3\ hr^{-1}$ (4.43×10^6 gallons per day), which requires 402 kW_e of electrical power to generate the required feed (operating) pressure (12 barg) for desalting the brackish water, containing 900 ppm of Total Dissolved Solids (TDS). Table 1 reports the nominal design specifications of the proposed BWRO plant. Table 2 shows the specifications of the FilmTech 8″ BW30-400 membrane, i.e., a spiral-wound module manufactured by Dow Chemical, chosen for simulation in this work.

A high-fidelity model (i.e., Modelica model) might provide an accurate reflection of reality but requires high computational power; thus, an approximation model (i.e., surrogate model) that mimics the behavior of the high-fidelity model as closely as possible while being computationally efficient to evaluate is constructed.

The *linear regressor*[1] is proposed to characterize the relationship shown in Eq. (1) between the feed flow rate m_f (i.e., a decision variable set by RAVEN) and the power consumption in the Feedwater Pump (FWP) P_{FWP} (in W_e):

$$P_{FWP} = k_0 + k_1 m_f \tag{1}$$

where k_1 and k_0 are the model-fitting parameters. Several simulations were conducted to estimate the model estimates by linear regression. Regression results for Eq. (1) are plotted in Figure 6. The estimated model-fitting parameters and the goodness of model fit (R^2 value) are listed in Table 3. Note that the simulation results showed that the dependency of the feed salinity S_f on P_{FWP} is negligible; hence, feed salinity was not considered in Eq. (1). The quality of the surrogate model fits compared to the Modelica model outputs indicates excellent model fits.

[1] The linear regressor is a least-squares fitting of the response of the system for a linear representation (linear regression).

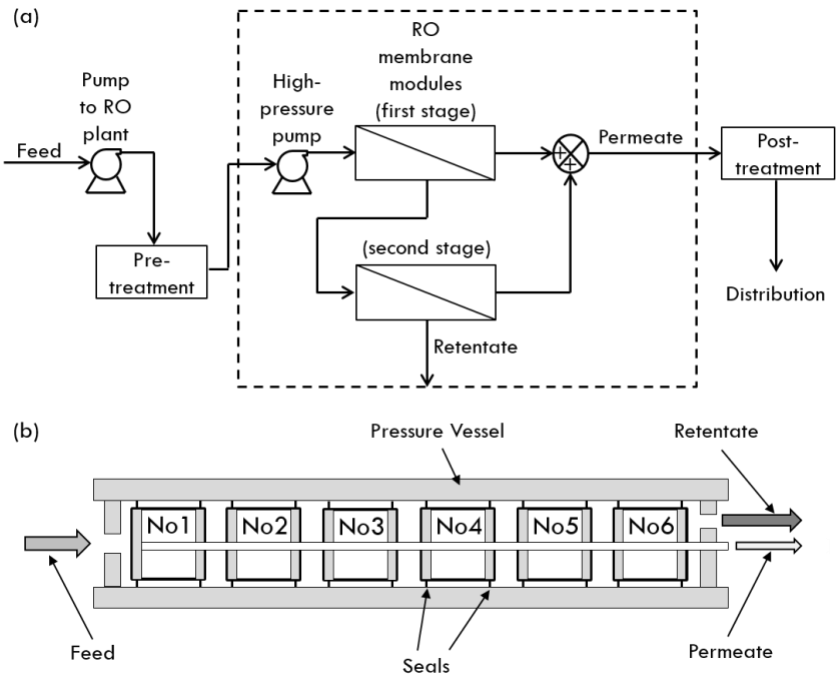

Figure 4: RO desalination: (a) process flow diagram for a two-stage BWRO plant and (b) schematic of an RO vessel, which consists of six membrane modules in series [12].

Table 1: BWRO plant specifications.

Symbol	Description	Unit	Value
ε_{pump}	Pump efficiency	%	80
ω	Pump shaft rotational speed	rpm	2240
V_{op}	Valve opening of the pneumatic pressure control valve	%	80
N_{VE}	Number of pressure vessels per HP pump	–	110
N_{ST}	Number of stages	–	2
N_M	Number of RO modules per one pressure vessel (or stage)	–	6
T_f	Feed temperature	°C	25
S_f	Feed salinity	ppm	900
p_f	Feed (operating) pressure	barg	12
p_p	Permeate pressure	barg	0
Q_p	Permeate volumetric flow rate	$m^3\ hr^{-1}$ [gal day^{-1}]	698 [4.43×10^6]
P_{BWRO}	Rated electrical load in the BWRO plant	kW_e	402
$\bar{S}_p$	Average permeate salinity (quality)	ppm	16.8
R_S	Salt rejection	%	99.4
R_{w1}	Water recovery in the first stage	%	47
R_{w2}	Water recovery in the second stage	%	62
R_w	Overall water recovery	%	80

Table 2: Model parameters for the FilmTech 8" BW30-400 membrane [12].

Symbol	Description	Unit	Value
l_{BR}	Brine channel length of an RO element	m	0.8665
h_{BR}	Brine channel height of an RO element	m	7.112×10^{-4}
h_{sp}	Spacer thickness	m	7.112×10^{-4}
w_{BR}	Brine channel width of an RO element	m	1.34
n_l	Number of leaves per one RO module	–	16
ϕ_{BR}	Overall void fraction of the brine channel	–	0.9
a_{sp}	Specific surface area of the spacer	m^{-1}	11.2×10^{3}
d_h	Hydraulic diameter	m	9.1×10^{-4}
A_m	Total membrane area per one RO module	m^2 [ft^2]	37.2 [400]
A_s	Membrane area occupied by precipitation	m^2 [ft^2]	1.86[a] [20]
α_1	Constant for solvent transport	–	8.646
α_2	Constant for solvent transport	bar^{-1}	0.0149
β_1	Constant for solute transport	–	14.65
L_{v0}	Intrinsic solvent transport parameter	m Pa^{-1} s^{-1}	1.042×10^{-11}
L_{s0}	Intrinsic solute transport parameter	m s^{-1}	1.333×10^{-8}

[a] Equivalent membrane fouling in terms of percentage at this value is 5%.

The proposed system was dynamically modeled with the *Modelica*[2] modeling language [17] using the commercially available Modelica-based modeling and simulation environment, i.e., *Dymola* version 2017 FD01 [18]. Figure 5 shows the top-level model for the BWRO plant implemented in Modelica.

As mentioned in the previous section, HP pumping only accounts for 90.4% of the total energy consumption in the BWRO facility P_{BWRO}; therefore, Eq. (2) is proposed to estimate the total energy consumption in the plant:

$$P_{BWRO} = {P_{FWP}}/{0.904} \tag{2}$$

Figure 7 and Figure 8 show the permeate flow rate m_p and salinity S_p, respectively, simulated by the high-fidelity model as functions of feed stream conditions. In these examples, an osmotic pressure correction factor F_π, defined by Eq. (5), was set to be 1.

As can see in Figure 7, the permeate flow rate increases as the feed flow rate increases for any given feed salinity. Also, at a given feed flow rate, it is expected to produce more permeate water with lower feed salinity. In Figure 8, the results show that the permeate salinity is inversely proportional to the feed flow rate (or equivalently the permeate flow rate) for any given feed salinity. In other words, the higher the feed flow rate, the purer the permeate stream. On the other hand, at a given feed flow rate, the permeate quality (or salt rejection) worsens as the feed salinity increases.

[2] Modelica is an object-oriented equation-based programming language, oriented toward computational applications with high complexity requiring high performance.

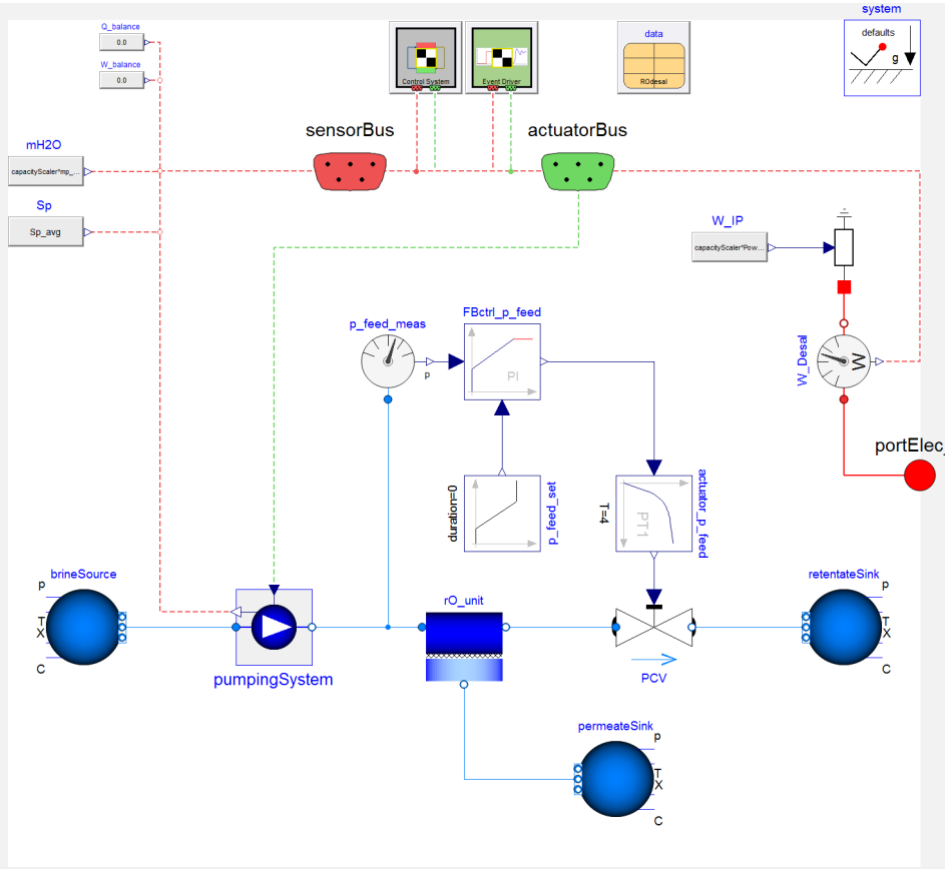

Figure 5: Top-level model for the BWRO plant implemented in Modelica.

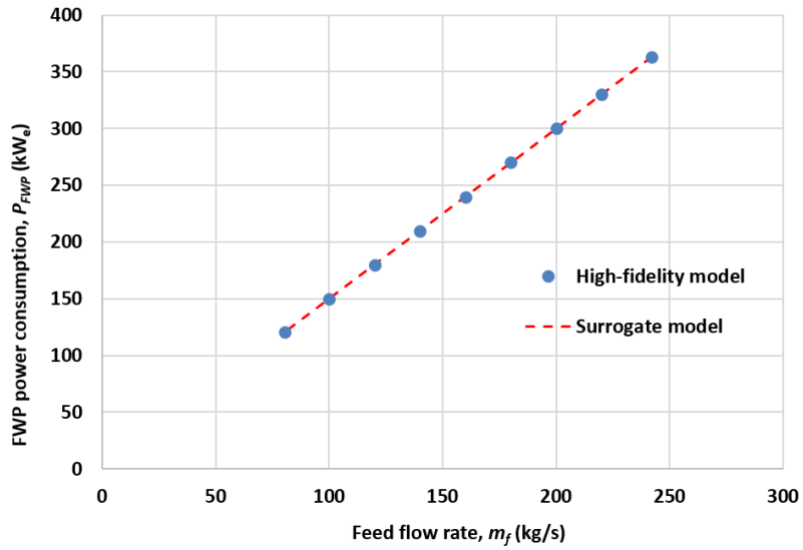

Figure 6: FWP power consumption (P_{FWP}) predicted by the high-fidelity (blue points) and surrogate (red dashed line) models.

Table 3: Model parameter estimates for Eq. (1).

Symbol	Description	Unit	Value
k_0	Model parameter	W_e	2.886×10^{-1}
k_1	Model parameter	W_e s kg^{-1}	1.500×10^{3}
R^2	Goodness of fit	–	1.000

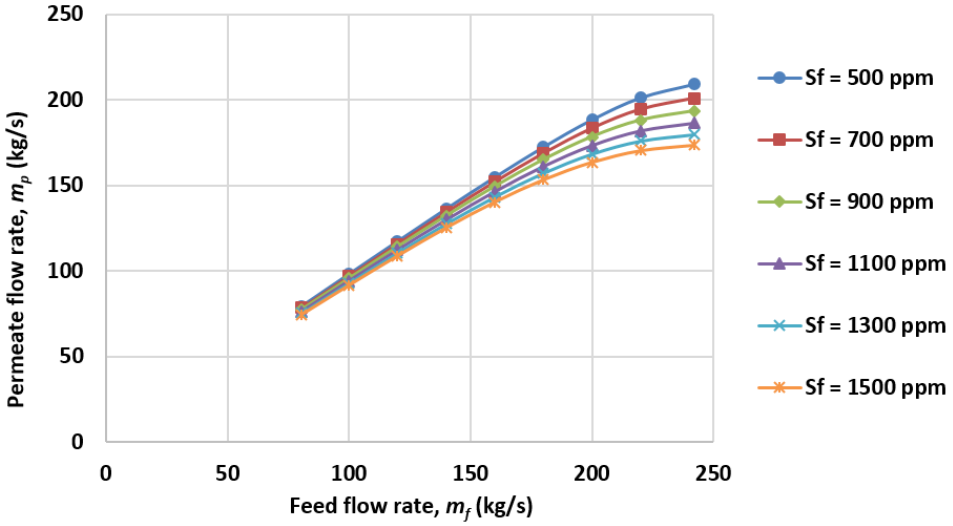

Figure 7: Permeate flow rate (m_p) versus feed flow rate (m_f) simulated for a range of feed salinity (S_f) by the high-fidelity model.

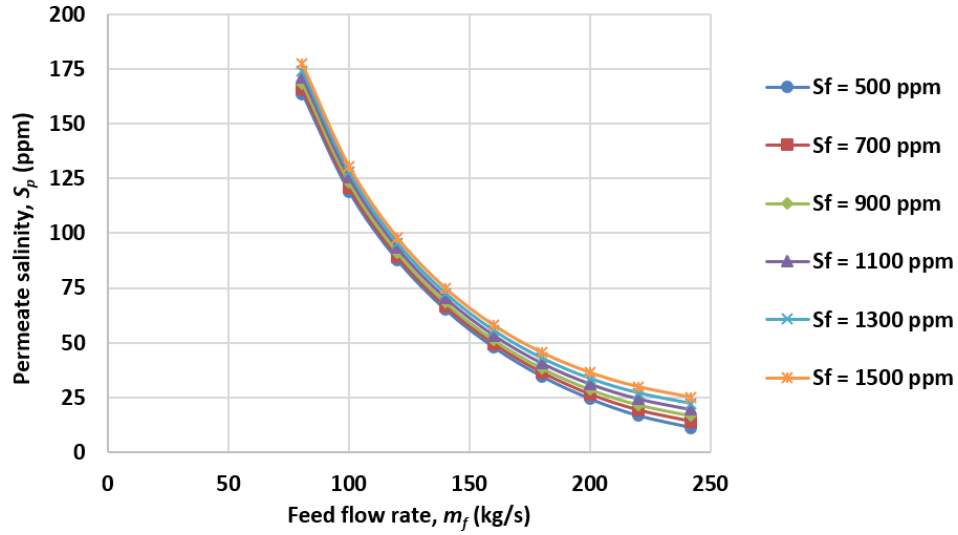

Figure 8: Permeate salinity (S_p) versus feed flow rate (m_f) simulated for a range of feed salinity (S_f) by the high-fidelity model.

In order to predict the permeate flow rate (in kg s^{-1}), the following set of equations is proposed:

$$m_p = k_0 + k_1 m_f + k_2 S_f + k_3 F_\pi + k_4 m_f S_f + k_5 m_f F_\pi + k_6 S_f F_\pi + k_7 m_f^2 + k_8 S_f^2 + k_9 F_\pi^2 \quad (3)$$

$$S_f = \sum_i C_{f,i} \quad (4)$$

$$F_\pi = \frac{\sum_i \frac{S_{f,i}}{MW_i} z_i}{\frac{S_f}{MW_{NaCl}} 2} \quad (5)$$

where k_0–k_9 are the model-fitting parameters, $S_{f,i}$ is the solute concentration of species i in the feed, MW_i is the molecular weight of species i, z_i is the number of valence electrons associated with species i, and MW_{NaCl} is the molecular weight of sodium chloride. The correction factor (F_π) takes into account the difference between the medium containing multiple solids (up to six solutes as mentioned previously) and the medium containing only Na^+ and Cl^- for the same concentration of TDS in the feed. Similarly, Eq. (6) is proposed to approximate the permeate salinity (in ppm) as a function of feed stream conditions:

$$S_p = k_0 + k_1 m_f + k_2 S_f + k_3 F_\pi + k_4 m_f S_f + k_5 m_f F_\pi + k_6 S_f F_\pi + k_7 m_f^2 + k_8 S_f^2 + k_9 F_\pi^2 \quad (6)$$

Figure 9 and Figure 10 show selected representative plots for m_p and S_p, respectively, simulated with the high-fidelity models (Modelica models) and the corresponding surrogate models fitted by nonlinear regression. The estimated model-fitting parameters and R^2 values are listed in Table 4. The surrogate models are superior in terms of the goodness of fit.

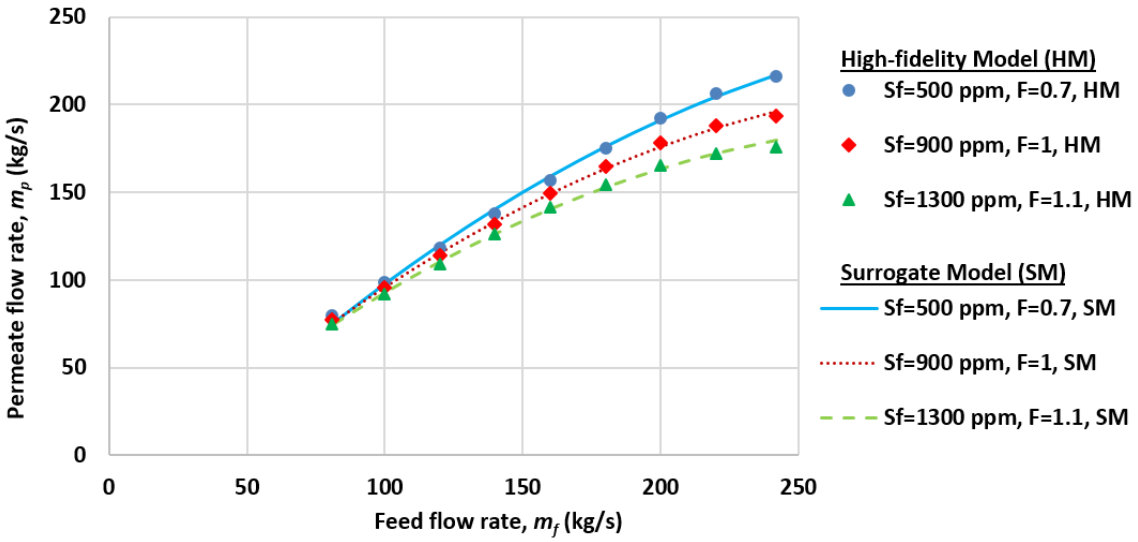

Figure 9: Permeate flow rate (m_p) predicted by the high-fidelity (points) and surrogate (lines) models.

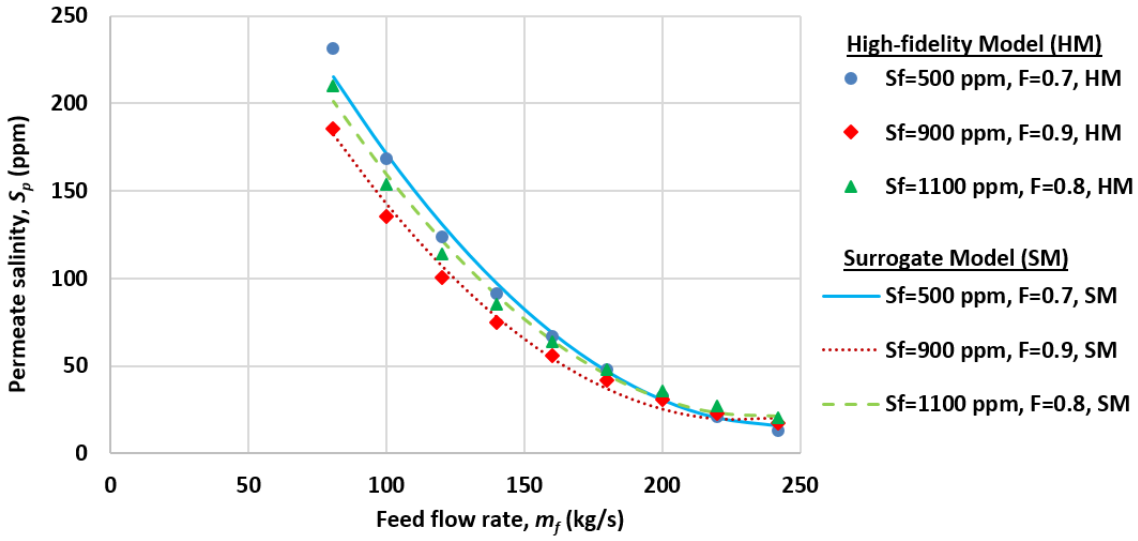

Figure 10: Permeate salinity (S_p) predicted by the high-fidelity (points) and surrogate (lines) models.

Table 4: Model parameter estimates for Eqs. (3) and (6).

Symbol	Description	Eq. (3)		Eq. (6)	
		Unit	Value	Unit	Value
k_0	Model parameter	kg s^{-1}	-68.25	ppm	7.041×10^{2}
k_1	Model parameter	–	1.828	ppm s kg^{-1}	-4.427
k_2	Model parameter	kg s^{-1} ppm^{-1}	2.684×10^{-2}	–	3.482×10^{-3}
k_3	Model parameter	kg s^{-1}	29.03	ppm	-4.151×10^{2}
k_4	Model parameter	ppm^{-1}	-1.820×10^{-4}	s kg^{-1}	1.007×10^{-5}
k_5	Model parameter	–	-1.966×10^{-1}	ppm s kg^{-1}	1.148
k_6	Model parameter	kg s^{-1} ppm^{-1}	-1.614×10^{-2}	–	3.376×10^{-3}
k_7	Model parameter	s kg^{-1}	-2.227×10^{-3}	ppm s^2 kg^{-2}	7.386×10^{-3}
k_8	Model parameter	kg s^{-1} ppm^{-2}	5.758×10^{-7}	ppm^{-1}	1.587×10^{-6}
k_9	Model parameter	kg s^{-1}	7.562×10^{-1}	ppm	85.38
R^2	Goodness of fit	–	0.998	–	0.991

The solute concentration of species i in the permeate $S_{p,i}$ is estimated as follows:

$$S_{p,i} = S_{f,i} \cdot y_{f,i} \tag{7}$$

$$y_{f,i} = {S_{f,i}}/{S_f} \tag{8}$$

where $y_{f,i}$ is the fraction of species i among TDS in the feed. The retentate (concentrate) flow rate m_r and the solute concentration of species i in the retentate stream $S_{r,i}$ can be calculated based on the law of mass conservation:

$$m_r = m_f - m_p \tag{9}$$

$$S_{r,i} = \frac{m_f S_{f,i} - m_p S_{p,i}}{m_r} \tag{10}$$

The retentate salinity S_r is the sum of $S_{r,i}$:

$$S_r = \sum_i S_{r,i} \tag{11}$$

3.1.2 CashFlow developments

RAVEN's CashFlow plugin is used in the N-R HES framework to map physical performance of a system into economic performance. The module is able to compute the NPV, the Internal Rate of Return (IRR) and the Profitability Index (PI). Furthermore, it is possible to conduct an NPV, IRR or PI search, i.e. CashFlow will compute a multiplicative value (for example, the production cost) so that the NPV, IRR or PI has a desired value. To fulfill the requirements of the APS cases on the cash flow calculations, the following extensions of the CashFlow plugin have been made:

CashFlow drivers

The CashFlow plugin allows definition of an arbitrary number of cash flows from which the indicators (NPV, PI, etc.) are computed. Each cash flow is of the form given in Eq. 12.

$$CF_y = m \cdot \alpha_y \left(\frac{driver_y}{ref}\right)^X \tag{12}$$

where *CF* is the cash flow for year y

m is an optional scalar multiplier

α is the multiplier of the cash flow for each year

ref is the reference for which α is given

X is the economy of scale factor, $0 < X < 1$ indicates an economy of scale while $X > 1$ indicates a diseconomy of scale.

driver is the cash flow driver. In previous versions of the CashFlow plugin, the driver was the same for all years for which the cash flow is computed, i.e. for all "y". With this update, the driver can be either a scalar or a vector with the length of the lifetime of the project. If it is a scalar, all $driver_y$ in Eq. 12 are the same for all years of the project life. If it is a vector, then each year of the project will have its corresponding value for the driver.

Tax and inflation

The CashFlow plugin can apply tax and inflation to the cash flows if needed. In previous versions of the plugin the tax and inflation rate were global inputs. That means the user could choose if tax (yes/no) and inflation (none, real or nominal) needed to be applied for each cash flow individually, but the same tax and inflation rates would apply for all cash flows. In the current version, the plugin allows different tax and inflation rates for each defined "component." A "component" is a collection of cash flows that share the same properties, such as lifetime and with this update also tax and inflation. If no tax or inflation rates are specified for a "component," the rates defined as "global" rates in the input will be applied.

Project management

As mentioned, the CashFlow plugin allows grouping of cash flows together into "components." A component is typically a part of the system that has the same lifetime and the same cash flows, i.e. for a battery or a plant. To compute the economic indicators (NPV, IRR, etc.), previous versions of the CashFlow plugin compute the Least Common Multiple (LCM) of all component lifetimes. Components with short lifetimes are re-built successively at the end of their lifetime until the LCM is reached. Running the global project to the LCM of all components guarantees that the NPV is computed for a time span so that all components reach their end of life in the same year. The individual component cash flows are repeated until the LCM is reached. For example, assume the calculation involves two components Component1 and Component2, with life times of 60 years and 40 years, respectively. The global project time will be 120 years where 2 successive Component1 and 3 successive Component2 will be built. For every 'building year', the cash flow for the last year (of the old component) and the year zero (for the newly built component) will be summed. Table 5 shows an example for illustration.

Table 5: Example cash flows for NPV calculation.

	Component 1		**Component 2**		
Year	**Comp. lifetime**	**Cash Flow (year)**	**Comp. lifetime**	**Cash Flow (year)**	**Total Net Cash flow**
0	0	CF_0^{Compo1}	0	CF_0^{Compo2}	$CF_0^{Compo1} + CF_0^{Compo2}$
1	1	CF_1^{Compo1}	1	CF_1^{Compo2}	$CF_1^{Compo1} + CF_1^{Compo2}$
…	..		…		
39	39	CF_{39}^{Compo1}	39	CF_{39}^{Compo2}	$CF_{39}^{Compo1} + CF_{39}^{Compo2}$
40	40	CF_{40}^{Compo1}	40 and 0	$CF_{40}^{Compo2} + CF_0^{Compo2}$	$CF_{40}^{Compo1} + CF_{40}^{Compo2} + CF_0^{Compo2}$
41	41	CF_{41}^{Compo1}	1	CF_1^{Compo2}	$CF_{41}^{Compo1} + CF_1^{Compo2}$
…	…		…		
59	59	CF_{59}^{Compo1}	19	CF_{19}^{Compo2}	$CF_{59}^{Compo1} + CF_{19}^{Compo2}$
60	60 and 0	$CF_{60}^{Compo1} + CF_0^{Compo1}$	20	CF_{20}^{Compo2}	$CF_{60}^{Compo1} + CF_0^{Compo1} + CF_{20}^{Compo2}$
61	1	CF_1^{Compo1}	21	CF_{21}^{Compo2}	$CF_1^{Compo1} + CF_{21}^{Compo2}$
…	…		…		
79	19	CF_{19}^{Compo1}	39	CF_{39}^{Compo2}	$CF_{19}^{Compo1} + CF_{39}^{Compo2}$
80	20	CF_{20}^{Compo1}	40 and 0	$CF_{40}^{Compo2} + CF_0^{Compo2}$	$CF_{20}^{Compo1} + CF_{40}^{Compo2} + CF_0^{Compo2}$
81	21	CF_{21}^{Compo1}	1	CF_1^{Compo2}	$CF_{21}^{Compo1} + CF_1^{Compo2}$
…	…		…		
119	59	CF_{59}^{Compo1}	39	CF_{39}^{Compo2}	$CF_{59}^{Compo1} + CF_{39}^{Compo2}$
120	60	CF_{60}^{Compo1}	40	CF_{40}^{Compo2}	$CF_{60}^{Compo1} + CF_{40}^{Compo2}$

The new developments for the CashFlow allow more flexibility in how the global project time and individual components are handled. The following new inputs have been made available in the current version of CashFlow:

<Global>input <ProjectTime>:	This is an optional input. If it is included in the input file, the global project time is not the LCM of all components, but the time indicated here.
<Component> input <StartTime>:	This is an optional input. If this input is specified for one or more components, the <Global> input <ProjectTime> is required. This input specifies the year in which this component will be built for the first time, i.e. when it will be included in the cash flows. The default is 0 and the component is built at the start of the project, i.e. at project year 0. For example, if the <ProjectTime> is 100 years, and for this component, the <StartTime> is 20 years, the cash flows for this component will be zero for years 0 to 19 of the project. Year 20 of the project will be year 0 for this component and so on (project year 21 will be component year 1, etc.).
<Component> input <Repetitions>:	This is an optional input. If this input is specified for one or more components, the <Global> input <ProjectTime> is required. This input specifies the number of times this component will be rebuilt. The default is 0, which indicates that the component will be rebuilt indefinitely until the project end (<ProjectTime>) is reached. Assume the <ProjectTime> is 100 years, and the component <Life time> is 20 years. Specifying 3 repetitions of this component will build 3 components in succession, at years 0, 20 and 40. For years 61 to 100 of the project, the cash flows for this component will be zero.

3.1.3 FVARMA developments

At the end of 2017, the Auto-Regressive Moving-Average (ARMA) algorithms in RAVEN had many essential elements for simulating time-dependent events based on training data [19, 20]. This includes using Fourier series to de-trend training data, using an empirical Cumulative Distribution Function (CDF) to normalize the residual, and reversing the process to produce new synthetic samples.

As the needs of ongoing projects in 2018 were considered, it became apparent there were some deficiencies in the ARMA that required feature expansion. First, each data set required an independent ARMA, and no correlation could be preserved between the sets. This means weather events and energy events that should exhibit correlation, such has unusually hot summer days and spikes in demand, could not be preserved in synthetic histories. Second, a separate ARMA was required for each data set, even if no correlation was observed. Allowing the training of multiple data sets in a single ARMA surrogate helps prevent risk of mismatching histories and provides a more convenient method to work with both the synthetic data and the surrogates themselves. Finally, the Fourier plus ARMA (FARMA) combination proved to be unsuitable for simulating solar irradiance when considered over multiple days, because of the lack of irradiation during the night. Additional algorithms were needed to allow accurate capturing of this kind of signal.

To address the lack of correlation, multiplicity of surrogates, and inability to capture solar irradiance data, the following new enhancements were implemented in the FARMA model.

Correlated ARMA

A methodology is available to extend the self-correlated data regression in the ARMA to consider additional data series. This treatment results in a vector of correlated data series trained in an ARMA, or Vector ARMA (VARMA). While the ARMA uses autoregression and moving average algorithms to

correlate data within its own history, the VARMA extends that correlation to consider the cross effects of regression terms in data series among each other. This allows capturing phenomena such as spikes in air temperature leading to spikes in demand.

To demonstrate this feature, a multivariate normal distribution was used to generate training data for two target variables, "A" and "B". Both share a mean of 42 and variance of 25, and the covariance between "A" and "B" is 22. The resulting training data is shown in the upper right of Figure 11. The correlation between the two is readily observed: increases in "A" tend to occur in tandem with increase in "B", and conversely. For clarity, no Fourier trends were included.

Once the VARMA was trained, a sample of the surrogate was taken, and the results considered. The two left-side figures in Figure 11 show the original data in comparison to the synthetic histories; as expected, they share little resemblance except in mean and variance. In the lower-right figure in Figure 11 the synthetic data is shown together, and they show the same kind of correlation exhibited in the original data. In this manner, correlation can be preserved in the creation of synthetic histories.

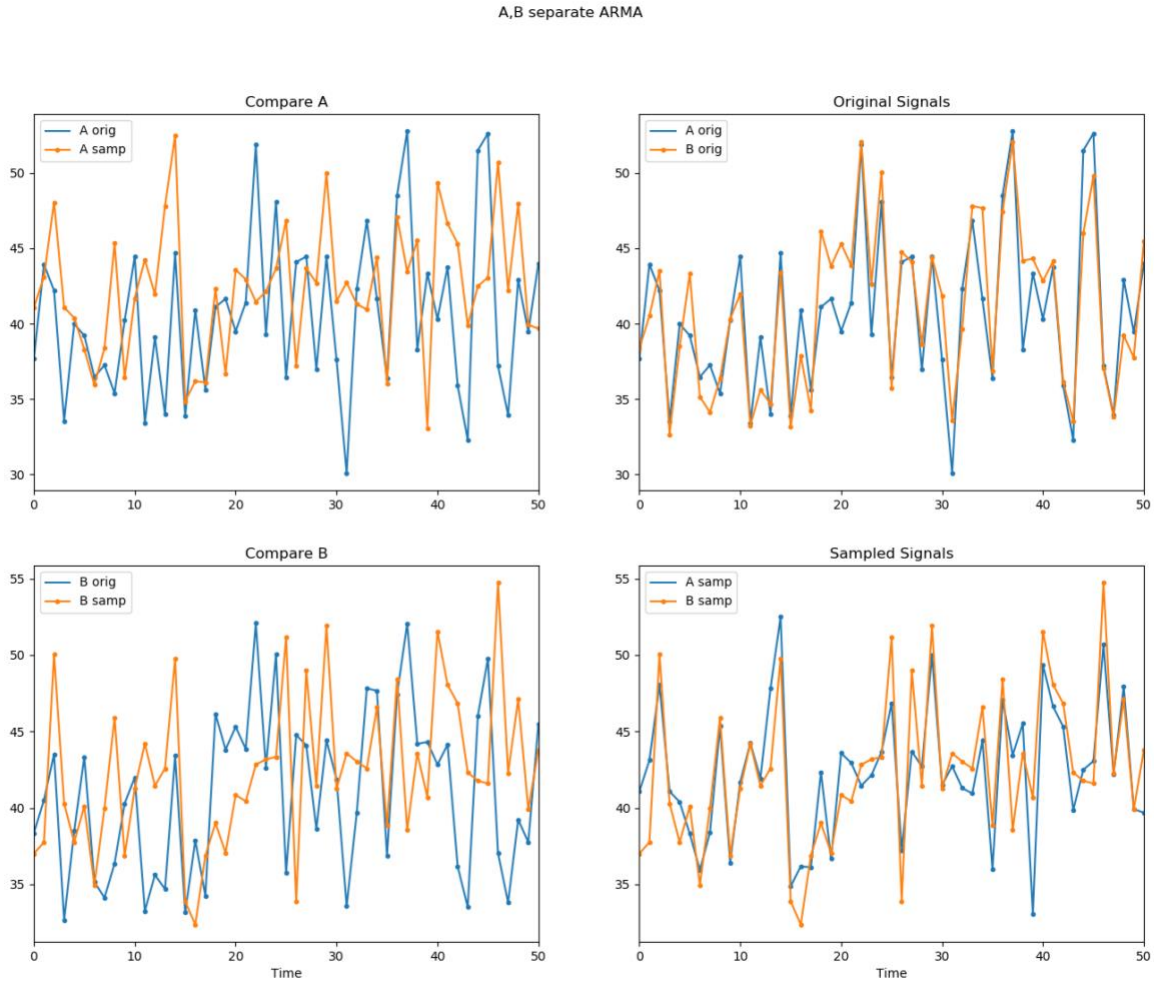

Figure 11: Correlated VARMA demonstration. Upper right: training data. Upper left: training versus synthetic for "A". Lower left: training versus synthetic for "B". Lower right: synthetic data.

Combined ARMA Models

To extend the portability, flexibility, and consistency of ARMA surrogate usage, the FARMA algorithm in RAVEN was expanded to train multiple targets in a single entity (Fourier plus VARMA (FVARMA)). Part of this work has been done in conjunction with the Fuel Cycle Option (FCO) campaign which shared the same needs. Due to timing constraints and the shared need, while NR-HES developed the theoretical formulation of the algorithm, a different team took charge of the deployment in RAVEN under FCO. As with previous efforts, the resulting surrogate was then portable between workflows as a single model that sampled all the trained targets simultaneously. Even if the targets are not correlated, the results originate from the same training data. In order to assure proper treatment of targets, the domain-limiting "out truncation" option was reworked to accept a list of the targets for whom a domain limitation should be applied, and a "specific Fourier" option was added to allow individual targets to make use of different base Fourier detrending periods.

By way of example, the wind speed ("Speed") and energy demand ("Demand") were considered for a week-long period. The composition of the signals is shown in Figure 12 and Figure 13. While Demand shows considerable stability in its day-to-day cycle, the wind shows very little daily trend and instead sees trends in a multi-hour period. Both of these targets were trained in the same FVARMA, but used different Fourier periods to capture their trends.

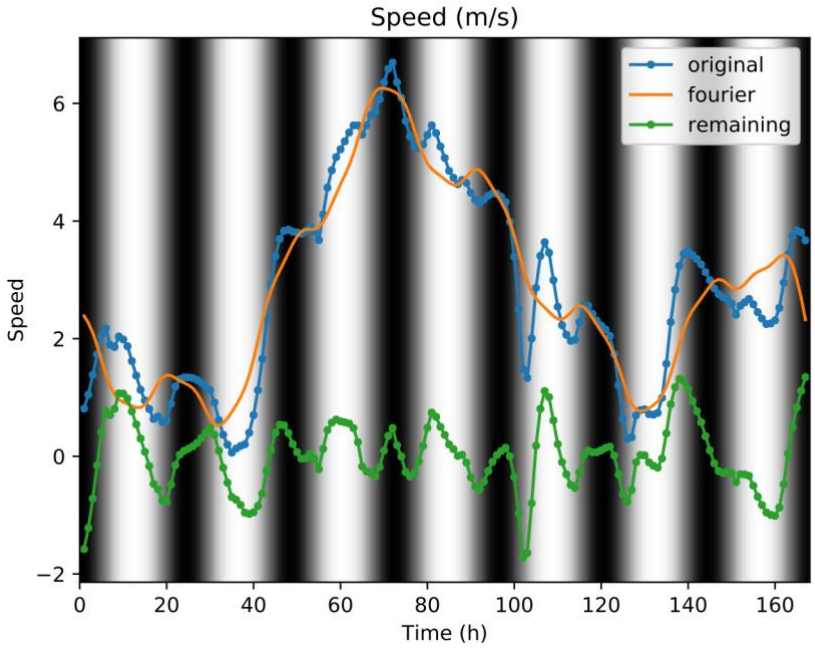

Figure 12: Wind Speed for a Week-Long Period in ERCOT North-Central Region, June 2007. Black and white background indicates day and night for better visibility of daily trends in the signal.

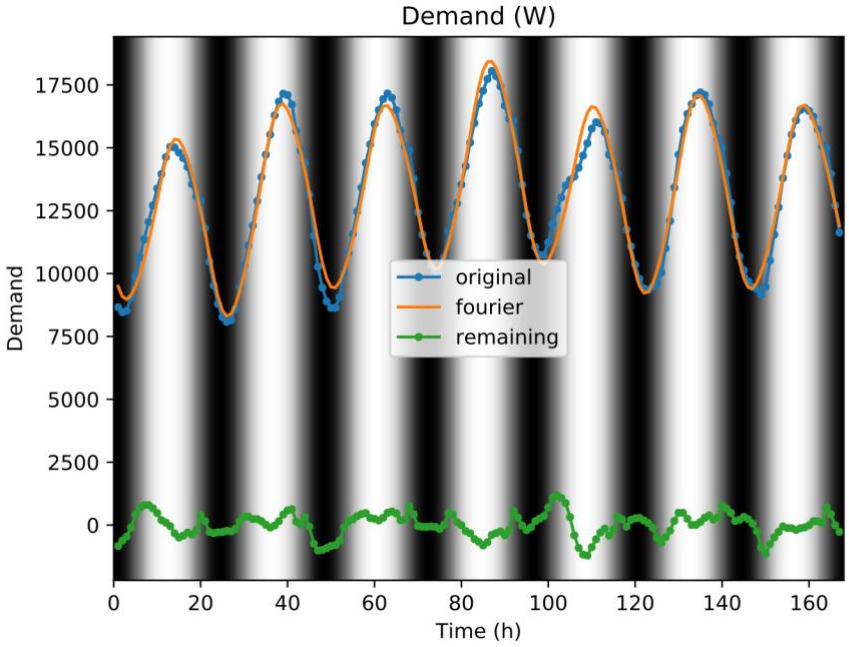

Figure 13: Energy Demand for a Week-Long Period in ERCOT North-Central Region, June 2007. Black and white background indicates day and night for better visibility of daily trends in the signal.

Zero-Filtering

Previous data analyzed (energy demand, wind speed) varied continuously throughout a 24-hour period, which made Fourier analysis a suitable tool to capture the behavior. Solar irradiance, measured as Global Horizontal Irradiance (GHI), however, has a single peak each day but a flat line at night. While the peaks are suitable for Fourier analysis, the flat lines are very difficult to capture using Fourier series. When the two are combined, the detrending stage often underestimates the daytime trends in an attempt to minimize error during the night, resulting in overestimating the variance during the day and introducing variance during the night, which should remain flat at zero. This can be seen in Figure 14. The orange line indicates the original training data, while the blue lines are the synthetic samples from the unfiltered, trained FVARMA. Note in the original training data there are two fairly normal days, followed by a day with significantly reduced irradiance for part of the day, introducing significant variance.

The unfiltered samples shown in Figure 14 demonstrate much smaller peak amplitudes on average, reaching only 400 W/m^2 on average instead of nearly 600. In addition, there is significant solar activity at night, with both negative and positive irradiance showing, when it should be zero.

To combat this phenomenon, an additional feature was added to the FVARMA called "zero filtering". When this filtering is requested, the algorithm takes note of the times in which the signal is nearly zero, then splits the construction of the FVARMA into two parts: one where the zero-filtered target is zero, and one that encompasses the remaining non-filtered time. An FVARMA is then trained for all targets during the non-filtered times, and for all except the zero-filtered target during filtered times. The results of these two FVARMAs are then recombined to create a consistent signal with correlations preserved for other targets during both night and day cycles, and correlations involving the GHI preserved during day cycles. An example of this is shown in Figure 15, especially in contrast to Figure 14. Note that the nighttime irradiance is precisely zero for all the nights, while there are still signals appropriate to the training data during the day.

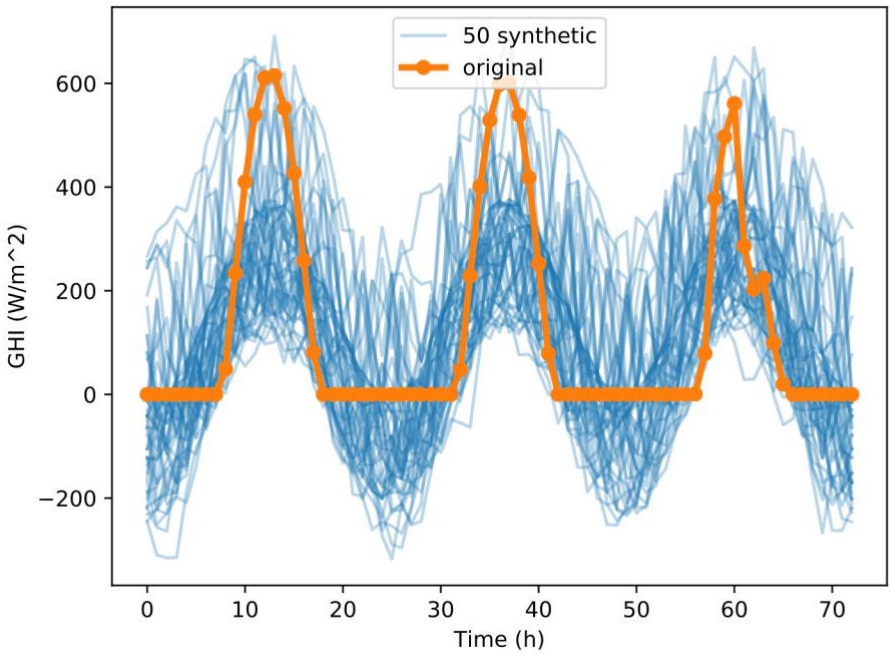

Figure 14: Global Horizontal Irradiance (GHI): Original and Unfiltered Synthetic Data, 3 days.

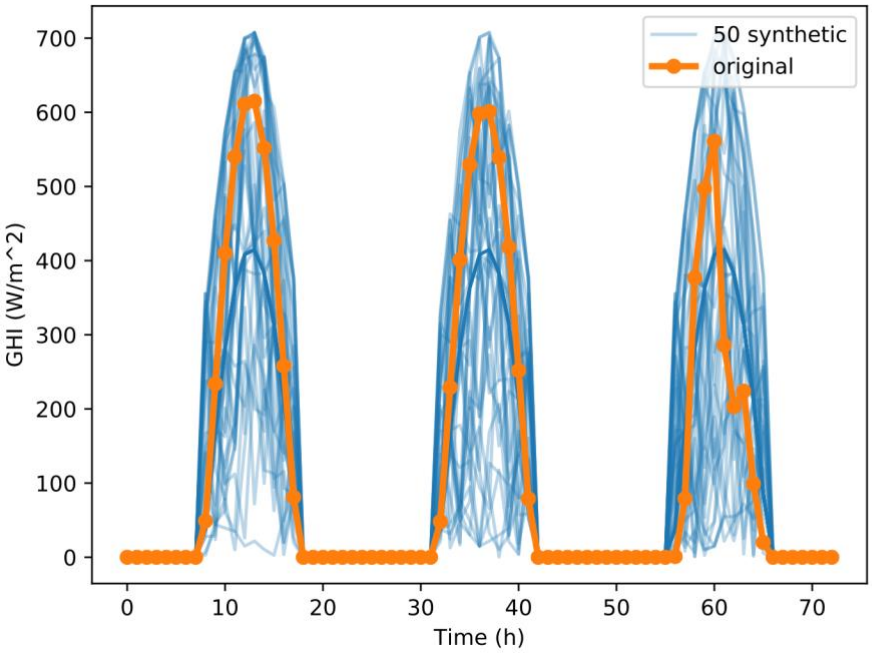

Figure 15: Global Horizontal Irradiance (GHI): Original and Zero-Filtered Synthetic Data, 3 days.

3.2 APS case model within N-R HES framework

This section describes how the three cases described in Section 2 are modeled using the N-R HES software framework. It also explains how the additional N-R HES framework developments detailed in the previous section (3.1) have been used. Before taking a closer look into the model, some nomenclature is introduced.

3.2.1 Nomenclature

This section summarizes the general nomenclature used for the APS case model within the N-R HES framework. It should be noted that the models and equations presented in the report may be using different units (Imperial, SI, chemical concentrations in dissolved ions or as equivalent of some other quantity, etc). The equations are implemented as presented, but the unit transformations performed are not presented here for easier reading of the equations.

Facilities Naming

WRF	Water Reclamation Facility.
RO1	Reverse osmosis plant after the WRF.
RO2	Reverse osmosis plant in Buckeye.
Pump	Pumping facility to inject brackish water in the pipeline in Buckeye.

Indexes

j	Index for years (1…J).
i	Index for month in year (1…12).
k	Index for days in a month (1…30).
l	Index for hours in a day (1…24).
ll	Index for hours in a year (1…8760).
J	NPP residual life (NumberOfYears in Table 6).

Facilities Characterization (WRF)

$W_{\underset{IN}{WRF}}$	WRF inflow [kg/month].
$W_{\underset{OUT}{WRF}}$	WRF treated water outflow [kg/month].
$\overrightarrow{PPM}_{\underset{IN}{WRF}}$	Chemistry of WRF inlet water (concentration of 6 tracked chemicals in [ppm]).
$\overrightarrow{PPM}_{\underset{OUT}{WRF}}$	Chemistry of WRF outlet water (concentration of 6 tracked chemicals in [ppm]).
$PPM_{cal\,\underset{OUT}{WRF}}$	WRF outlet calcium concentration (as $CaCO_3$) [ppm].
$PPM_{mag\,\underset{OUT}{WRF}}$	WRF outlet magnesium concentration (as $CaCO_3$) [ppm].
$PPM_{sod\,\underset{IN}{WRF}}$	WRF inlet sodium concentration [ppm].
$PPM_{sod\,\underset{OUT}{WRF}}$	WRF outlet sodium concentration [ppm].
$PPM_{alk\,\underset{OUT}{WRF}}$	WRF outlet total alkalinity (as $CaCO_3$) [ppm].
$PPM_{cl^-\,\underset{IN}{WRF}}$	WRF inlet chloride concentration [ppm].
$PPM_{cl^-\,\underset{OUT}{WRF}}$	WRF outlet chloride concentration [ppm].
$PPM_{sul\,\underset{OUT}{WRF}}$	WRF outlet sulfate concentration [ppm].
E_{WRF}	Electricity consumption function for the WRF [MWh/month].

F_{WRF} Fixed cost of WRF [$/capacity].
V_{WRF} Variable (and fixed) cost function of the WRF excluded electricity [$/volume].
$CAPEX_{WRF}$ Unit capital cost of WRF [$/capacity].

Facilities Characterization (RO1)

C_{RO1} Capacity of RO1 [kg/s]
$W_{\substack{RO1 \\ OUT}}$ RO1 treated clean water (permeate) [kg/month].
$W_{\substack{RO1 \\ Waste}}$ RO1 waste stream [kg/s].
$\overrightarrow{PPM}_{\substack{RO1 \\ OUT}}$ Chemistry of clean RO1 outlet (permeate) water (concentration of 6 tracked chemicals in [ppm]).
$\overrightarrow{PPM}_{\substack{RO1 \\ Waste}}$ Chemistry of RO1 waste water (concentration of 6 tracked chemicals in [ppm]).
E_{RO1} Electricity consumption function for the RO1 [Wh/month].
F_{RO1} Fix cost for RO1 [$/capacity (kg/s)].
V_{RO1} Variable cost function of the RO1 excluded electricity [$/volume].
$CAPEX_{RO1}$ Unit capital cost for RO1 [$/capacity (kg/s)].

Facilities Characterization (RO2)

C_{RO2} Capacity of RO2 [kg/s]
$W_{\substack{RO2 \\ OUT}}$ RO2 treated clean water (permeate) [kg/s].
$W_{\substack{RO2 \\ Waste}}$ RO2 waste stream [kg/s].
$\overrightarrow{PPM}_{\substack{RO2 \\ OUT}}$ Chemistry of clean RO2 outlet (permeate) water (concentration of 6 tracked chemicals in [ppm]).
$\overrightarrow{PPM}_{\substack{RO2 \\ Waste}}$ Chemistry of RO2 waste water (concentration of 6 tracked chemicals in [ppm]).
E_{RO2} Electricity consumption function for the RO2 [Wh/month].
F_{RO2} Fix cost for RO2 [$/capacity (kg/s)].
V_{RO2} Variable cost function of the RO2 excluded electricity [$/volume].
$CAPEX_{RO2}$ Unit capital cost for RO2 [$/capacity (kg/s)].

Facilities Characterization (Evaporation Pond)

W_{EvP} Water inflows in the evaporation ponds [kg/month].
$W_{blowdown}$ Water blown down from the PVGS cooling towers to the evaporation ponds [kg/month].
$\overrightarrow{PPM}_{blowdown}$ Water chemistry of blown down from the PVGS cooling towers to the evaporation ponds (concentration of 6 tracked chemicals in [ppm]).

Facilities Characterization (Brackish water pumping station)

C_{RO1} Capacity of the brackish water pump [kg/s].
E_{Pump} Electricity consumption function for the brackish water pump [kWh/month].
F_{Pump} Fix cost for brackish water pump [$/capacity (kg/s)].
V_{Pump} Variable cost function of the brackish water pump excluded electricity [$/volume].
$CAPEX_{Pump}$ Unit capital cost for brackish water pump [$/capacity (kg/s)].

Global quantities

$P_{E,W}$	Wholesale electricity price [$/MWh] (EL_wholesale_price in Table 6).
$P_{E,R}$	Retail electricity price [$/MWh] (EL_wholesale_price + EL_RetWholeDiff in Table 6).
$P_{E,Hub}$	Electricity price at the PV Hub [$/MWh].
P_{Br}	Price of brackish water [$/acre-foot] (PBrackish in Table 6).
P_{eff}	Price structure of effluent water [$/acre-foot]. This includes multiple tiers and a dependency on the year.
$Penalty$	The non-usage fee payed for water not used [$].
$HouseLoad$	The PVGS house load [MW] (HouseLoad in Table 6).
$WACC_{APS}$	Weighted Average Cost of Capital (WACC) (APS) [%].
$WACC_{PV}$	WACC (APS PVGS) [%].
Inf	Projected inflation rate [%].
Tax	Corporate tax rate [%].
D_j	Depreciation % at year j [%].
α	Fraction of water outgoing from the WRF to the RO1 [%]. This is a constant for a given evaluation of the model (RO1_split in Table 6).
W_{PV}	PVGS cooling water needs [kg/month]. This is an input to the model (Cooling in Table 6). Different values by month can be input.
$\overrightarrow{PPM_{PV}}$	PVGS cooling water chemistry (concentration of 6 tracked chemicals in [ppm]).
PPM_{PVmax}	Acceptable maximum chloride concentration in the PVGS cooling water [ppm]. This is an input to the model (limit_clo_ppm in Table 6).
$BlowD$	Amount of water blown down from the PVGS cooling towers to the evaporation ponds [%]. This is an input the model (Blowdown in Table 6).
W_{eff}	Effluent water bought from the SROG [kg/month]. This is not an input, but has to be solved for a given set of inputs.
$\overrightarrow{PPM_{eff}}$	Chemistry of effluent water (concentration of 6 tracked chemicals in [ppm]). This is an input to the model (Chem_cal_eff, Chem_mag_eff, Chem_sod_eff, Chem_alk_eff, Chem_clo_eff, Chem_sul_eff in Table 6). Different values by month can be input.
W_{Br}	Brackish water pumped from ground water [kg/month]. This is an input to the model (W_brackish in Table 6). Different values by month can be input.
$\overrightarrow{PPM_{Br}}$	Chemistry of brackish water (concentration of 6 tracked chemicals in [ppm]). This is an input to the model (Chem_cal_brackish, Chem_mag_brackish, Chem_sod_brackish, Chem_alk_brackish, Chem_clo_brackish, Chem_sul_brackish in Table 6). Different values by month can be input.
$NPP_{Variable}$	Variable cost of the PVGS NPP [$/production].
NPP_{Fixed}	Fixed cost of the PVGS NPP [$/capcaity].
$PowAPS$	Power share of PVGS belonging to APS [MW] (PowAPS in Table 6).
$PowAPS\%$	Power share of PVGS belonging to APS [%] (PowAPS% in Table 6).
ED_{Net}	Electricity Net Demand [MW].
$ES_{APS\ PV}$	Electricity sold by APS of PVGS shares [$/y].

3.2.2 Overall data flow

Figure 16 shows the overall data flow of the APS cases as modeled in the N-R HES framework. As one can see, first a "sampler" in RAVEN provides all the inputs needed by the subsequent models. A list of all inputs provided by the sampler is given in Table 6. This "sampler" can be any sampler available in RAVEN, for example a "Grid Sampler" to run sensitivity studies on the inputs or an optimizer to find an optimal set of inputs with respect to a target variable, e.g. the maximum NPV. The sampled inputs are then distributed to the subsequent models in the framework. Note that the sampler only provides inputs to the physical

models, i.e. “ARMA PostP”, “APS Model” and “NPV PreP” in Figure 16. The economics are treated by the RAVEN CashFlow plugin (“NPV” in Figure 16) and its inputs are collected in a separate input file (see Section 4.1).

Table 6: Model inputs provided by the RAVEN “sampler”.

Variable name in model	**Description**
RO1_split	The percentage of water that goes to the RO after the WRF (α in Figure 1 to Figure 3). The unit is [%].
NumberOfYears	The number of years considered in the Cash Flow calculation for the global project lifetime. The unit is [years].
PowAPS	Nominal PVGS power output. The unit is [W].
PowAPS%	Share of APS at PVGS. The input unit is [%].
EL_wholesale_price	Retail electricity price. The unit is [$/MWh].
EL_RetWholeDiff	Difference between retail and wholesale price [$/MWh].
HouseLoad	APS house load. The unit is [W].
Blowdown	The percentage of water that goes from the cooling towers to the evaporation ponds. The unit is in [%].
PBrackish	Brackish water price. The unit is [$/acre-foot].
W_brackish	Amount of brackish water blend with the SROG water. 12 different values, one for every month can be input. The unit is [kg].
Chem_cal_brackish	Calcium concentration in brackish water. The unit is [ppm].
Chem_mag_brackish	Magnesium concentration in brackish water. The unit is [ppm].
Chem_sod_brackish	Sodium concentration in brackish water. The unit is [ppm].
Chem_alk_brackish	Total alkalinity (as $CaCO_3$) in brackish water. The unit is [ppm].
Chem_clo_brackish	Chloride concentration in brackish water. The unit is [ppm].
Chem_sul_brackish	Sulfate concentration (as SO_4) in brackish water. The unit is [ppm].
limit_clo_ppm	Chloride limit in the PVGS cooling water system. The unit is [ppm].
Cooling	Amount of cooing water needed at the cooling towers. 12 different values, one for every month can be input. The unit is [kg].
Chem_cal_eff	Calcium concentration (as $CaCO_3$) in effluent water. 12 different values, one for every month can be input. The unit is [ppm].
Chem_mag_eff	Magnesium concentration (as $CaCO_3$) in effluent water. 12 different values, one for every month can be input. The unit is [ppm].

Chem_sod_eff	Sodium concentration in effluent water. 12 different values, one for every month can be input. The unit is [ppm].
Chem_alk_eff	Total alkalinity (as $CaCO_3$) in effluent water. 12 different values, one for every month can be input. The unit is [ppm].
Chem_clo_eff	Chloride concentration in effluent water. 12 different values, one for every month can be input. The unit is [ppm].
Chem_sul_eff	Sulfate concentration in effluent water. 12 different values, one for every month can be input. The unit is [ppm].

For the APS cases, the first model run by the framework is the one that computes the physics of the system, i.e. tracks the water quantities and chemical compositions from the water acquisition points through the WRF and RO to the PVGS cooling towers and finally into the evaporation ponds. This physical model is shown in Figure 16 as "APS model" and described in more detail in Section 3.2.4.

Next, the "Correlated ARMA" (FVARMA) is run to prepare the stochastic input data for the economic analysis. The FVARMA generates correlated synthetic data for the APS internal demand, the non-curtailable rooftop solar (rPV) production and the PV Hub price. A description of how the net demand and PV Hub prices are generated for the lifetime of the project is given in Section 3.2.3.

Then, the NPV pre-processor ("NPV PreP" in Figure 16) is run. This module will compute the cash flow drivers needed by the NPV modules. For example, "NPV PreP" will compute the electricity consumption of the RO. This drives the electricity cost cash flow that is computed by the NPV module. "NPV PreP" receives the outputs from the APS model, i.e. water mass flows and chemical compositions of the water at different points in the system. In addition, the needed inputs from the sampler as well as the net demand and PV Hub prices form the FVARMA are also passed to the NPV preprocessor. Finally, the cash flow drivers are passed to the NPV modules. The NPV module runs three times, one time for each APS case considered in this study. The NPV module computes all the cash flows from the input cash flow drivers, applies taxation, inflation if needed and discounts the cash flows to finally compute the NPV for each case. For case two, instead of the NPV itself, the cash flow module computes the Levelized Cost of Water (LCOW), i.e. the cost of the water produced by the RO2, so that the overall system NPV is zero. The "NPV PreP" and NPV modules including all the cash flows considered in this problem are described in detail in Section 3.2.5.

Finally, the outputs of the NPV modules, i.e. the NPVs for cases 1 and 2 as well as the LCOW for case 2 are passed back to the sampler in RAVEN. For parametric studies on the inputs, the passed back results are just stored in a file together with the inputs for further analysis, like plotting. If the sampler is an optimizer, the results are used to construct a gradient and a decision is made as to how the inputs need to be changed to move toward a more optimal solution. The optimizer iterates until it converges on the optimum or the maximum number of iterations is reached. The inputs and outputs for all iteration steps of the optimizer are stored in a file for subsequent analysis, e.g. to make plots.

3.2.3 FVARMA and "ARMA PostP"

As mentioned, the FVARMA produces the synthetic time histories for the APS internal demand, the rPV production as well as the PV electricity hub price. It is worth mentioning that no industrial solar is considered in the evaluation, since per APS policy industrial solar is considered curtailable. First, synthetic shapes for one year for all of these data are produced and passed into the subsequent models. The choice of

input parameters for the FVARMA model (like Fourier frequencies for de-trending, ARMA model time history parameters "P" and "Q", etc.) is crucial for the model to produce good synthetic data [19]. In addition, these parameters strongly depend on the shape of the input training data. The measured input training data as well as a study on the parameters to be used for the APS data in the FVARMA model, i.e. an APS data analysis, is provided later in Section 4.1.2.

Once the data is generated, the demand and rPV solar generation are passed into the ARMA postprocessor "ARMA PosP". The postprocessor scales the demand and solar data from the FVARMA for future years and computes the net demand for the length of the project ("NumberOfYears" in Table 6). The postprocessor currently supports two scaling options to produce the future net demand. ("Forecast" in the postprocessor input):

- The demand is scaled exponentially with an exponent that can be input in the postprocessor as "DemandScalingFactor" while the rPV is scaled linearly with the coefficient "rPVAddedCapacity".
- Both the demand and the rPV are scaled exponentially using the "DemandScalingFactor".

The first-year demand is taken directly from the sampled FVARMA. Subsequent years are scaled by the user input value. Similarly, the first year of rPV generation is taken directly from the rPV FVARMA. For the rPV the user can choose between two growth models: an exponential scaling, like for the demand, or a linear model with a fixed addition per year. In the second case, the user inputs the rPV scaling factor in units of MW added per year. To apply this capacity addition to generation numbers appropriately, a capacity factor profile is calculated. The input rPV generation is divided by the initial rPV capacity (660 MW) in each hour of the year. The capacity factors are multiplied by the yearly capacity addition and added to the generation that corresponds to the same hour. This method ensures that the capacity addition does not add generation in hours that did not have generation in the first year. This assumes that each year's capacity additions occur at the beginning of the year.

After demand and rPV generation are scaled, rPV generation is subtracted from demand to develop a net demand profile. rPV is considered "must take" generation by APS, meaning that the utility is required to use all the generation rPV produces. Subtracting the rPV production from demand ensures that all the rPV generation is used to meet demand. The net demand is then passed into the larger cash flow model.

The synthetic electricity prices for the PV electricity hub are directly passed into the "NPV PreP" module. The synthetic data generated for one year is repeated for the length of the project.

3.2.4 APS model

As mentioned, the physics of the system are computed by the "APS model" in the software framework. The "APS model" tracks the water quantities (mass flows) and chemical composition through the system from the water acquisition point to the cooling towers and eventually evaporation ponds. The time discretization for all variables is monthly. The concentrations (in ppm) of six different dissolved solids are tracked ($\overrightarrow{PPM}$), namely:

- Calcium
- Magnesium
- Sodium
- Total Alkalinity
- Chloride
- Sulfate.

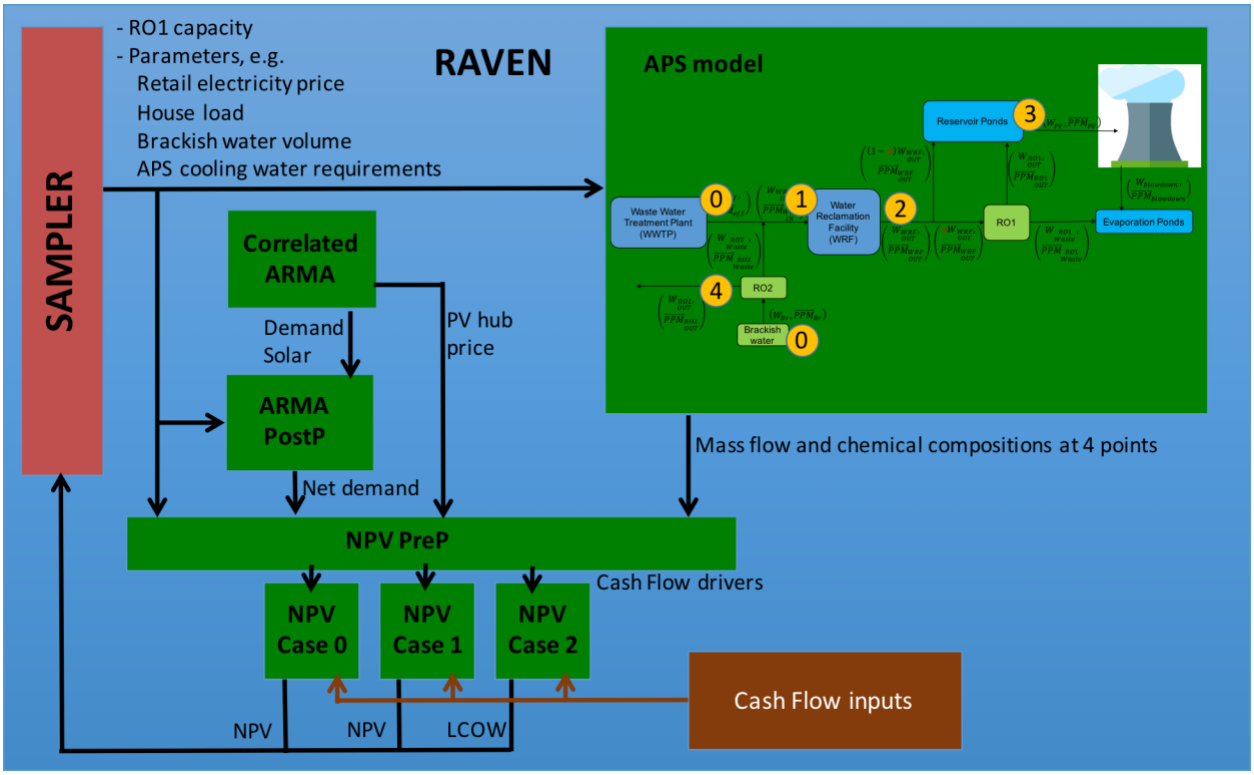

Figure 16: Data flow of the APS case model inside the N-R HES software framework.

The inputs to the model are:

- The cooling water needed by the cooling towers (W_{PV}).
- The maximum acceptable chloride concentration in the water at the cooling towers (PPM_{PVmax}).
- The effluent water chemistry, i.e. the concentrations of the six above mentioned chemicals ($\overrightarrow{PPM}_{eff}$) at the WWTP.
- The amount of brackish water pumped (W_{Br}).
- The brackish water chemistry, i.e. the concentrations of the six above mentioned chemicals ($\overrightarrow{PPM}_{Br}$) at the brackish water pump.

Looking at the above model inputs, one can see that W_{PV} is an input while W_{eff} is an unknown. Ideally, the transfer functions of the RO and WRF can be inverted and the system can be solved from the back, i.e. starting from the cooling towers (point 3 (W_{PV}) in Figure 16) and go back to the water acquisition points (point 0 (W_{eff}) in Figure 16). Unfortunately, the system is not analytically invertible and has to be solved iteratively. The "Brent" root finding algorithm [21] has been used to find W_{eff} for the above inputs. Therefore, the system's equations are implemented in a "forward" manner from the water acquisition (point 0 in Figure 16) to the evaporation ponds (point 3 in Figure 16) and then subject to the "Brent" algorithm.

The "reservoir ponds" are not modeled in this first version of the APS model. It is assumed that the monthly production of cooling water matches exactly the PVGS cooling water needs for each month ($W_{PV,i} = \underset{OUT}{W_{RO1,i}} + (\alpha - 1)\underset{OUT}{W_{WRF,i}}, \forall i$) and there is no possibility to store produced water for later use. This assumption allows solution of the problem for each month independently, i.e. $W_{eff,i}$ can be found solely as a function of the above inputs at month "i".

The current version of the APS model allows one to change the allowable maximum chloride concentration at the cooling towers. The model uses the input water quantities if the maximum chloride concentration is lower than 450 ppm without scaling, i.e. there is no gain in water consumption for lower chloride concentrations ($W_{PV}\ if\ PPM_{\mathrm{PVmax}} \leq 450ppm$). On the other hand, if the input maximum chloride concentration is larger than 450 ppm, the water need for the cooling towers is scaled linearly, i.e.

$$(W_{PV} \cdot \frac{PPM_{\mathrm{PVmax}}}{450}\ if\ PPM_{\mathrm{PVmax}} > 450ppm). \tag{13}$$

All needed cash flow drivers (electricity consumption, mass flow rate, etc.) can be computed when the mass flow rate and chemical composition of the water at the four points indicated in Figure 16 are known (see numbers 0-4 in "APS model" in Figure 16).

Point 0

The first point where knowledge of the water flow is needed is at the water source. In particular, the effluent water characteristics at the WWTP outlet (W_{eff} and $\overrightarrow{PPM}_{eff}$) and the water characteristics at the brackish water pump (W_{Br} and $\overrightarrow{PPM}_{Br}$) must be known. As mentioned, W_{Br}, $\overrightarrow{PPM}_{Br}$ and $\overrightarrow{PPM}_{eff}$ are inputs while W_{eff} is found iteratively.

Points 1 and 4

The next point at which knowledge of the water characteristics is needed is point 1 in Figure 16 ($W_{\underset{IN}{WRF}}$ and $\overrightarrow{PPM}_{\underset{IN}{WRF}}$). There are three cases: the first is when RO2 is not present and no brackish water is pumped (CASE 0); the second is when brackish water is pumped, but the RO2 is still not built (CASE 1); and, finally, the third case includes the brackish water pump and the RO2 (CASE 2).

In CASE 0, the water conditions at the WRF inlet are the conditions at the WWTP outlet, i.e.

$$W_1^{CASE0} = W_{\underset{IN}{WRF}} = W_{eff} \tag{14}$$

$$\overrightarrow{\mathrm{PPM}}_1^{\mathrm{CASE0}} = \overrightarrow{\mathrm{PPM}}_{\underset{\mathrm{IN}}{\mathrm{WRF}}} = \overrightarrow{\mathrm{PPM}}_{\mathrm{eff}}. \tag{15}$$

If the RO2 is not present but brackish water is pumped, i.e. in CASE 1 where the brackish water is directly injected into the WRSS, the needed quantities at point 1 are

$$W_1^{CASE1} = W_{\underset{IN}{WRF}} = W_{eff} + W_{Br} \tag{16}$$

$$\overrightarrow{PPM}_1^{CASE1} = \overrightarrow{PPM}_{\underset{IN}{WRF}} = \frac{\overrightarrow{PPM}_{eff} W_{eff} + \overrightarrow{PPM}_{Br} W_{Br}}{W_{eff} + W_{Br}}. \tag{17}$$

Finally, there is the case where the RO2 is present (and brackish water is pumped), i.e. CASE 2. In this case the brackish water is first treated in the RO2 and the waste stream is then injected into the WRSS while the permeate clean water can be sold for profit. Therefore, to compute the water characteristics at point 1, we first need to find the water characteristics at the outlet of RO2 (permeate and waste stream). For that we use the RO transfer function ($f_{\text{transfer RO}}$) defined in Section 3.1.1. The capacity of RO2 is the maximum brackish water mass flow it sees during the year, i.e.

$$C_{RO2} = \max_i(W_{Br,i}). \tag{18}$$

Knowing C_{RO2}, the permeate conditions (which are the water characteristics at point 4 in Figure 16) can be obtained as

$$W_4 = W_{\underset{OUT}{RO2}} = f_{transfer\ RO}(W_{Br}, \overrightarrow{PPM}_{Br}, C_{RO2}) \tag{19}$$

$$\overrightarrow{PPM_4} = \overrightarrow{PPM}_{\substack{RO2\\OUT}} = f_{transfer\ RO}(W_{Br}, \overrightarrow{PPM_{Br}}, C_{RO2}). \quad (20)$$

Furthermore, the waste water characteristics for RO2 are found with

$$W_{\substack{RO2\\Waste}} = f_{transfer\ RO}(W_{Br}, \overrightarrow{PPM_{Br}}, C_{RO2}) \quad (21)$$

$$\overrightarrow{PPM}_{\substack{RO2\\Waste}} = f_{transfer\ RO}\left(W_{Br}, \overrightarrow{PPM_{Br}}, C_{RO2}\right). \quad (22)$$

Finally, knowing the RO2 waste water characteristics, the water conditions at point 1 for CASE 2 can be found as follows:

$$W_1^{CASE2} = W_{\substack{WRF\\IN}} = W_{eff} + W_{\substack{RO2\\Waste}} \quad (23)$$

$$\overrightarrow{PPM_1^{CASE2}} = \overrightarrow{PPM}_{\substack{WRF\\IN}} = \frac{\overrightarrow{PPM_{eff}} W_{eff} + \overrightarrow{PPM}_{\substack{RO2\\Waste}} W_{\substack{RO2\\Waste}}}{W_{eff} + W_{\substack{RO2\\Waste}}}. \quad (24)$$

Point 2

Next, the water characteristics at point 2, i.e. at the WRF outlet, need to be found. For that the WRF transfer function is used ($f_{transfer\ WRF}$):

$$W_2 = W_{\substack{WRF\\OUT}} = f_{transfer\ WRF}\left(W_{\substack{WRF\\IN}}, \overrightarrow{PPM}_{\substack{WRF\\IN}}\right) \quad (25)$$

$$\overrightarrow{PPM_2} = \overrightarrow{PPM}_{\substack{WRF\\OUT}} = f_{transfer\ WRF}\left(W_{\substack{WRF\\IN}}, \overrightarrow{PPM}_{\substack{WRF\\IN}}\right) \quad (26)$$

For the WRF transfer function, it is assumed that all chemical concentrations can be reduced to a fixed value, except sodium and chloride, which are just passed through, i.e. not changed in the WRF. The values to which the other chemical concentrations are reduced are the average WRF outlet concentrations for the year 2017 [22]. All the WRF inlet water is treated, i.e. the WRF has no waste stream. The implemented equations for $f_{transfer\ WRF}$ are as follows:

$$W_{\substack{WRF\\OUT}} = W_{\substack{WRF\\IN}} \quad (27)$$

$$PPM_{cal\,\substack{WRF\\OUT}} = 90.6 \quad (28)$$

$$PPM_{mag\,\substack{WRF\\OUT}} = 32.1 \quad (29)$$

$$PPM_{sod\,\substack{WRF\\OUT}} = PPM_{sod\,\substack{WRF\\IN}} \quad (30)$$

$$PPM_{alk\,\substack{WRF\\OUT}} = 32.3 \quad (31)$$

$$PPM_{cl^-\,\substack{WRF\\OUT}} = PPM_{cl^-\,\substack{WRF\\IN}} \quad (32)$$

$$PPM_{sul\,\substack{WRF\\OUT}} = 223.0 \quad (33)$$

Point 3

Finally, the water characteristics at the PVGS cooling towers must to be known (point 3 in Figure 16, W_{PV} and $\overrightarrow{PPM_{PV}}$). Two cases exist: First, CASE 0 where the RO1 is not present and second CASE 1 & CASE 2 where RO1 is built.

In the case where the RO1 is not present, the PVGS cooling tower water characteristics are the same as at the WRF outlet, i.e.

$$W_3^{CASE0} = W_{PV} = W_{\underset{OUT}{WRF}} \tag{34}$$

$$\overrightarrow{PPM}_3^{CASE0} = \overrightarrow{PPM}_{PV} = \overrightarrow{PPM}_{\underset{OUT}{WRF}} \tag{35}$$

In the case where the RO1 is present, to compute the water characteristics at point 3 we first need to find the water characteristics at the outlet of RO1 (permeate and waste stream). For that we use the RO transfer function ($f_{\text{transfer RO}}$) defined in Section 3.1.1. First, the capacity of RO1 (C_{RO1}) is found so that the RO1 permeate together with the water mixed back from the WRF outlet can satisfy the PVGS cooling tower needs at all times. Intuitively, this condition should happen for $\max_i(W_{PV,i})$, but the RO efficiency is non-linear and a larger RO could be needed for less W_{PV}. Therefore, the capacity of RO1 is solved for iteratively.

Knowing C_{RO1}, the permeate conditions can be obtained as

$$W_{\underset{OUT}{RO1}} = f_{transfer\ RO}(\alpha W_{\underset{OUT}{WRF}}, \overrightarrow{PPM}_{\underset{OUT}{WRF}}, C_{RO1}) \tag{36}$$

$$\overrightarrow{PPM}_{\underset{OUT}{RO1}} = f_{transfer\ RO}(\alpha W_{\underset{OUT}{WRF}}, \overrightarrow{PPM}_{\underset{OUT}{WRF}}, C_{RO1}). \tag{37}$$

Similarly, the waste water characteristics for RO1 are found with

$$W_{\underset{Waste}{RO1}} = f_{transfer\ RO}(\alpha W_{\underset{OUT}{WRF}}, \overrightarrow{PPM}_{\underset{OUT}{WRF}}, C_{RO1}) \tag{38}$$

$$\overrightarrow{PPM}_{\underset{Waste}{RO1}} = f_{transfer\ RO}\left(\alpha W_{\underset{OUT}{WRF}}, \overrightarrow{PPM}_{\underset{OUT}{WRF}}, C_{RO1}\right). \tag{39}$$

Finally, knowing the RO1 water characteristics, the water conditions at point 3 for CASE 1 and CASE 2 can be found as follows:

$$W_3^{CASE1,2} = W_{PV} = (1-\alpha)W_{\underset{OUT}{WRF}} + W_{\underset{OUT}{RO1}} \tag{40}$$

$$\overrightarrow{\mathrm{PPM}}_3^{\mathrm{CASE1,2}} = \overrightarrow{\mathrm{PPM}}_{\mathrm{PV}} = \frac{\overrightarrow{\mathrm{PPM}}_{\underset{\mathrm{OUT}}{\mathrm{WRF}}}(1-\alpha)\mathrm{W}_{\underset{\mathrm{OUT}}{\mathrm{WRF}}} + \overrightarrow{\mathrm{PPM}}_{\underset{\mathrm{OUT}}{\mathrm{RO1}}}\mathrm{W}_{\underset{\mathrm{OUT}}{\mathrm{RO1}}}}{(1-\alpha)\mathrm{W}_{\underset{\mathrm{OUT}}{\mathrm{WRF}}} + \mathrm{W}_{\underset{\mathrm{OUT}}{\mathrm{RO1}}}}. \tag{41}$$

Evaporation ponds

The amount of water going to the evaporation points is computed as follows

$$W_{EP} = W_{\underset{Waste}{RO1}} + W_{blowdown} \tag{42}$$

where

$$W_{blowdown} = W_{PV} \cdot BlowD. \tag{43}$$

3.2.5 Economics ("NPV PreP" and "NPV")

This section details the NPV PreP and NPV modules in Figure 16. These modules compute all the cash flows considered in the economics analysis of the different cases studied. The cash flow analysis is calculated using a differential approach, which means:

$$\Delta NPV_{Case} = NPV_{Case} - NPV_{Ref} \tag{44}$$

If $\Delta NPV_{Case} > 0$ it indicates that the case under current consideration is better than the reference situation (in our case the status quo CASE 0). Differential analysis assumes that the following values are not changing between the different cases:

- F_{WRF}
- $CAPEX_{WRF}$
- NPP_{Variable}
- NPP_{fixed}

CASE 0 (Status Quo)

To evaluate CASE 0 we try to isolate the cash flow, or, better, the part that could be affected by the water supply strategy, which is seen by APS as the owner of 29.1% ($PowAPS\%$) of PVGS. Considering the 29.1% ownership of the PVGS by APS, we should consider 29.1% of the cooling water related expenses ($NPV^0_{\substack{Water\\APS}}$) and the whole amount of electricity sold of the APS quota ($NPV^0_{\substack{El\\APS}}$).

We assume that

$$NPV^0_{APS} = PowAPS\% \cdot NPV^0_{\substack{Water\\PV}} + NPV^0_{\substack{El\\APS}} \tag{45}$$

$$NPV^0_{\substack{Water\\PV}} = \sum_{j=1}^{J} \frac{(1-Tax)}{(1+WACC_{PV})^j}\left\{-CW_j^0 - CV_j^0 - CE_j^0\right\} \tag{46}$$

where:

- CW_j^0 Total annual costs from water acquisition.
- CV_j^0 Total annual water costs from variable sources (excluded electricity and water).
- CE_j^0 Total annual water costs from electricity consumption.

The total annual cost from water acquisition (CW_j^0) is computed as follows:

$$CW_j^0 = \sum_{i=1}^{12}\left(P_{eff,j}(W_{eff,i})\right) + Penalty_j\left(W^0_{eff,j}\right) \tag{47}$$

where:

- $P_{eff,j}(W_{eff,i})$ Monthly effluent water price as a function of the amount of effluent water bought by month [23]. This function includes multiple tiers, i.e. the first x acre-feet have a certain price [$/acre-foot], then the next y acre-feet have a different price, etc. In addition, the price differs from year to year.
- $Penalty_j\left(W^0_{eff,j}\right)$ Yearly penalty for non-usage [23]. If at the end of the year, there is less water bought than contracted, a penalty for that "non-used" amount has to be played. The penalty is 20% of the average cost over the different tiers for that year. It is assumed that the contracted amount of water is 80000 acre-feet/year minus the planned amount of brackish water bought, i.e.

$$Penalty_j = \left[\left(80000 - \sum_{i=1}^{12}\left(W_{Br,i}\right)\right) - \sum_{i=1}^{12}\left(W_{eff,i}\right)\right] \cdot 0.2 \cdot avg(P_{eff,tiers,j}) \tag{48}$$

The annual variable and fixed costs that come from water treatment (CV_j^0) for CASE 0 are only incurred by the WRF, i.e.

$$CV_j^0 = \sum_{i=1}^{12}\left(V_{WRF}(W_{eff,i}, \overrightarrow{PPM}_{eff,i})\right) \tag{49}$$

The variable cost function for the WRF is as follows [24]:

$$V_{WRF}(W, \overrightarrow{PPM}) = C_{CaO} \cdot D_{CaO} \cdot W + C_{Na2CO3} \cdot D_{Na2CO3} \cdot W + 6.719 \cdot 10^{-5} \cdot W + 1.366 \cdot 10^6 + 5.851 \cdot 10^{-5} \cdot W \tag{50}$$

where

$$D_{CaO} = 0.00075 \left[\frac{PPM_{mag}}{[PPM_{mag}]_o} + \frac{[PPM_{cal}]}{[PPM_{cal}]_o} \right] \quad (51)$$

$$D_{Na2CO3} = 0.0070 \frac{D_{CaO}}{(D_{CaO})_o} \quad (52)$$

and

- C_{CaO} Cost of lime [\$/lb]. (0.1 \$/lb)
- C_{Na2CO3} Cost of soda ash [\$/lb]. (0.17 \$/lb)
- D_{CaO} Dosage of lime [lb/gal].
- $(D_{CaO})_o$ Average lime dosage [lb/gal] (0.0015 lb/gal).
- D_{Na2CO3} Dosage of soda ash [lb/gal].
- PPM_{mag} Magnesium concentration [ppm].
- $[PPM_{mag}]_o$ Average magnesium concentration [ppm] (142.1 ppm).
- PPM_{cal} Calcium concentration [ppm].
- $[PPM_{cal}]_o$ Average Calcium concentration [ppm] (187.5 ppm).
- $1.366 \cdot 10^6$ Fixed cost for one month [\$].

The cost function V_{WRF} assumes the following:

- Principal chemical costs are for lime (CaO) and Soda Ash (Na_2CO_3) addition – relatively smaller chemical cost components (CO_2, Acid, Hypochlorite, and Polyfloc) are assumed independent of hardness and are lumped together as a residual cost that is a function of volume treated.
- Ca and Mg are the principal constituents for treatment. SiO_2 and PO_4 do not drive the lime and ash dosage.
- Chemical usage is baselined to average dosage over the year 2017.
- Chemical unit costs (\$/lb_m) are based on average 2017 values.
- Manpower, contract services and labor, and maintenance materials are assumed a fixed cost and are based on 2017 actuals for WRF.

The annual electricity costs that come from water treatment (CE_j^0) for CASE 0 are only incurred by the WRF. Note that the WRF is considered PVGS house-load and therefore the wholesale price of electricity ($P_{E,W}$) is considered, i.e.

$$CE_j^0 = \sum_{i=1}^{12} \left(E_{WRF}(W_{eff,i}) \cdot P_{E,W} \right) \quad (53)$$

The electricity consumption function for the WRF is as follows [24]:

$$E_{WRF}(W) = 714 + 1.8 \cdot 10^{-6} \cdot W \quad (54)$$

The electricity consumption function E_{WRF} assumes the following:

- Power costs are based on off-site demands (Hassayampa Pump Station (HPS) and cathodic protection) and WRF on-site demands (house loads).
- The on-site WRF power load is estimated to be 2.5 times the HPS loads at normal operating conditions with a baseload demand of 20% (lighting, etc.).

We can now consider the cash flow to APS from selling electricity produced by PVGS, which is:

$$NPV^{0}_{\substack{El\\APS}} = \sum_{j=1}^{J} \frac{(1-Tax)}{(1+WACC_{PV})^{j}} ES^{0}_{\substack{APS\,PV\\j}} \tag{55}$$

where $ES_{\substack{APS\,PV\\j}}$ is the yearly total revenue of electricity sold by APS of their PVGS share.

Given the level of the net demand there are 3 different possible situations. The time discretization for the net demand is hourly. First, the APS power available is computed by

$$PowAPS_{cor} = PowAPS - PowAPS\%\,(HouseLoad + E_{WRF}) \tag{56}$$

The three situations are then (evaluated for each hour):

- $ED_{Net} \geq PowAPS_{cor} \Longrightarrow ES^{0}_{APS\,PV,ll} = PowAPS_{corr} \cdot P_{E,R}$
- $0 \leq ED_{Net} < PowAPS_{cor} \Longrightarrow ES^{0}_{APS\,PV,ll} = ED_{Net} \cdot P_{E,R} + (PowAPS_{cor} - ED_{Net}) P_{E,Hub}$
- $ED_{Net} \leq 0 \Longrightarrow ES^{0}_{APS\,PV,ll} = PowAPS_{cor} \cdot P_{E,Hub}$

Once the electricity sold for each hour has been evaluated, these values can be summed to find the yearly electricity revenue.

$$ES^{0}_{\substack{APS\,PV\\j}} = \sum_{ll}^{8760} ES^{0}_{APS\,PV,ll} \tag{57}$$

CASE 1 (brackish water acquisition and RO1)

As for CASE 0, we start from the NPV decomposition to APS from water and electricity sold.

$$NPV^{1}_{APS} = PowAPS\% \cdot NPV^{1}_{\substack{Water\\APS}} + NPV^{1}_{\substack{El\\APS}} \tag{58}$$

First, we evaluate the portion coming from the water:

$$NPV^{1}_{\substack{Water\\APS}} = \sum_{j=1}^{J} \left\{ \frac{(1-Tax)\left(-CV^{1}_{j,WRF} - CE^{1}_{j,WRF}\right)}{(1+WACC_{PV})^{j}} \right\} + \sum_{j=1}^{J} \left\{ \frac{(1-Tax)\left(-CV^{1}_{j,RO1} - CE^{1}_{j,RO1} - CF^{1}_{j,RO1}\right)}{(1+WACC_{PV})^{j}} \right\} +$$
$$\sum_{j=1}^{J} \left\{ \frac{(1-Tax)\left(-CV^{1}_{j,Pump} - CE^{1}_{j,Pump} - CF^{1}_{j,Pump}\right)}{(1+WACC_{PV})^{j}} \right\} + \sum_{j=1}^{J} \left\{ \frac{Tax\left(D_j CAPEX^{1}_{RO1} C^{1}_{RO1} + D_j CAPEX_{Pump} C_{Pump}\right)}{(1+WACC_{PV})^{j}} \right\} -$$
$$CAPEX^{1}_{RO1} C^{1}_{RO1} - CAPEX_{Pump} C_{Pump} + \sum_{j=1}^{J} \left\{ \frac{(1-Tax)\left(-CW^{1}_{j,Br} - CW^{1}_{j,eff}\right)}{(1+WACC_{PV})^{j}} \right\} \tag{59}$$

where,

For the WRF:

- $CV^{1}_{j,WRF}$ WRF annual costs from variable sources (excluded electricity and water). This quantity is computed the same way as for CASE 0 (see Eq. 49).
- $CE^{1}_{j,WRF}$ WRF annual costs from electricity consumption. This quantity is computed the same way as for CASE 0 (see Eq. 53).

For the RO1 [25]:

- $CV^{1}_{j,RO1}$ RO1 annual costs from variable sources (excluded electricity and water).
- $CF^{1}_{j,RO1}$ RO1 annual costs from fixed sources. $CV^{1}_{j,RO1} + CF^{1}_{j,RO1}$ is assumed to be 1% of the capex.

- $CE^1_{j,RO1}$ RO1 annual costs from electricity consumption. The amount of electricity used by the RO1 ($E^1_{j,WRF}$) is provided by the RO1 model (see Section 3.1.1). The cost is then computed by $CE^1_{j,WRF} = E^1_{j,WRF} \cdot P_{E,R}$. Note that RO1 is not considered PVGS house load and consequently the retail price of electricity is applied ($P_{E,R}$).

For the brackish water pump [26]:

- $CV^1_{j,Pump}$ Brackish water pump annual costs from variable sources (excluded electricity).
- $CF^1_{j,Pump}$ Brackish water pump annual costs from fixed sources. $CV^1_{j,Pump} + CF^1_{j,Pump}$ is assumed to be 2000 $/month independent of the pump size.
- $CE^1_{j,Pump}$ Brackish water pump annual costs from electricity consumption. The amount of electricity used by the brackish water pump ($E^1_{j,Pump}$) is proportional to the reference that pumping 400 acre-foot need 136500 kWh of power. The cost is then computed by $CE^1_{j,Pump} = E^1_{j,Pump} \cdot P_{E,R}$. Note that the pump is not considered PVGS house load and consequently the retail price of electricity is applied ($P_{E,R}$).

Water acquisition cost:

- $CW^1_{j,eff}$ Total annual costs from effluent water acquisition. This quantity is computed the same way as for CASE 0 (see Eq. 47).
- $CW^1_{j,Br}$ Total annual costs from brackish water acquisition. This is $CW^1_{j,Br} = \sum_i^{12} W_{Br,i} \cdot P_{Br}$.

For the component of the NPV that arises from APS electricity sales two factors need to be accounted for:

- The electricity to APS disposal is decreased/increased by $PowAPS\%$ times the variation of electricity consumption at the WRF.
- The baseload is increased by the amount of electricity used by RO1.

$$\mathrm{NPV}^1_{\substack{\mathrm{El}\\ \mathrm{APS}}} = \sum_{\mathrm{j}=1}^{\mathrm{J}} \frac{(1-\mathrm{Tax})}{(1+\mathrm{WACC_{PV}})^{\mathrm{j}}} \mathrm{ES}^1_{\substack{\mathrm{APS\ PV}\\ \mathrm{j}}} \tag{60}$$

The electricity revenue is computed in the same way as for CASE 0. First, the power available to APS is decreased by $PowAPS\%$ of the electricity used in the WRF and the house load. Second, the net demand is raised by the additional electricity use associated with the RO plant and the brackish water pump (since not considered PVGS house load). The equations analogue to CASE 0 are:

$$PowAPS^1_{cor} = PowAPS - PowAPS\% \ (HouseLoad + E^1_{WRF}) \tag{61}$$

$$ED^1_{Net,cor} = ED_{Net} + E^1_{RO1} + E^1_{Pump} \tag{62}$$

The three situations are then evaluated for each hour:

- $ED_{Net,cor} \geq PowAPS_{cor} \Longrightarrow ES^1_{APS\ PV,ll} = PowAPS^1_{cor} \cdot P_{E,R}$
- $0 \leq ED_{Net,cor} < PowAPS_{cor} \Longrightarrow ES^1_{APS\ PV,ll} = ED_{Net,cor} \cdot P_{E,R} + (PowAPS^1_{cor} - ED_{Net,cor})P_{E,Hub}$
- $ED_{Net,cor} \leq 0 \Longrightarrow ES^1_{APS\ PV,ll} = PowAPS^1_{cor} \cdot P_{E,Hub}$

Once the electricity sold for each hour is evaluated, it can be summed to find the yearly electricity revenue:

$$ES^1_{\substack{APS\ PV\\ j}} = \sum_{ll}^{8760} ES^1_{APS\ PV,ll} \tag{63}$$

CASE 2 (RO2 for potable water from brackish and RO1 for clean PVGS cooling water)

For CASE 2, we assume that the potable water plant is owned solely by APS. This situation introduces two new cash flows, one is the revenue generated from RO2 directly to APS and the second arises from an increase in the operational costs at PVGS WRF and RO1 that needs to be compensated by APS.

Rather than calculating the NPV, which requires knowledge of the price at which the potable water is sold, this case computes an LCOW, i.e. the water price that will compensate the difference in cost APS is seeing compared to CASE 0, in which no ROs are built:

$$0 = NPV^{2}_{\substack{El\\APS}} - NPV^{0}_{\substack{El\\APS}} + NPV^{2}_{\substack{Water\\APS}} - NPV^{0}_{\substack{Water\\APS}} + \sum_{j=1}^{J} \frac{(1-Tax)}{(1+WACC_{PV})^{j}} \left\{ W_{\substack{RO2\\OUT,j}} \cdot LCOW \right\} \quad (64)$$

First, we evaluate the portion coming from the water (except the revenue from potable water sales):

$$NPV^{2}_{\substack{Water\\APS}} = \sum_{j=1}^{J} \left\{ \frac{(1-Tax)\left(-CV^{2}_{j,WRF} - CE^{2}_{j,WRF}\right)}{(1+WACC_{PV})^{j}} \right\} + \sum_{j=1}^{J} \left\{ \frac{(1-Tax)\left(-CV^{2}_{j,RO1} - CE^{2}_{j,RO1} - CF^{2}_{j,RO1}\right)}{(1+WACC_{PV})^{j}} \right\} +$$
$$\sum_{j=1}^{J} \left\{ \frac{(1-Tax)\left(-CV^{2}_{j,RO2} - CE^{2}_{j,RO2} - CF^{2}_{j,RO2}\right)}{(1+WACC_{PV})^{j}} \right\} + \sum_{j=1}^{J} \left\{ \frac{(1-Tax)\left(-CV^{2}_{j,Pump} - CE^{2}_{j,Pump} - CF^{2}_{j,Pump}\right)}{(1+WACC_{PV})^{j}} \right\} +$$
$$\sum_{j=1}^{J} \left\{ \frac{Tax\left(D_j CAPEX^{2}_{RO1} C^{2}_{RO1} + D_j CAPEX^{2}_{RO2} C^{2}_{RO2} + D_j CAPEX_{Pump} C_{Pump}\right)}{(1+WACC_{PV})^{j}} \right\} - CAPEX^{2}_{RO1} C^{2}_{RO1} - CAPEX^{2}_{RO2} C^{2}_{RO2} -$$
$$CAPEX_{Pump} C_{Pump} + \sum_{j=1}^{J} \left\{ \frac{(1-Tax)\left(-CW^{2}_{j,Br} - CW^{2}_{j,eff}\right)}{(1+WACC_{PV})^{j}} \right\} \quad (65)$$

where,

For the WRF:

- $CV^{2}_{j,WRF}$ WRF annual costs from variable sources (excluded electricity and water). This quantity is computed the same way as for CASE 0 (see Eq. 49).
- $CE^{2}_{j,WRF}$ WRF annual costs from electricity consumption. This quantity is computed the same way as for CASE 0 (see Eq. 53).

For the RO1:

- $CV^{2}_{j,RO1}$ RO1 annual costs from variable sources (excluded electricity and water).
- $CF^{2}_{j,RO1}$ RO1 annual costs from fixed sources. $CV^{2}_{j,RO1} + CF^{2}_{j,RO1}$ is assumed to be 1% of the capex.
- $CE^{2}_{j,RO1}$ RO1 annual costs from electricity consumption. The amount of electricity used by the RO1 ($E^{2}_{j,WRF}$) is provided by the RO1 model (see Section 3.1.1). The cost is then computed by $CE^{2}_{j,WRF} = E^{2}_{j,WRF} \cdot P_{E,R}$. Note that RO1 is not considered PVGS house load and consequently the retail price of electricity is applied ($P_{E,R}$).

For the RO2:

- $CV^{2}_{j,RO2}$ RO2 annual costs from variable sources (excluded electricity and water).
- $CF^{2}_{j,RO2}$ RO2 annual costs from fixed sources. $CV^{2}_{j,RO2} + CF^{2}_{j,RO2}$ is assumed to be 1% of the capex.
- $CE^{2}_{j,RO2}$ RO2 annual costs from electricity consumption. The amount of electricity used by the RO2 ($E^{2}_{j,WRF}$) is provided by the RO2 model (see Section 3.1.1). The cost is then computed by $CE^{2}_{j,WRF} = E^{2}_{j,WRF} \cdot P_{E,R}$. Note that RO2 is not considered PVGS house load and consequently the retail price of electricity is applied ($P_{E,R}$).

For the brackish water pump:

- $CV^2_{j,Pump}$ Brackish water pump annual costs from variable sources (excluded electricity).
- $CF^2_{j,Pump}$ Brackish water pump annual costs from fixed sources. $CV^2_{j,Pump} + CF^2_{j,Pump}$ is assumed to be 2000 $/month independent of the pump size.
- $CE^2_{j,Pump}$ Brackish water pump annual costs from electricity consumption. The amount of electricity used by the brackish water pump ($E^2_{j,Pump}$) is proportional to the reference that pumping 400 acre-foot need 136500 kWh of power. The cost is then computed by $CE^2_{j,Pump} = E^2_{j,Pump} \cdot P_{E,R}$. Note that the pump is not considered PVGS house load and consequently the retail price of electricity is applied ($P_{E,R}$).

Water acquisition cost:

- $CW^2_{j,eff}$ Total annual costs from effluent water acquisition. This quantity is computed the same way as for CASE 0 (see Eq. 47).
- $CW^2_{j,Br}$ Total annual costs from brackish water acquisition. This is $CW^2_{j,Br} = \sum_i^{12} W_{Br,i} \cdot P_{Br}$.

For the component of the NPV that arises from APS electricity two factors need to be accounted for:

- The electricity that APS is able sell from its PVGS's share is decreased/increased by $PowAPS\%$ times the variation of electricity consumption at the WRF.
- The baseload is increased by the amount of electricity used by RO1.

$$NPV^2_{\substack{El \\ APS}} = \sum_{j=1}^{J} \frac{(1-Tax)}{(1+WACC_{PV})^j} ES^2_{\substack{APS\,PV \\ j}} \tag{66}$$

The electric revenue is computed in the same way as for CASE 0. First, the power available to APS is decreased by $PowAPS\%$ of the electricity used in the WRF and the house load. Second, the net demand is increased by the additional electricity usage of the RO plants and the brackish water pump (not considered PVGS house load). The equations analogous to CASE 0 are:

$$PowAPS^2_{cor} = PowAPS - PowAPS\% \, (HouseLoad + E^2_{WRF}) \tag{67}$$

$$ED^2_{Net,cor} = ED_{Net} + E^2_{RO1} + E^2_{RO2} + E^1_{Pump} \tag{68}$$

The three situations are then evaluated for each hour:

- $ED_{Net,cor} \geq PowAPS_{cor} \Longrightarrow ES^2_{APS\,PV,ll} = PowAPS^2_{cor} \cdot P_{E,R}$
- $0 \leq ED_{Net,cor} < PowAPS_{cor} \Longrightarrow ES^2_{APS\,PV,ll} = ED_{Net,cor} \cdot P_{E,R} + (PowAPS^2_{cor} - ED_{Net,cor}) P_{E,Hub}$
- $ED_{Net,cor} \leq 0 \Longrightarrow ES^2_{APS\,PV,ll} = PowAPS^2_{cor} \cdot P_{E,Hub}$

Once the electricity sold for each hour has been evaluated, it can be summed to find the yearly electricity revenue.

$$ES^2_{\substack{APS\,PV \\ j}} = \sum_{ll}^{8760} ES^2_{APS\,PV,ll} \tag{69}$$

4. SIMULATIONS

This chapter presents the results of the economic analysis for the APS cases introduced in the previous chapters. First, the input data and assumptions are discussed. After that, in the second section of this chapter, the results of the analysis including the sensitivity studies performed for selected inputs are presented and discussed.

4.1 Input data and assumptions

As mentioned, this section presents the model inputs. The assumptions made in the physical modeling (water flows and chemical compositions) as well as in the cash flows have already been discussed in Section 3.2. This section first discusses the model inputs that are assumed not to have a stochastic nature. After that, in a second section, the inputs that are assumed to have a stochastic nature are presented.

4.1.1 Non-stochastic input data

This first section presents the inputs that are assumed to be non-stochastic, i.e. 'fixed values'. These values include the inputs presented in Table 6 as well as the economic parameters such as tax, inflation rate, etc. Inputs that have a corresponding sensitivity study performed are indicated with the 'reference value' colored in red [22-32].

NumberOfYears	J	[years]	**27, 47**
PowAPS	$PowAPS$	[MW]	**1130**
PowAPSPercent	$PowAPS\%$	[%]	**29.1**
EL_wholesale_price	$P_{E,W}$	[$/MWh]	**30.0, 35.0, 40.0**
EL_RetWholeDiff	$P_{E,diff}$ This is the difference between wholesale and retail price, i.e. $P_{E,R} = P_{E,W} + P_{E,diff}$	[$/MWh]	**10.0**
HouseLoad	HouseLoad	[MW]	**66.0**
Blowdown	$BlowD$	[%]	**5.0**
PBrackish	P_{Br}	[$/acre-foot]	**25.0**
PEffluent	P_{eff} structure is a multi-tier structure where water becomes more expensive as more water is purchased. In addition, the water becomes more expensive from year to year.	[$/acre-foot]	The effluent water price
W_brackish	W_{Br} No variation during the year has been considered, i.e. the same amount of brackish water is purchased every month.	[kg/month]	**493392742.0 (400 AF/month), 1480178226.0 (1200 AF/month), 2960356452.0 (2400 AF/month), 4933900000.0 (4000 AF/month)**
Chem_cal_brackish	$PPM_{Br,cal}$	[ppm]	**180.0**
Chem_mag_brackish	$PPM_{Br,mag}$	[ppm]	**80.0**
Chem_sod_brackish	$PPM_{Br,sod}$	[ppm]	**780.0**
Chem_alk_brackish	$PPM_{Br,alk}$	[ppm as $CaCO_3$]	**244.0**

Chem_clo_brackish	$PPM_{Br,clo}$	[ppm]	**799.0**
Chem_sul_brackish	$PPM_{Br,sul}$	[ppm as SO_4]	**1180.0**
limit_clo_ppm	$PPM_{PV,max}$	[ppm]	**450.0**, **500.0**
Cooling[3]	W_{PV} **6201290803.93, 8168938593.87, 8653282665.24, 7018621424.36,**	[kg/month] **7060244743.00, 8460301824.30, 7994877443.22, 6859696025.94**	**6712122441.70, 5004499622.53, 8728961426.39, 5072610507.56,**
Chem_cal_eff[3]	$PPM_{eff,cal}$	[ppm as $CaCO_3$]	**194.0, 222.0, 175.3, 193.3, 181.2, 165.5, 187.0, 157.8, 198.8, 190.7, 188.5, 196.8**
Chem_mag_eff[3]	$PPM_{eff,mag}$	[ppm as $CaCO_3$]	**140.0, 154.0, 139.5, 135.7, 132.4, 139.3, 150.8, 141.8, 143.0, 139.3, 146.0, 142.8**
Chem_sod_eff[3]	$PPM_{eff,sod}$	[ppm]	**264.0, 250.0, 215.0, 250.0, 297.0, 293.5, 383.7, 258.0, 284.5, 229.3, 182.3, 244.5**
Chem_alk_eff[3]	$PPM_{eff,alk}$	[ppm as $CaCO_3$]	**163.0, 175.0, 169.3, 160.0, 154.4, 164.0, 161.0, 151.4, 153.5, 159.7, 169.5, 166.5**
Chem_clo_eff[3]	$PPM_{eff,clo}$	[ppm]	**301.0, 345.0, 292.5, 292.5, 359.0, 445.5, 477.0, 448.8, 471.0, 353.7, 168.0, 286.0**
Chem_sul_eff[3]	$PPM_{eff,sul}$	[ppm]	**215.0, 248.0, 186.5, 186.5, 167.0, 191.5, 185.8, 195.0, 177.8, 164.0, 159.0, 183.5**
Forecast	*N/A*	[option select]	See Section 3.2.3.Two different rPV and demand growth models have been considered. One where the **demand scales exponentially with 3.3% while the rPV grows linearly adding 200 MW/year**. The second model considerers that both, the demand and rPV grow exponentially 3.3% per year.
DiscoutRate	$WACC_{PV} = WACC_{APS}$	[%]	**5, 10, 15**
Inflation	Inf	[%]	**3**
Tax	Tax	[%]	**21.0**
Depreciation	D_j	[%]	A 15 years MACRS accelerated depreciation table is used for the RO plants while a 7 year MACRS is used for the brackish water pump.
CAPEX RO	$CAPEX_{ROx}$	[$/(kg/s)]	**64800.0**
Economy RO	X	[-]	**1.0** This is the economy of scale factor (See Eq. 12) for the ROs. A factor of 1.0 means there is no economy and no dis-economy of scale, i.e. an RO with double the capacity will cost double.
CAPEX Pump	$CAPEX_{Pump}$	[$/(kg/s)]	**2105.3**

[3] Note that these values are not a sensitivity study, but reflect the change during the year.

Economy Pump	X	[-]	**1.0**

This is the economy of scale factor (See Eq. 12) for the brackish water pump. A factor of 1.0 means there is no economy and no dis-economy of scale, i.e. a pump with double the capacity will cost double.

4.1.2 Stochastic input data

In addition to the non-stochastic inputs, the APS problem also has some inputs that are stochastic, namely the hourly rPV production, the raw APS demand and the PV Hub price. Traditionally, to analyze such a system, one would use historical data only. To remove this limitation, the capability of the N-R HES framework to generate stochastic time series (FVARMA) can be used. The model is used to create from limited databases of time histories an unlimited number of representative time histories that are never exactly the same as, but are statistically similar to, the time histories in the databases. The unlimited source of time histories can then be used to perform statistical analysis of the economic performance of the model. The advantage of using such systemic histories is that with historic data only the system can only be analyzed for that exact data, while averaging over multiple synthetic histories will lead to an analysis for the average of future possible behaviors. It should be noted that the FVARMA reproduces the stochasticity of the data to be applied to future data, but does not include any growth/inflation projections, i.e. the FVARMA produces an unlimited amount of "today's" data.

The detailed functioning of the FVARMA is explained in [19, 20] and Section 3.1.3, but its functioning is summarized here briefly. First, the training data is de-trended with a set of Fourier frequencies that the user can choose. This is used to capture and remove seasonal, weekly and daily (day/night) trends in the data. The residual data after the de-trending is assumed to contain only the stochastic noise. This noise is normalized and the VARMA portion of the algorithm is used to model it. The user can input the autocorrelation length parameters "P" and "Q" for the VARMA model. Once the FVARMA model is trained, an unlimited number of synthetic data series can be generated.

Having multiple stochastic data, such as electricity price and demand or renewable generation, intuition tells us that there might be correlations between these data not only in the longer trends, but also in the stochastic portion of the data. The correlation of the data in the general trends is captured by the Fourier, e.g. the correlation that demand and solar production are both low at night is captured by the individual Fourier de-trending for the two data. In addition to these correlated trends, there are also correlated stochastic events, like a hot day in summer where solar production spikes and at the same time (air conditioning) demand also spikes. This type of stochastic correlation is not captured by the ARMA algorithm. To try to capture this, the recently developed correlated Vector ARMA (FVARMA, see Section 3.1.3) has been used for the data in this study.

Model inputs

Demand and rPV generation datasets from APS were used for training [28-30, 32, 33]. The demand dataset is historical data from 2016 with an hourly resolution. The rPV generation, also an hourly resolution, corresponds to 12 different days, a representative day for each month, ordered and repeated to make up one year. The datasets are representative of 2016, a leap year, and therefore have 8784 hours in total. The model developed can run on either 8784-hour or standard 8760-hour sets. Finally, hourly PV Hub price data for 2016 downloaded from [33] has been used.

FVARMA Training and Sampling

In all cases, input data is passed into RAVEN to train a FVARMA which is then saved for later sampling. Several different FVARMA analyses are presented here. The first configuration trains separate FVARMA models for the demand and the rPV generation. The second uses a single FVARMA to investigate the correlation between the rPV generation and demand. The third case is also a correlated, but

rather than training the FVARMA over the entire year, six separate correlated FVARMAs are trained (2 months each). The analysis has shown that (see later in this section) training over the entire year leads to an average variance that does not reproduce the seasons well, i.e. has a too large of a variance in the winter months and a too small of a variance for the summer months. For the subsequent APS case analysis, the correlated FVARMA is split in 2 month blocks that correlate demand and the rPV is used. In addition, the PV Hub price is also sampled by the FVARMA.

All the FVARMAs analyzed utilize a filter that disregards the rPV zero generation periods in correlation so that they do not affect the demand values. After the FVARMA models are trained, RAVEN samples each of them, creating the synthetic demand and solar generation data. The synthetic data is then passed by RAVEN to a linked external model ("ARMA PostP" in Figure 16), where it is scaled and combined to form a net demand profile.

Uncorrelated demand and rPV analysis

The FVARMA input parameters used in this case are as follows: The Fourier series are calculated for 1 year, 30 days, 1 day, and 3 hours for both FVARMAs. The correlation length for the FVARMA is set to 2 hours and the out truncation is set to positive, forcing the FVARMA to output non-negative values for demand and rPV.

The synthetic demand data output by the FVARMA model was verified to be statistically similar to the input data. Table 7 displays the average and standard deviations, as compared to the original demand data. Figure 17 shows the outputs from the FVARMA model, sampled 50 different times. Three representative days in June are plotted, showing that the FVARMA can create synthetic data with relative accuracy.

Table 7: Statistical properties of training and synthetic demand.

	Real Demand	**Synthetic Demand**	**% Difference**
Average	3490.3	3488.2	0.1%
Standard Deviation	1011.3	1001.3	1.0%

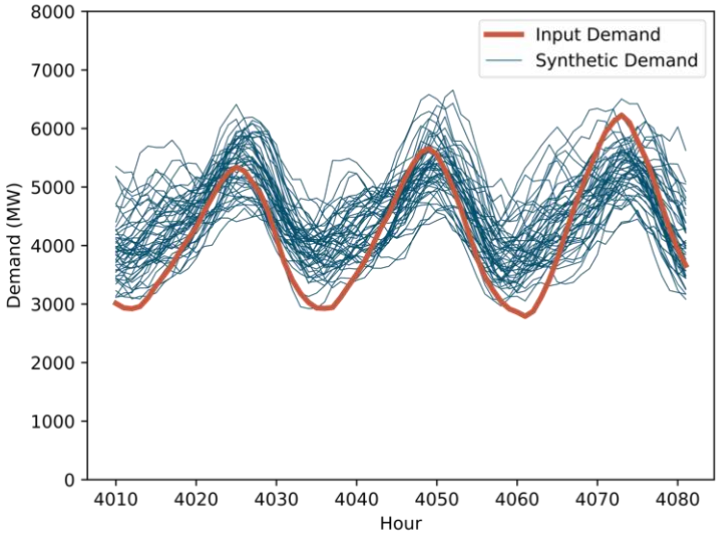

Figure 17: Synthetic demand and input demand over three representative days.

On the other hand, the synthetic rPV data is not as statistically similar to its training data because the FVARMA algorithm has difficulty with long periods of the same value, such as when the generation is zero at night (no periodicity). When the model is sampled, the output has significant solar generation in the nighttime hours. This is illustrated in Figure 18, where the input generation profile is zero but the majority of the 50 synthetic generation profiles have generation at night. To remedy this, the rPV generation profile was post-processed to ensure generation is only available in the same hours as the input generation data. The smoothing is also displayed in Figure 18. This results in the slight over estimation of rPV generation.

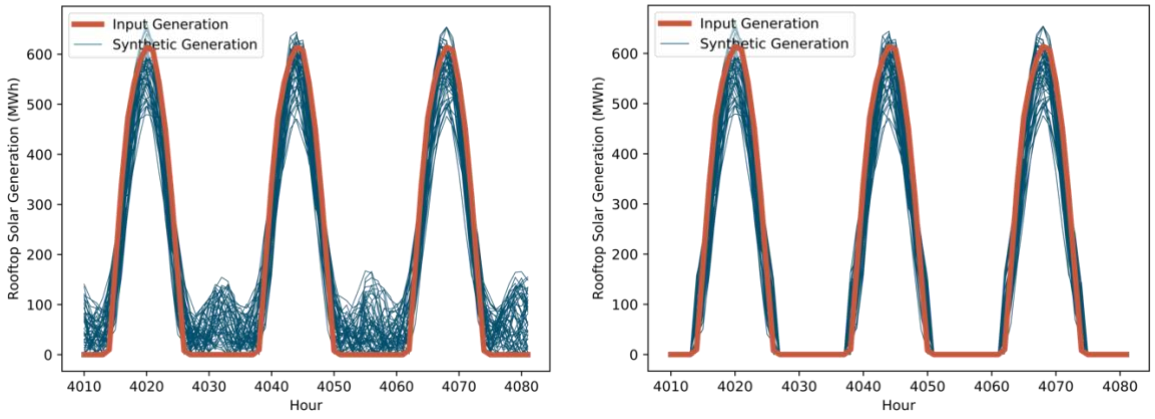

Figure 18: rPV actual generation vs. synthetic generation over three representative days. The plot on the left is direct output from the FVARMA model. The plot on the right is with postprocessing to ensure that the generation is zero at night.

A statistical comparison of the input data, synthetic data, and synthetic data with post processing is shown in Table 8. The synthetic generation average and standard deviation have 1.1% and 3.7% error, respectively.

Table 8: Statistical properties for training, synthetic, and smoothed rPV Generation.

	Real rPV Generation	**Synthetic rPV Generation**	**Synthetic rPV Generation with Smoothing**
Average	152.9	154.6	149.7
Standard Deviation	204.8	197.6	194.8

Correlated demand and rPV (with rPV Generation Adjustment) analysis

The correlated FVARMA parameters are similar, but designating the rPV production in the zeroFilter node tells the FVARMA not to correlate the datasets when production is zero. In those instances, only the demand FVARMA is trained and the rPV generation will be set to zero. The correlated with zeroFilter inputs are as follows: The Fourier series are calculated for 1 year, 3 months, 30 days, 1 day, and 3 hours for both FVARMAs. The correlation length for the FVARMA is set to 6 hours and the out truncation is set to positive, forcing the FVARMA to output non-negative values for demand and rPV.

Because the correlated FVARMA has issues with zero generation at night, a processor was developed to correlate the demand and rPV generation only at times of rPV generation. Table 9 and Table 10 show the statistical characteristics of the synthetic data from correlated FVARMA. The model was sampled 50 times; three representative days in June are plotted in Figure 19.

Table 9: Statistical properties of training data and synthetic demand for correlated FVARMA with adjustment.

	Real Demand	**Synthetic Demand**	**% Difference**
Average	3490.3	3136.4	11.3%
Standard Deviation	1011.3	831.2	21.7%

Table 10: Statistical properties for real and synthetic rPV Generation for correlated FVARMA with adjustment.

	Real rPV Generation	**Synthetic rPV Generation**	**% Difference**
Average	152.9	137.5	11.1%
Standard Deviation	204.8	182.1	16.0%

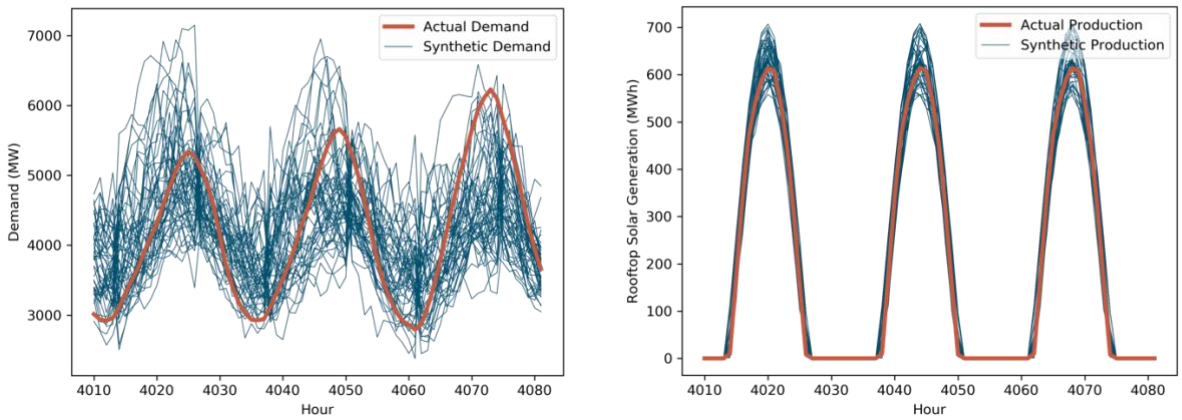

Figure 19: Output of correlated FVARMA with adjustment for demand and rPV for three representative days.

"Correlated FVARMA Split" used for APS analysis

When training the FVARMA over one year, the model would miss some of the features on shorter time horizons. For example, the variance was high in the winter months because the model had trained over the whole year, including the summer peak. To remedy this, the dataset was split into 6 equal length time series and an individual FVARMA was trained for each of these two-month sections. The synthetic data output from each FVARMA was reassembled into a one-year time series. Figure 20 compares the results from the single, one-year FVARMA and the six, two-month FVARMAs. The split FVARMA case leads to much better matching of the winter months with a lower overall variance. Additionally, a 3-day representative period in June is plotted with data from the split FVARMAs (Figure 21). The data agrees better than the single FVARMA method in the above Section. Furthermore, to investigate the variance in the data, 10000 synthetic histories were produced for demand, rPV and hub price. That leads to a statistical error of $1/\sqrt{10000} = 1\%$. The means and variances are presented in Figure 22 (demand), Figure 23 (rPV) and Figure 24 (hub price). The 6 distinct variance regions for the split FVARMA can clearly be seen for the demand and hub price. This result confirms that using the yearly average variance is less accurate than the split. For the rPV, however, the reason why mean and variance are "solid blocks" rather than lines is that during the night hours the mean and variance is always zero.

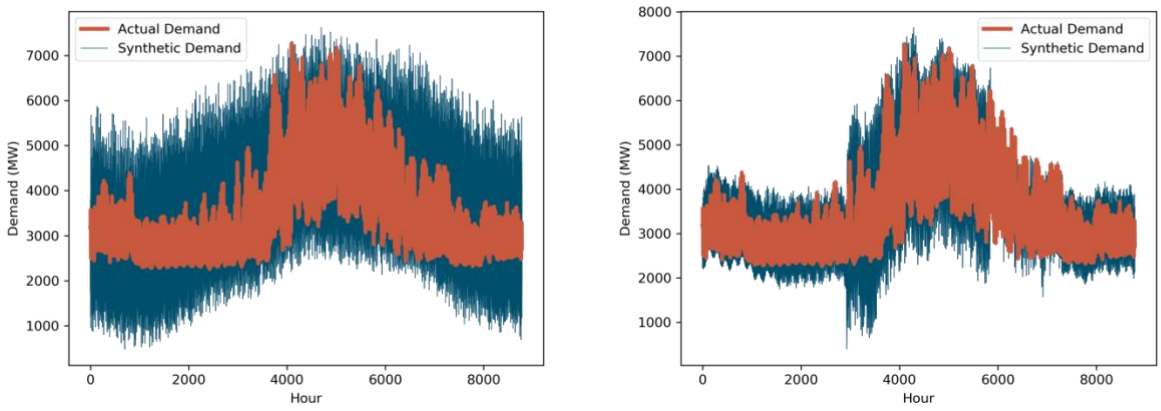

Figure 20: One-year synthetic demand vs actual demand. The plot on the left is data sampled from the one-year FVARMA and the right is data sampled from the six, two-month FVARMAs.

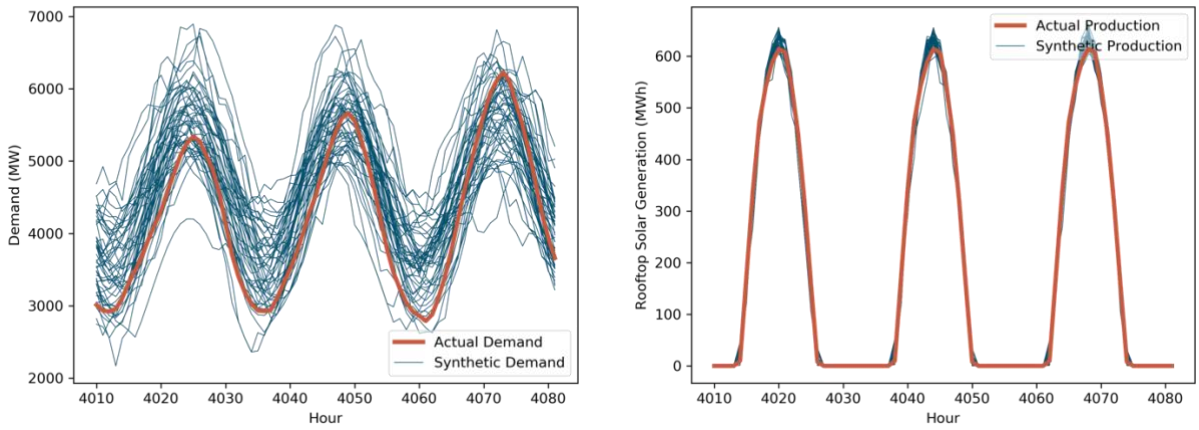

Figure 21: Output of two-month correlated FVARMA with zeroFilter demand and rPV for three representative days.

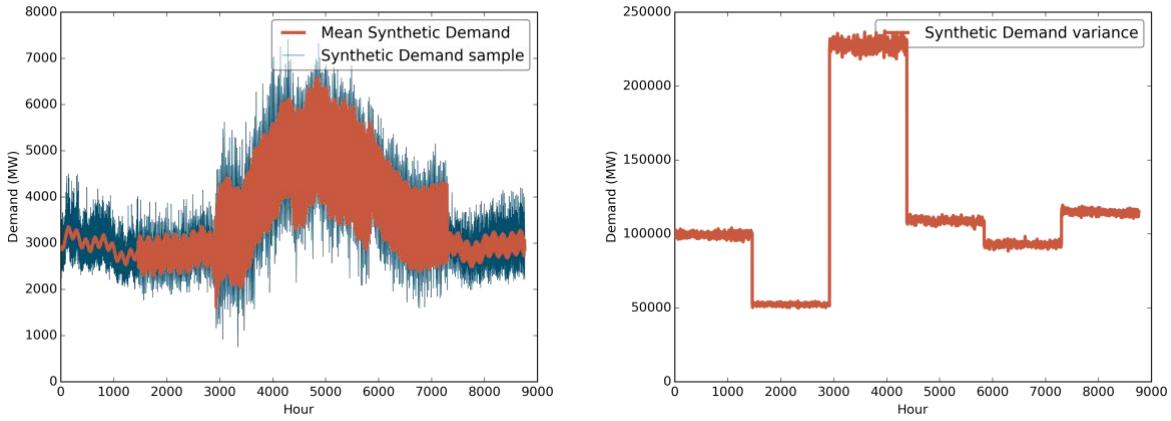

Figure 22: Results of 10^4 runs: Mean and variance for synthetic demand.

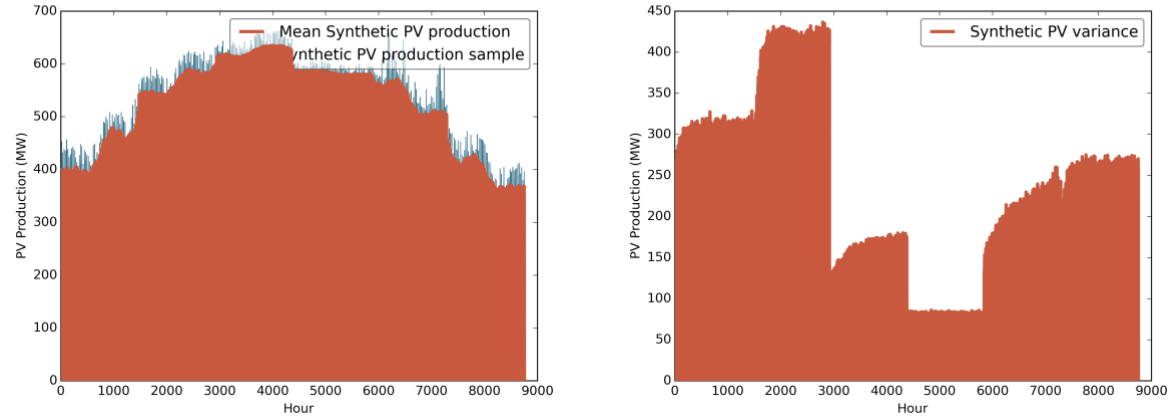

Figure 23: Results of 10^4 runs: Mean and variance for synthetic rPV production.

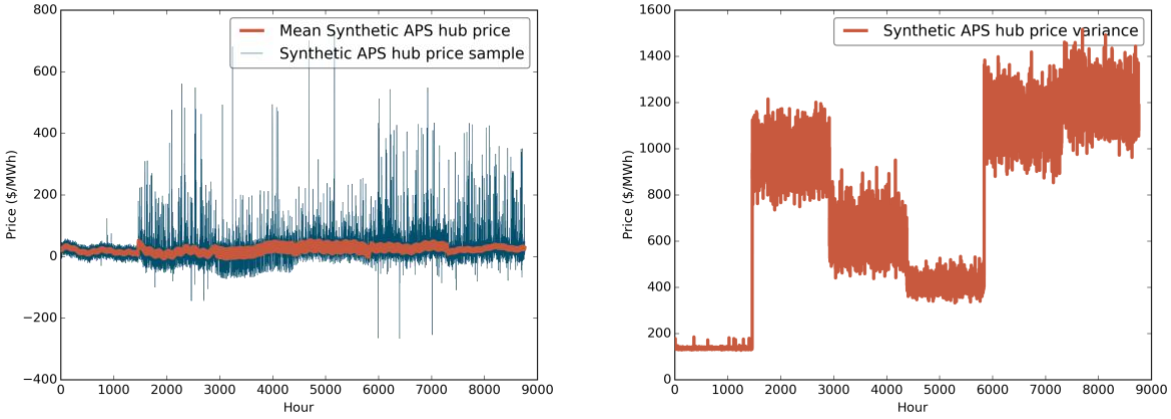

Figure 24: Results for 10^4 runs: Mean and variance for synthetic hub price production.

Thus far we have confirmed that the FVARMA prediction ability to produce each data separately is statistically meaningful. The next section discusses how we can also capture the stochastic (short term) correlation between demand and rPV or demand and hub price.

Figure 25 shows a 2-week period of demand and rPV data, including both the input training data and several synthetic histories. Two cases are shown: the case where the two signals are trained and sampled independently (uncorrelated) and the case where the two signals have been trained and sampled with the correlated FVARMA. One can see that there is no difference in correlated and uncorrelated synthetic data. This result indicates that no (stochastic, short term) correlation is present between the data. Furthermore, it can be seen from the rPV plots that each day is the same, destroying any possibility for short-term correlation between the demand and the rPV. As mentioned previously, the available rPV data provided by APS contains only one typical day for each month.

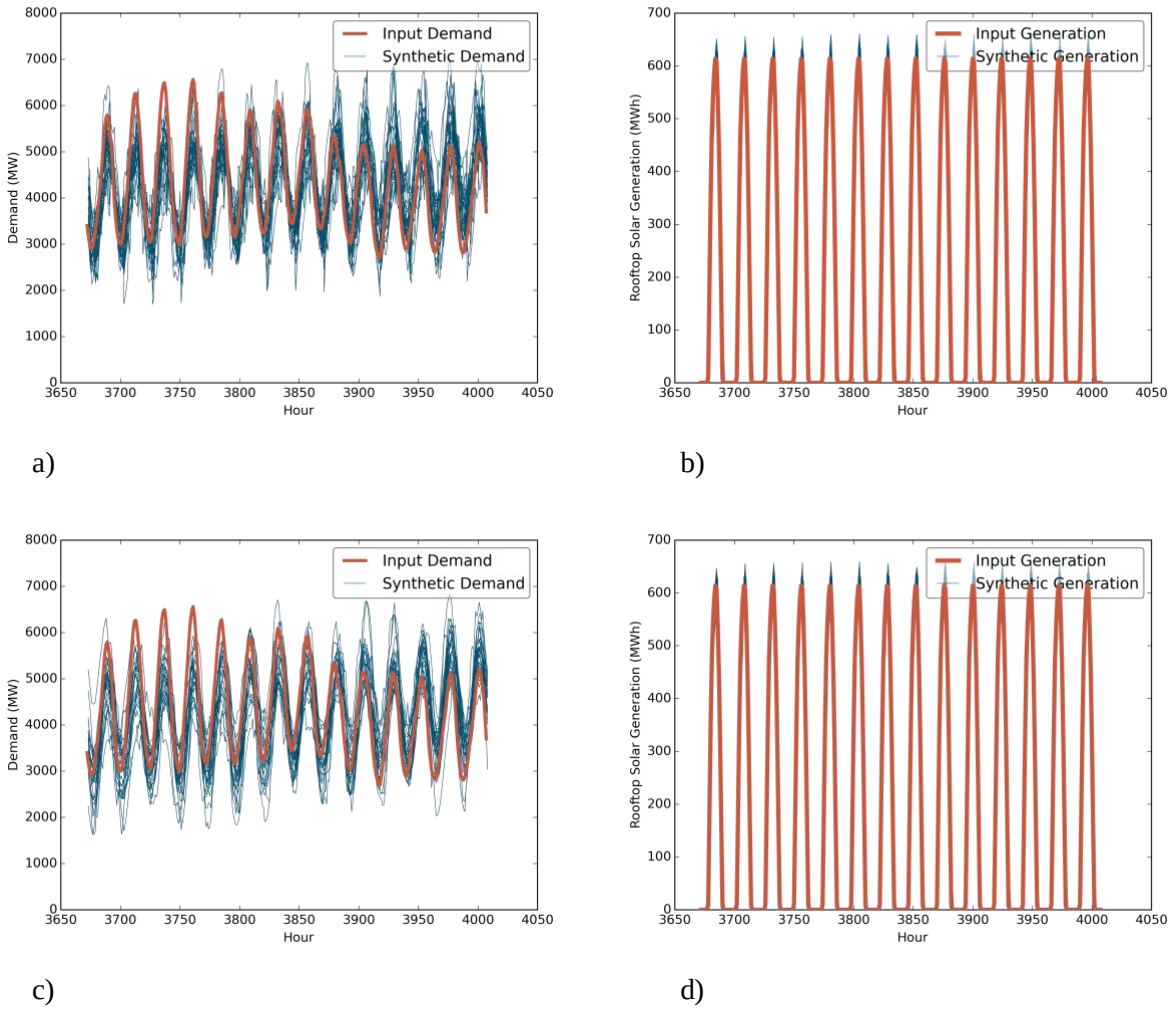

Figure 25: Two-week period of demand and rPV generation: a) demand, uncorrelated FVARMA, b) rPV, uncorrelated FVARMA, c) demand, correlated FVARMA and d) rPV, correlated FVARMA.

To demonstrate that the correlation analysis works as well on real data in addition to the test case shown in Section 3.1.3, the day and night cycle has been removed from the Fourier trends and has been pushed into the FVARMA portion of the model. As mentioned, the correlation of demand and rPV generation, with both being low during the night and high during the day, is normally captured by the Fourier de-trending. Training a correlated FVARMA where the highest Fourier frequency is one week will push the day/night cycle into the noise of the signal that is treated by the FVARMA. If this noise is not correlated between the signals demand could go up while rPV goes down, but if the correlation is found by the model then the two signals should move up and down together. Since in this testing scenario the days are pushed inside the noise, actual days and nights are only statistically represented, i.e. there is no day and night anymore, but we should still see the correlated rise and fall of demand and rPV. The results shown in Figure 26 confirm that the correlated FVARMA is working as intended. One can see that even the delay in demand and rPV present in the training data is captured by the correlated FVARMA.

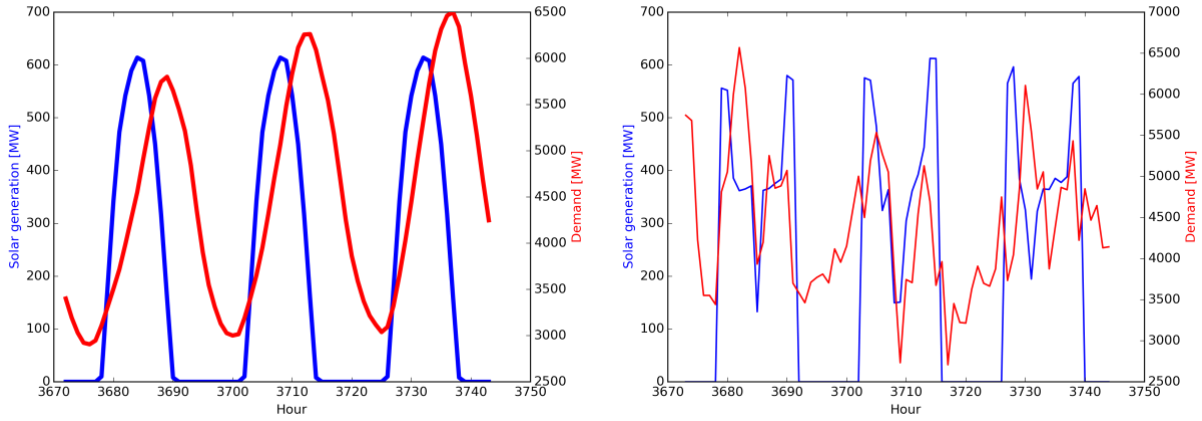

Figure 26: Left) Three-day training data for demand and rPV; Right) Synthetic data with correlated FVARMA where lowest Fourier frequency is 1-week (for demonstration purposes only).

Similar to the demand and rPV, Figure 27 shows a 2-week period of correlated demand and hub price. This figure also shows no apparent (stochastic, short term) correlation between the training data.

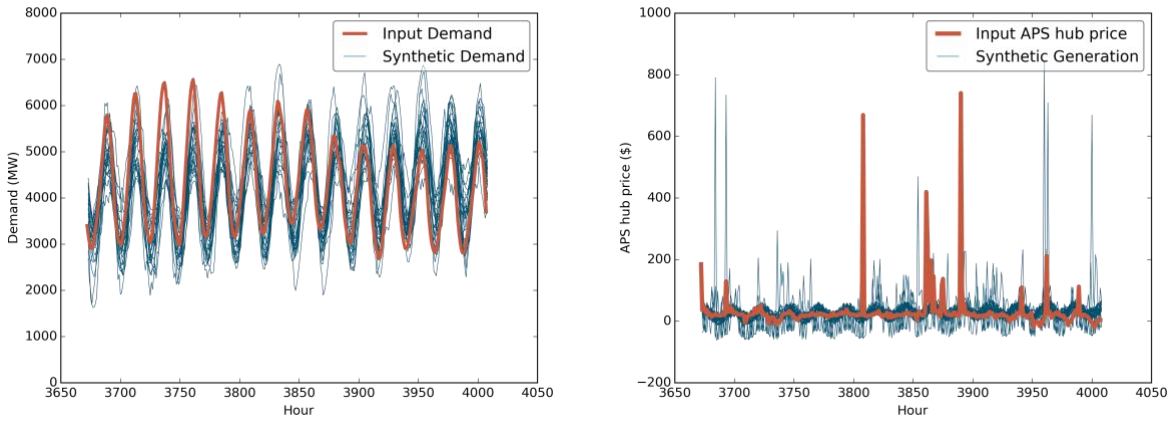

Figure 27: 2-week period of demand and hub price: correlated FVARMA.

In conclusion, the following observations are made:

- Reproduced demand, rPV and hub price data can be statistically meaningful with the FVARMA model when 2-month blocks are trained individually instead of the full year. It is suggested for future work that the "arbitrary" 2 month blocks are replaced by a cluster analysis, i.e. so that FVARMAs can be trained on groups of similar weeks or days throughout the year. It is believed that this will increase the quality of the synthetic data even further.
- The FVARMA can reproduce signals with "flat regions" (e.g. zero production during the night) like the rPV generation with the help of the "zero filter" capability developed for the FVARMA module. However, it is suggested that additional signal treatment methods (in addition to Fourier) that are capable of capturing capped data, such as spikes, are assessed for use in the FVARMA model.
- It has been shown that the recently implemented correlated FVARMA capability is working as intended. However, (after removing the long term trends and correlations by Fourier de-trending) no correlation could be found between the demand and the rPV or the demand and the hub price in the stochastic portion of the signal, although it is suspected that correlation exists and is an important driver for the economic analysis. Concerning the rPV data, higher resolution data is needed to be able to perform a correlation analysis. For the hub price it is assumed that there is no actual correlation or it is so weak or delayed that we cannot capture it. Further investigations for the input data are needed to gain a better understanding of whether correlation exists and, if so, how much.

Net demand and hub price forecast

Using the sampled demand and rPV generation, a net demand profile can be generated for future years. Net demand profiles for the two possible growth scenarios are shown. Figure 28 shows the demand forecast for the next 27 years (the remaining operating license period for PVGS). This is the same for both scenarios, i.e. a 3.3% growth per year. Figure 29 shows that the rPV production grows for the two scenarios where the rPV grows exponentially at 3.3% and, alternately, linearly at 200 MW/year. Finally, Figure 30 shows the resulting net demand for the two cases.

One can see the resulting high variance and very large summer peaks by 2045. The rPV generation, in the case of linear scaling at 200 MW/yr, has a capacity of 6060 MW in the final year. The linear solar capacity additions are relatively small when compared to the demand, which increases exponentially.

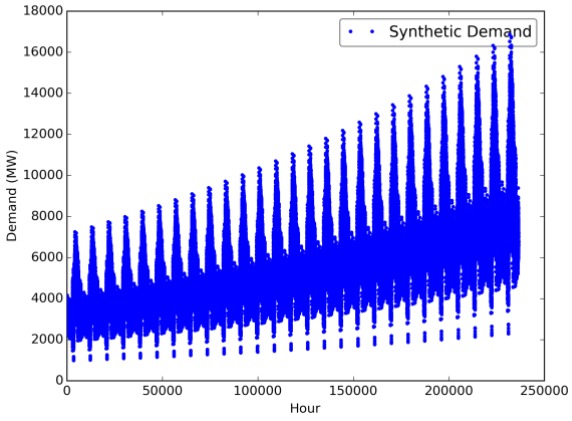

Figure 28: Exponential demand growth at 3.3%/year.

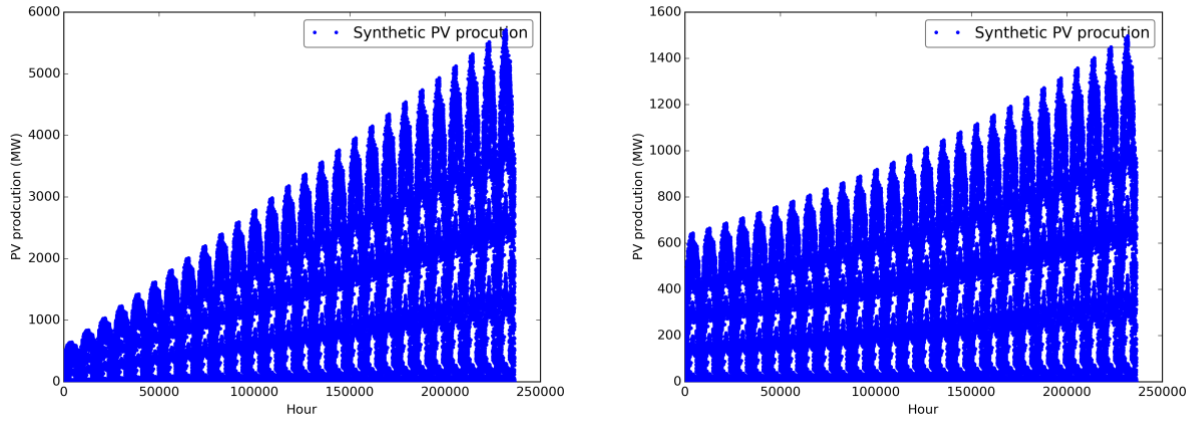

Figure 29: rPV growth: Left) linear at 200MW/year; Right) exponential at 3.3%/year.

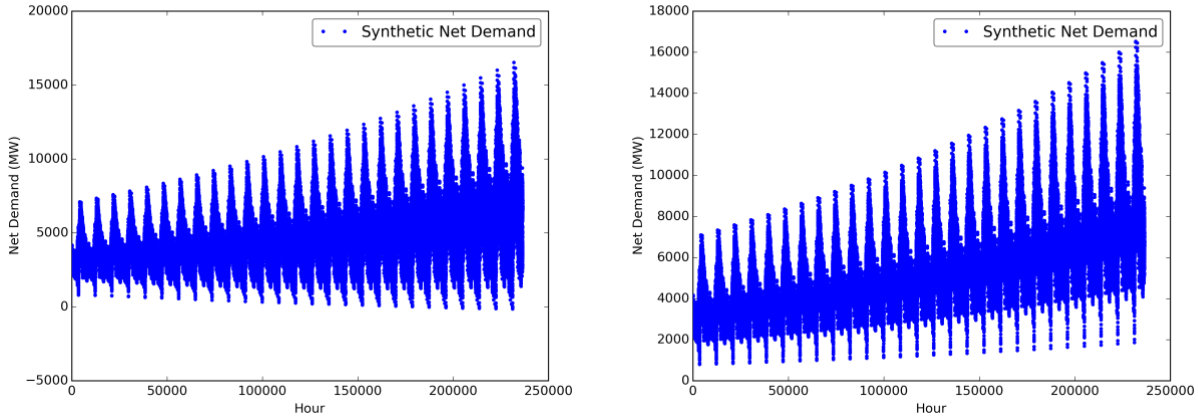

Figure 30: Net demand growth: Left) using rPV linear at 200MW/year; Right) using rPV exponential at 3.3%/year.

In conclusion, the following observations are made:

- Depending on the net demand forecast model, the variance of the net demand changes considerably. Future work is needed to understand which forecast model (in general, not just out of the two presented here) is right for this type of analysis.
- There is no forecast for the hub price. In addition, PV is considered a price taker at the hub and cannot influence its price.

4.2 APS case simulations

This section presents the simulation results for the three APS cases using the input data in Section 4.1. First, the "reference" for the three cases is presented (red values in Sect. 4.1.1) followed by the sensitivity studies.

4.2.1 Reference case

The reference case uses the input data marked in red in Section 4.1.1. This data is summarized again for convenience in Table 11. Before the overall economic results for the reference case are shown and discussed, more detailed results are presented for the physics of the model (water flow and chemical composition throughout the system). Furthermore, a detailed breakdown of the cash flows is presented as well for selected cases.

Table 11: Reference input values for APS cases.

Parameter	Reference value
Net demand future projection	Demand exponential/rPV linear
Brackish water amount	5000 AF/year
Max Cl^- concentration	450 ppm
Wholesale price	35 $/MWh
Discount rate	10 %
Project lifetime	27 years

Detailed physical model results for selected cases

Once the inputs in Table 11 are fixed, the problem has one additional degree of freedom: RO1_split, the percentage of water that goes to the RO1 after the WRF. RO1_split is directly proportional to the capacity of RO1. In practice, there is an optimum RO1 capacity that is unknown *a priori*. The optimum RO1 capacity is the capacity that produces the maximum chloride concentration allowable in the cooling water reservoirs. The optimum RO1 capacity will be discussed in the overall economics results later in this chapter. However, this goal in this section is to show some detailed model results that provide a foundation for the overall results presented later. Reference case results for two values of RO1_split are shown, i.e. 20% and 80%.

First, to understand the physics model, Figure 31 to Figure 33 show the water flows for CASE 0, 1 and 2 throughout the system (20% and 80% RO1_split). The figures show the monthly water flows for one year. All other years are the same, calculated through the lifetime of the project (NumberOfYears).

As one can see, for CASE 0 the water flow for RO1_split 20% and 80% are the same since in CASE 0 no RO1 is built (e.g., this case provides a baseline for the other cases). Furthermore, since the WRF has no waste stream, the effluent water from the WWTP, the WRF inflow and outflow, and the water flow into the reservoirs are equal and match the PVGS water consumption in all months except July and September. In these two months the effluent water chloride concentration is higher than the limit of 450 ppm and, therefore, the "requested" PVGS water consumption (shown as blue dots in Figure 31 to Figure 33) has been adjusted according to Eq. 13 to account for the increased water consumption if $ppm(Cl^-)>450$. This adjustment is only done for CASE 0. CASE 1 and CASE 2 always match the "requested" PVGS water. The chloride concentration in these two cases can be adjusted by changing the size of RO1.

For CASE 1, one can see that the amount of effluent water purchased in the case of RO1_split 80% is somewhat bigger than in the RO1_split 20% case. This is due to the fact that the RO1 waste stream is bigger (see "Water RO1 in" and "Water RO1 out" in the Figures) for the bigger RO1 (RO1_split 80%). Consequently, to get the same amount of water to the cooling towers in both cases (RO1_split 20% and 80%), the amount of effluent water in the RO1_split 80% has to be bigger (for the same amount of brackish water purchased in both cases). It is worth mentioning that in both cases (RO1_split 20% and 80%), the recovery ratio of RO1, i.e. the amount of clean water compared to the waste stream is almost the same (see Figure 34) and always > 80%. Finally, in CASE 2 the brackish water is purified in RO2 and the waste of RO2 is injected into the WRSS. In the reference case presented here, the amount of brackish water purchased is relatively small compared to the PVGS water needs. Therefore, although the RO2 waste stream is considerably less than the brackish water acquired, the change in needed effluent water between CASE 1 and CASE 2 is too small to be seen in the plots. That is not true if more brackish water is purchased and purified in RO2.

After tracking the water through the system, we can next look to the evaporation ponds. The water flow to these ponds is the combined flow from the cooling tower blowdown and the RO1 waste stream. Figure 35 shows the blowdown from the cooling towers for the status quo (CASE 0). As for the water flows discussed previously, RO1 is not built for CASE 0 and the blowdown for RO1_split 20% and 80% are the same. Consequently, only one figure is shown.

Since the water flows for CASE 1 and CASE 2 are similar (see above), the blowdowns and RO1 waste streams are similar as well. Note that the RO waste stream not only depends on the inlet water flow but also on the water chemistry. Therefore, for the RO waste streams to be similar between CASE 1 and CASE 2, \ the RO inlet water chemistry should also be similar, which it is (see discussion on water chemistry later in this Section). Consequently, results are only shown for CASE 1 (for RO1_split 20% and 80%) in Figure 36. One can see that while the blowdown from the cooling towers stays constant, the RO1 waste stream quadruples for the bigger RO1.

It is worth noting that the overall plots presented later always indicate the maximum blowdown during the year corresponding to the green triangles in Figure 35 and Figure 36. This is the most conservative assumption for the economics analysis. The evaporation pond model could be refined in future iterations of the model.

Next, we can investigate the variation of the chemical compositions throughout the model. Since the behavior is similar for CASE 0, 1 and 2 as well as for the different RO1 sizes, plots are only shown for CASE1, RO1_split 20%, in Figure 37.

As one can see, for the small amount of brackish water acquired (compared to the overall PVGS water needs), the chemical composition of the effluent and brackish water blend is still close to the effluent chemistry. Then, all the chemicals are reduced to a constant value in the WRF except chloride and sodium. One should note that for calcium, in some months the constant value to which the WRF reduced the calcium concentration is actually higher than the inlet concentration. The chemical transfer model of the WRF could be refined in the future to avoid such unphysical behavior (even though the effect on the economics is negligible). Even if more brackish water is acquired, the chemical composition of the water at the outlet of the WRF is always the same (except for chloride and sodium), but the WRF chemical consumption and therefore the Operation and Maintenance (O&M) cost will change for changing WRF inlet chemistry. That said, it becomes clear now why the RO1 waste streams are similar between CASE 1 and CASE 2, although the water chemistry at the water source is quite different (effluent water blend with brackish water vs. RO2 waste stream): The RO1 inlet conditions are determined by the WRF outlet (which are constant), not the water source.

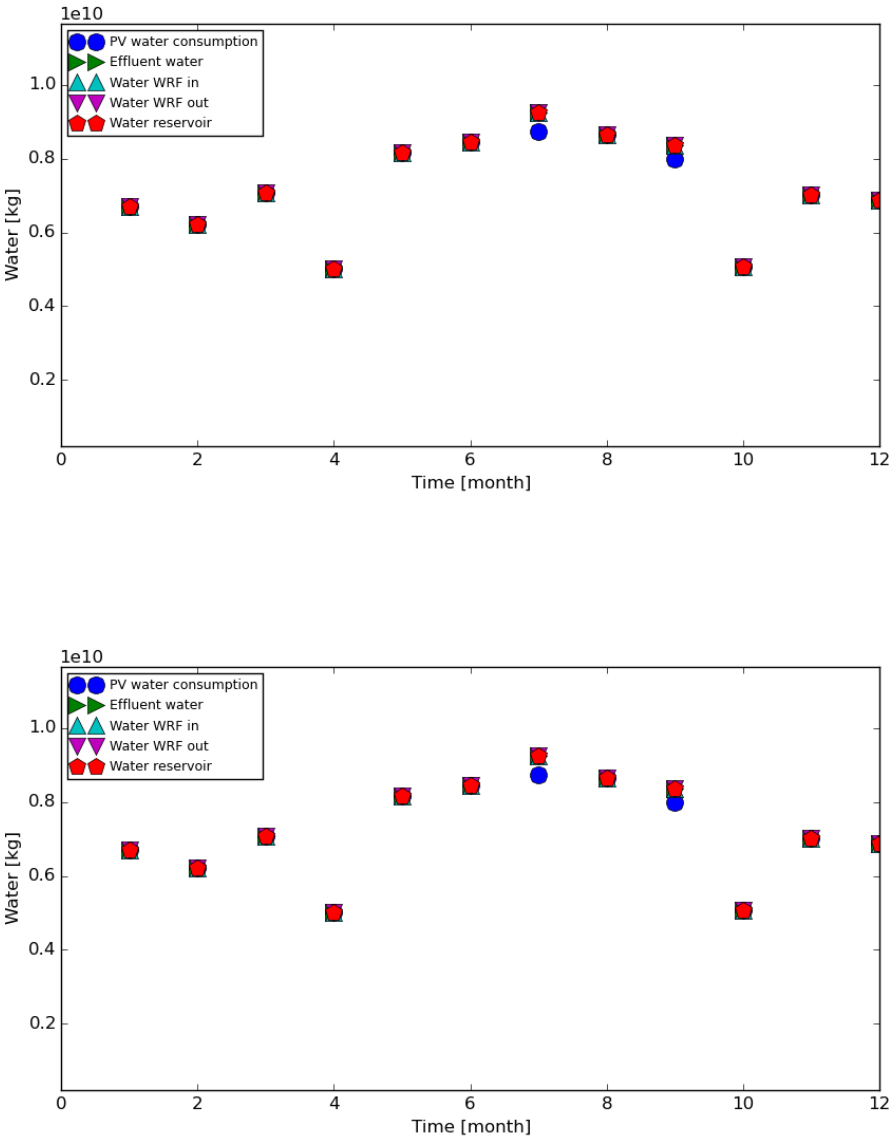

Figure 31: Reference CASE 0, monthly water flows through the system for one year. Top) RO1_split 20%; Bottom) RO1_split 80%.

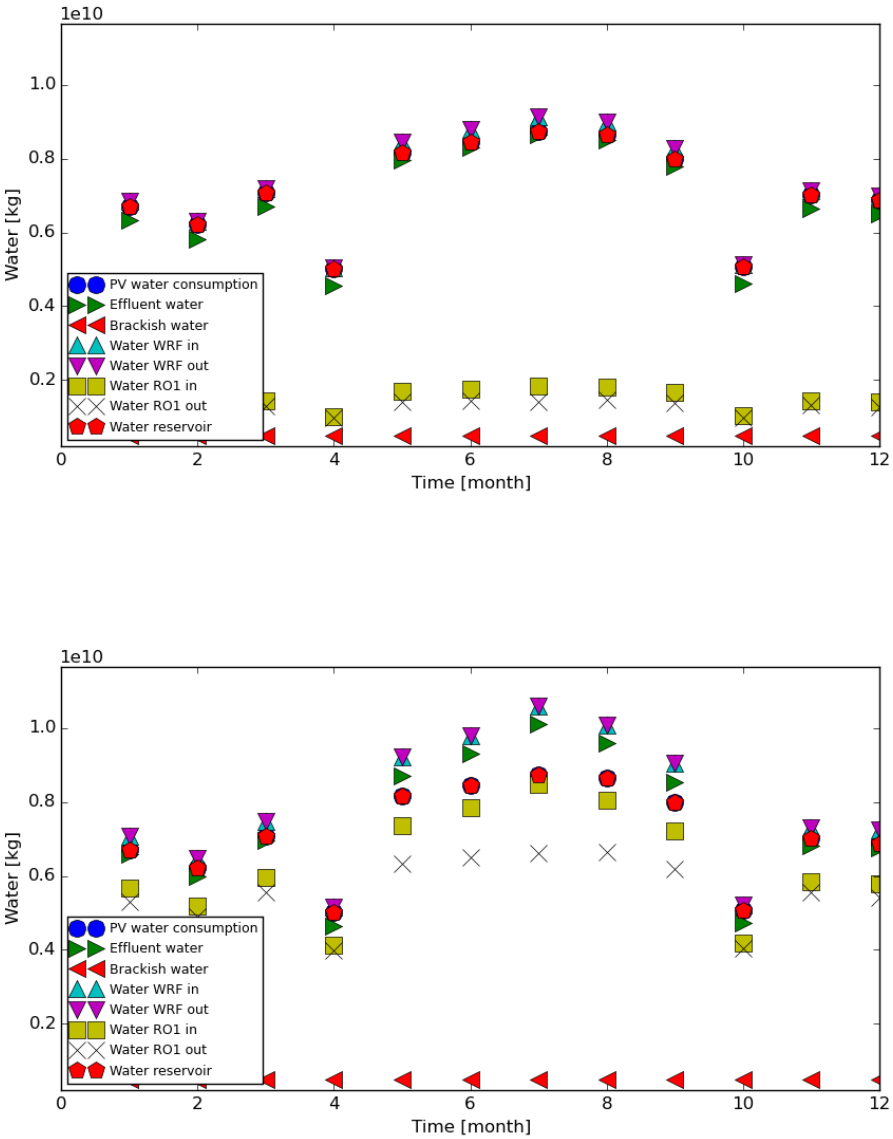

Figure 32: Reference CASE 1, monthly water flows through the system for one year. Top) RO1_split 20%; Bottom) RO1_split 80%.

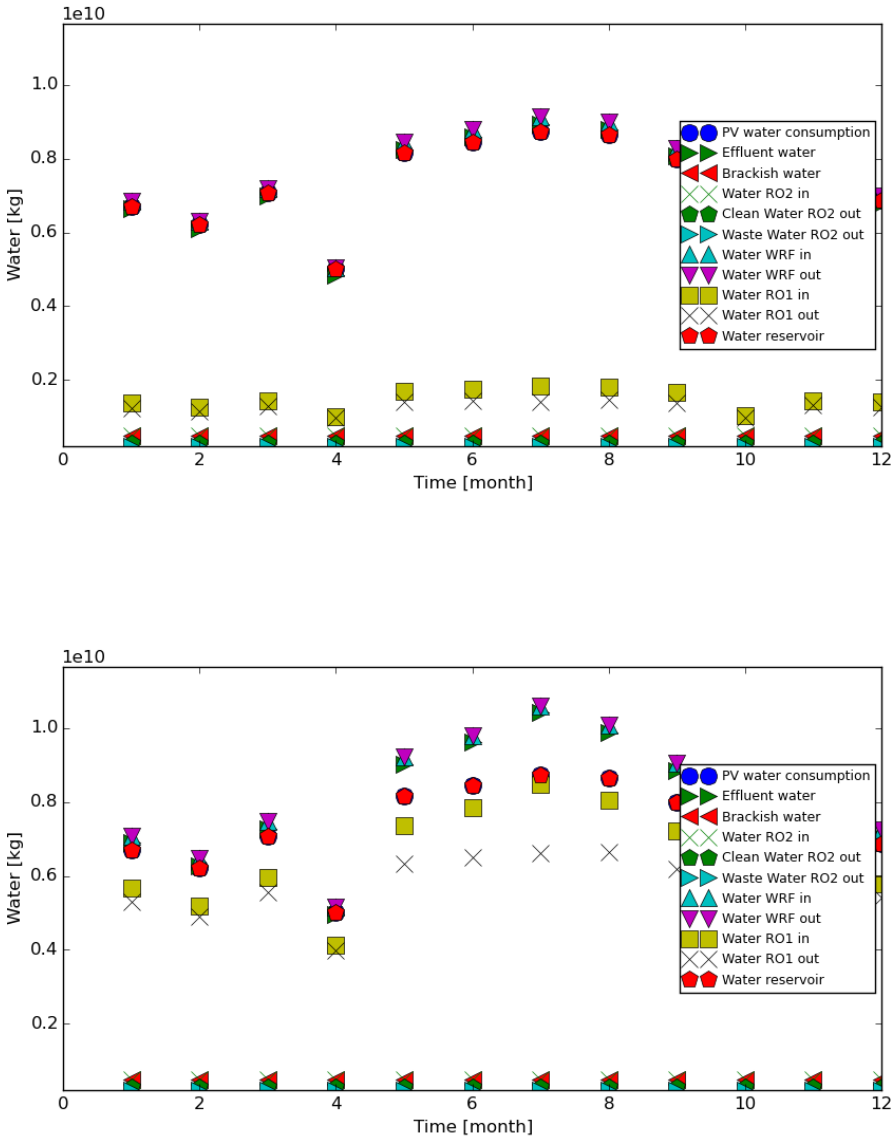

Figure 33: Reference CASE 2, monthly water flows through the system for one year. Top) RO1_split 20%; Bottom) RO1_split 80%.

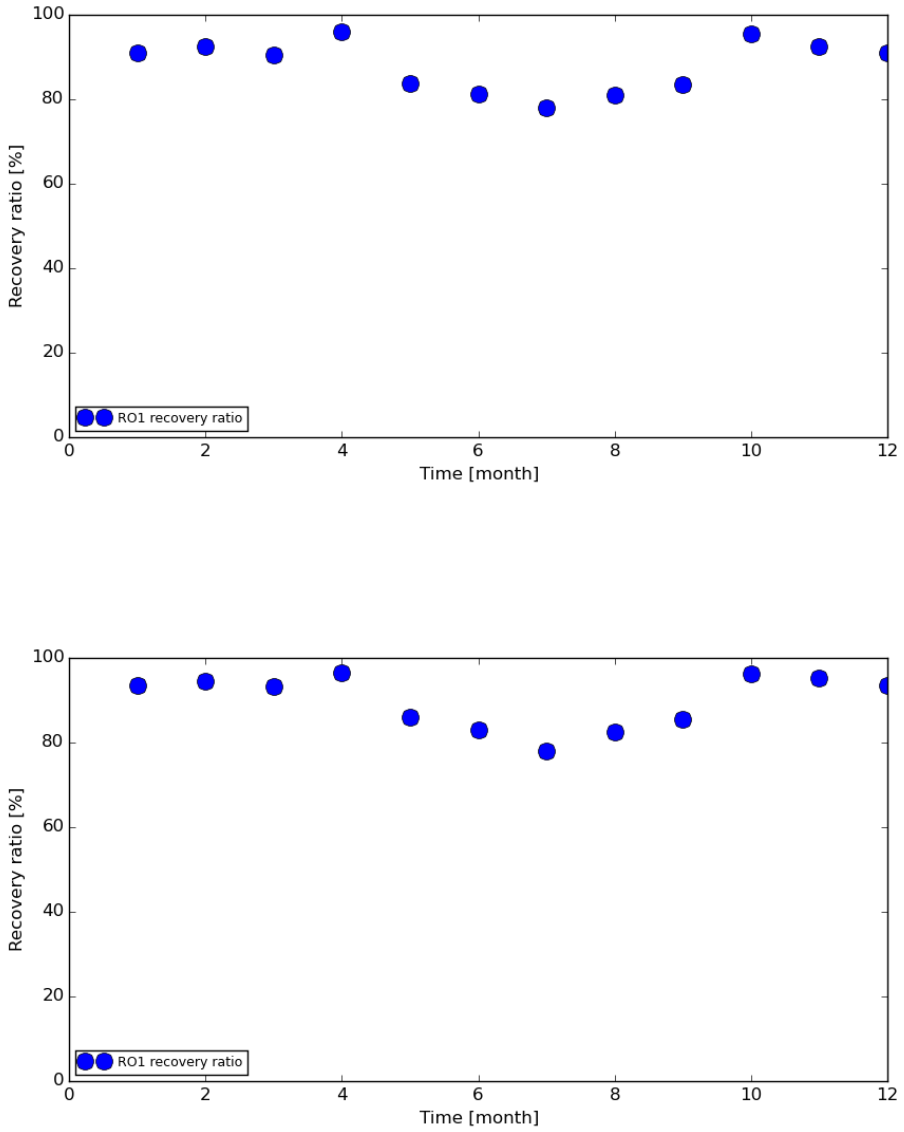

Figure 34: Reference CASE 1, monthly recovery ratio for RO1 for one year. Top) RO1_split 20%; Bottom) RO1_split 80%.

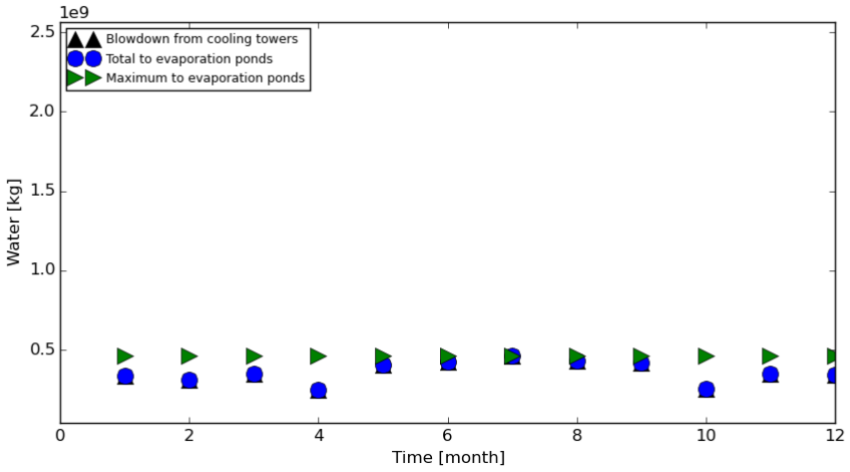

Figure 35: Reference CASE 0, monthly water flows to the reservoir ponds for one year.

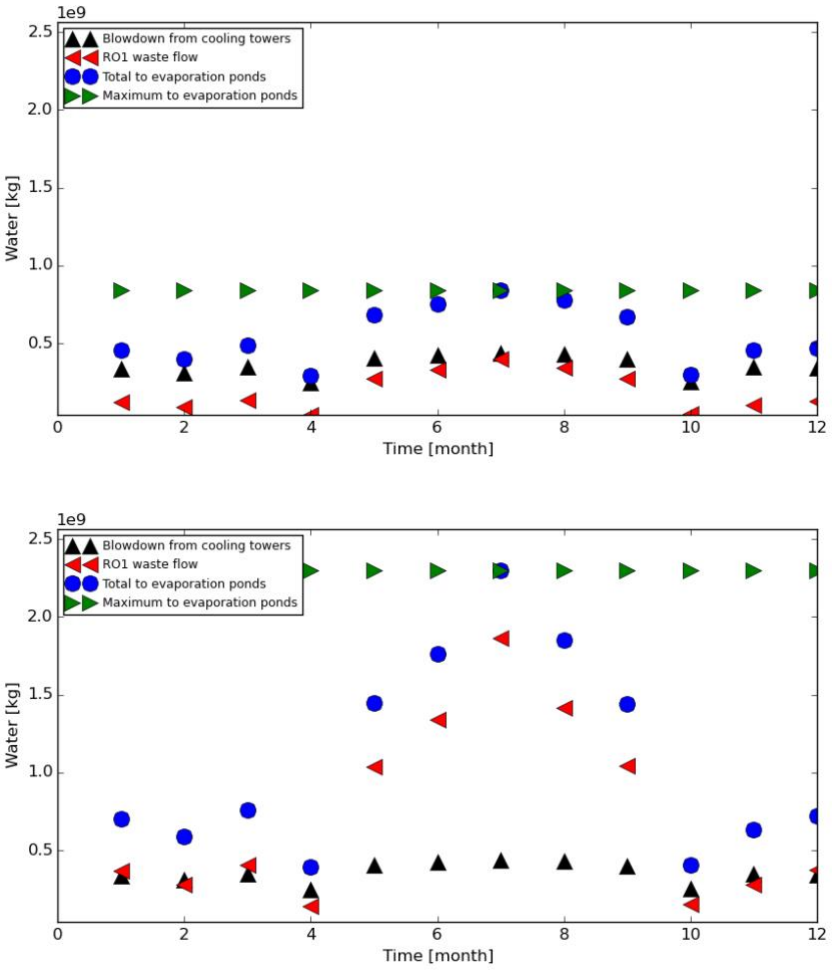

Figure 36: Reference CASE 1, monthly water flows to the reservoir ponds for one year. Top) RO1_split 20%; Bottom) RO1_split 80%.

It should be mentioned that, even though the RO model considers the effect of all 6 tracked chemicals at its inlet and computes concentrations for all of them at the RO1 permeate clean water stream, only the RO1 outlet chloride concentration is shown in Figure 37. Chloride is the limiting factor for the cooling water towers, while the other chemicals are already brought below their limits by the WRF and are further reduced by the RO1.

It is worth noting that, similar to the water flows to the evaporation ponds, the overall plots presented later always indicate the maximum chloride concentration during the year (corresponding to the maximum of the pentagons in the "Chloride" plot in Figure 37). This is the most conservative assumption for the economics analysis. The reservoir pond model should be refined in future iterations of the model to yield a more realistic average chloride concentration.

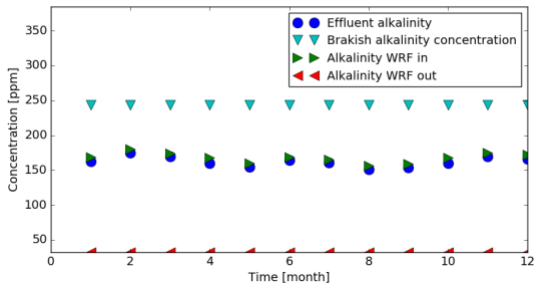

Alkalinity

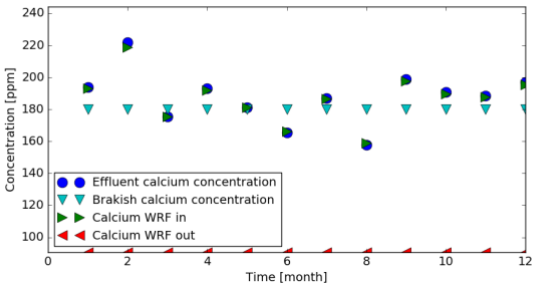

Calcium

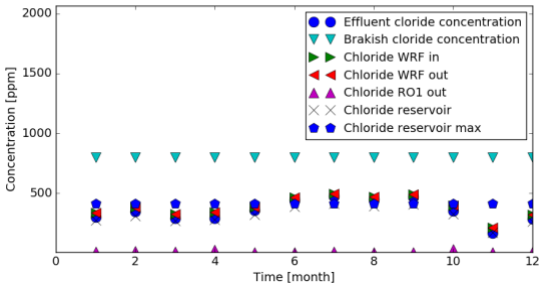

Chloride

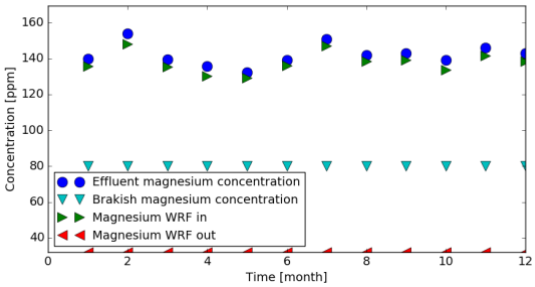

Magnesium

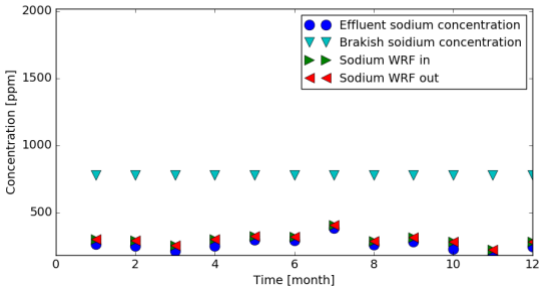

Sodium

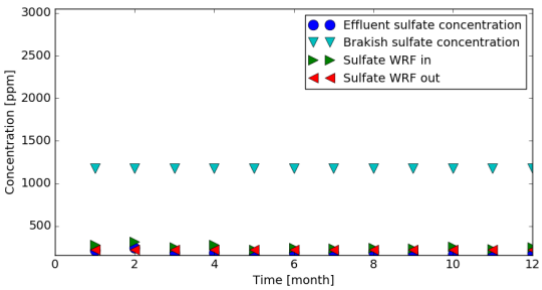

Sulfates

Figure 37: Reference CASE 1, monthly water chemistry (6 tracked chemicals) through the system for one year; RO1_split 20%.

Detailed economics snapshots for selected cases

After looking at the physical model in detail, we can have the same detailed look at the economic model of the system. In the same manner as before, results for CASE 0, 1 and 2 are shown for the reference inputs and for RO1_split 20% and 80%.

Table 12 shows a breakdown of the relevant cash flows for CASE 0. Recall that only cash flows that vary between CASE 0, 1, and 2 are considered with an overall differential NPV analysis as the final goal. One can see that the effluent water acquisition costs are roughly ten times higher than the electricity cost for the WRF. Furthermore, for CASE 0, since no RO1 is built, the values for RO1_split 20% and 80% should be the same. One can see that they are indeed the same for the cash flows that don't depend on the stochastic inputs, but vary slightly for "APS electricity sales" which depend on the PV Hub price, a stochastic input that changes for every evaluation of the model.

Table 13 shows the relevant cash flows for CASE 1 while Table 14 shows them for CASE 2. Looking at the water acquisition cost (effluent and brackish), one can see that for the small amount of brackish water considered in the reference case, the savings in effluent water cost are less than 5% in CASE 1 (RO1_split 20%) and are nullified for the larger RO case. For CASE 2, where the purified brackish water is sold and nearly all the cooling water has to be purchased from the effluent source (the RO2 waste contributes some water), the effluent water cost is even higher than in CASE 0 (to compensate for the RO1 waste stream).

Looking at the WRF O&M and electricity costs, one can see that the higher chemical concentrations in the WRF inlet stream for CASE 1 and 2 raise these costs by a maximum of 2%. The RO electricity cost is comparable to the one in the WRF per water unit, i.e. the RO electricity cost is comparable to the WRF for the large RO1, but only a fraction (~20%) in the case of RO1_split 20%.

Furthermore, one can see that the RO1 capital cost varies between $45 million (RO1_split 20%) and $211 million (RO1_split 80%), while the capex for RO2 (for ~5000 AF/year brackish water) is ~$12 million. As mentioned in the economics section, there is no economy of scale considered in the current model and it needs to be further investigated if the capex is still meaningful for such a small RO.

Since the amount of brackish water acquired in CASE 1 and 2 and RO1_split 20% and 80% is the same, the brackish water capex and the electricity cost are equal for all cases.

Table 12: Reference CASE 0, cash flow breakdown. Values shown for the first year of the project lifetime. RO1_split 20% and 80% (in million $).

RO1_split	**20%**	**80%**
Effluent water cost [year 1]	10.40	10.40
WRF Variable O&M	25.43	25.43
WRF electricity	1.75	1.75
APS electricity sales	437.18	437.21

Table 13: Reference CASE 1, cash flow breakdown. Values shown for the first year of the project lifetime. RO1_split 20% and 80% (in million $).

RO1_split	**20%**	**80%**
Effluent water cost	9.84	10.41
Brackish water cost	0.12	0.12
WRF Variable O&M	25.48	26.14
WRF electricity	1.77	1.88
RO1 CAPEX	45.66	211.83
RO1 electricity usage	0.37	1.57
Brackish pump CAPEX	0.40	0.40
Brackish elect. usage	0.07	0.07
APS electricity sales	437.17	437.16

Table 14: Reference CASE 2, cash flow breakdown. Values shown for the first year of the project lifetime. RO1_split 20% and 80% (in million $).

RO1_split	**20%**	**80%**
Effluent water cost	10.25	10.79
Brackish water cost	0.12	0.12
RO2 CAPEX	12.33	12.33
RO2 electricity usage	0.12	0.12
WRF Variable O&M	25.51	26.19
WRF electricity	1.77	1.88
RO1 CAPEX	45.69	212.46
RO1 electricity usage	0.37	1.57
Brackish pump CAPEX	0.40	0.40
Brackish elect. usage	0.07	0.07
APS electricity sales	437.17	437.16

Detailed economics related to the PV Hub price

As discussed in the APS case description (see Chapter 2), the analysis considers two options to save money: a) The hope of having to trade less at the PV Hub (for potentially low or even negative prices) by adding APS baseload (addition of RO1 and RO2); b) Better economy from savings in water acquisition (effluent vs. brackish plus RO). The above tables suggest that for the small amount of brackish water considered, building RO1 is not economical, but it might become economical for larger amounts of brackish water acquired (discussed later in the sensitivity studies, Section 4.2.2). Furthermore, it appears that savings from raising the APS baseload with the ROs is of limited effect, as discussed below.

Figure 38 shows the number of hours during each year of the project at which APS has to sell electricity at the PV Hub ($ED_{Net} < PowAPS_{cor}$) as well as the yearly average price at which electricity has been sold at the hub. First, one can see that the number of hours at which electricity has to be sold at the hub increases during the project lifetime, reaching a maximum before going back down. This is expected and reflects the future behavior of the net demand volatility with the increasing rPV, i.e. the demand grows exponentially, while rPV grows linearly and the slope is the same for both at about 20 years into the project. Furthermore, one can see that the average price at which APS sold at the hub is around 8 $/MWh, which is lower than the retail price, i.e. it is beneficial to sell at the retail price compared to at the hub. This encourages APS to increase the baseload, as discussed. On the other hand, as one can see from Figure 38, APS only has to electricity at the hub for 20 hours/year, which is negligible. In addition, the difference of when APS has to sell at the hub in the status quo (CASE 0) and CASE 1 or 2 is even smaller (difference between green tringles and blue dots). Keep in mind that it is this difference that provided the improved economics by adding the additional baseload in the form of RO1 and RO2. It should be considered that this result depends on the stochastic nature of the PV Hub price. To account for that, 10000 samples have been run for this analysis and the mean and standard deviations of the hours sold at the hub, as well as its mean hub price, are shown in Figure 39 and Figure 40. One can see that the conclusions made from the single time history remain true for the 10000 run averages.

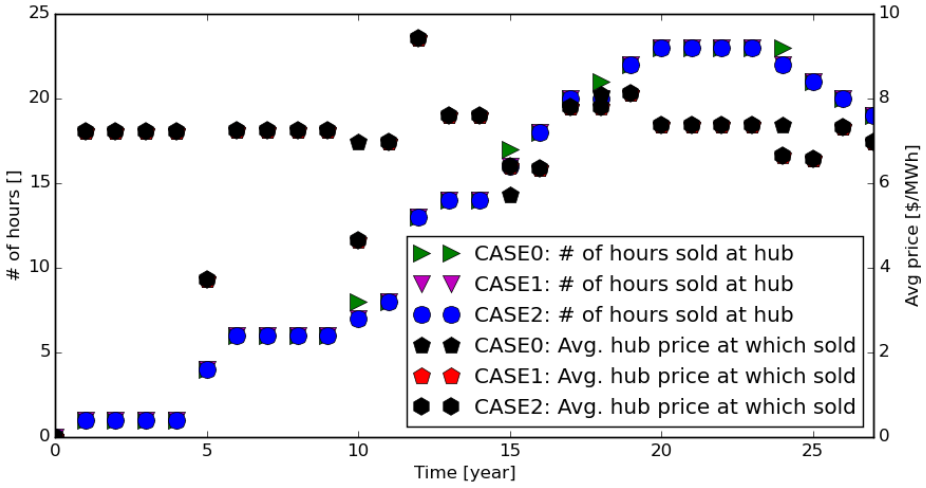

Figure 38: Reference cases, yearly number of hours when electricity is sold at the PV Hub and the average hub price at which electricity has been sold for each year of the project lifetime.

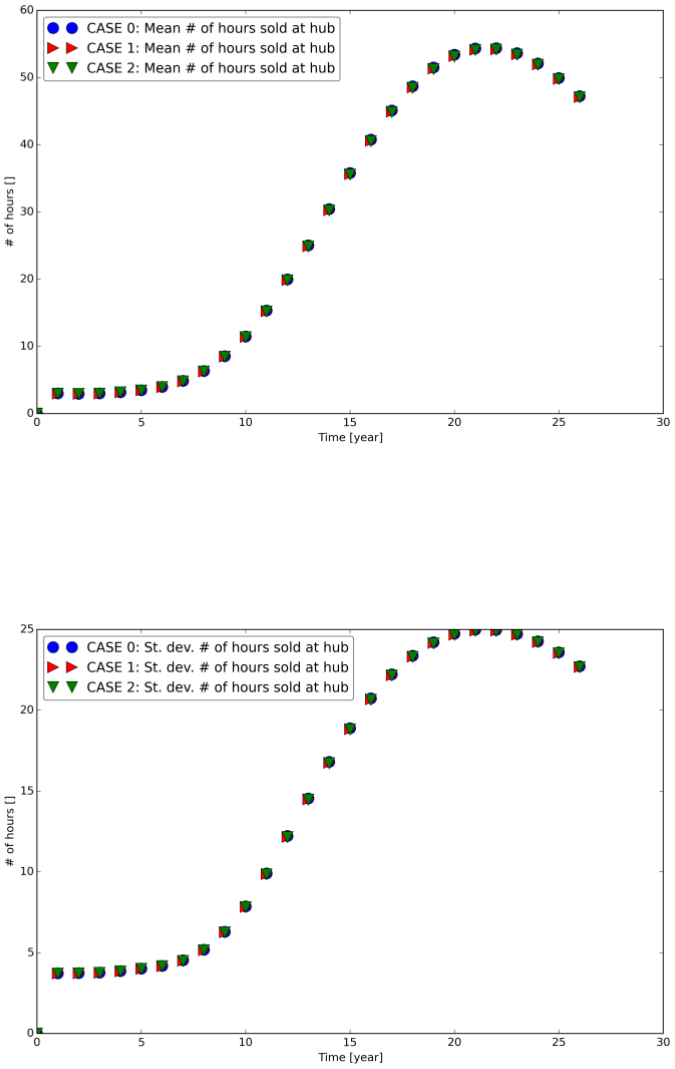

Figure 39: Results for 10^4 runs: Mean and standard deviation for number of hours during a year when electricity has to be sold at the PV Hub.

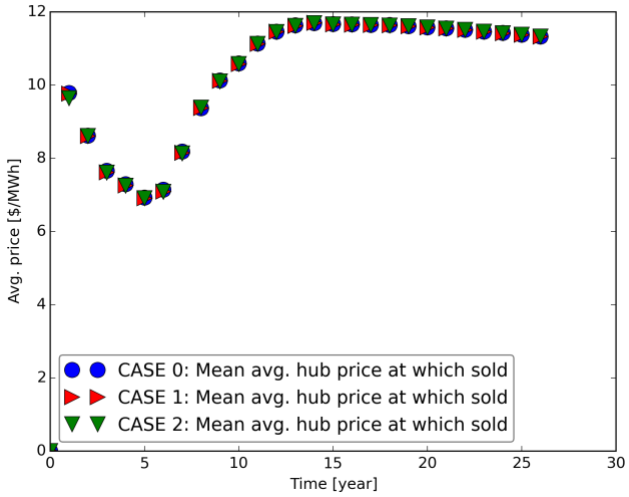

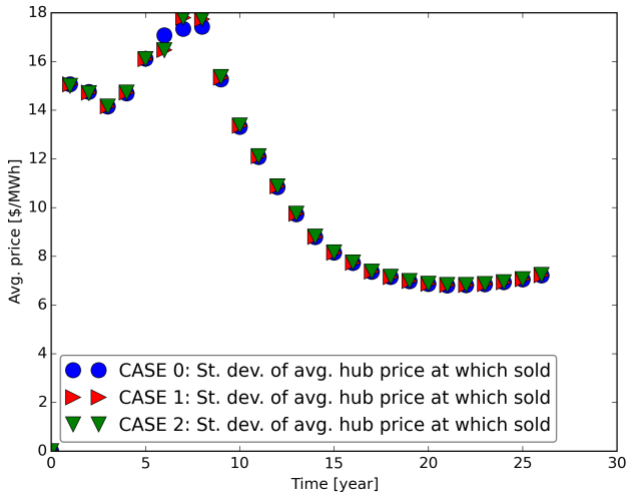

Figure 40: Results for 10^4 runs: Mean and standard deviation for yearly average hub price when electricity has to be sold at the PV Hub.

To assess the maximum value of the PV Hub, one could assess the opportunity to take ("buy") electricity from the hub when its price is negative. Figure 41 shows the number of hours (for each year during the project) for which the internal APS demand is bigger than the APS power share of PVGS ($ED_{Net} > PowAPS_{cor}$) and, at the same time, the hub price is negative (mean and standard deviation of 10000 runs). During these hours, APS could decide to curtail all its assets (except PVGS) and cover the demand with the hub. In that case, APS could cover the demand and make money from the hub. The maximum of this "opportunity revenue" could be calculated by $(ED_{Net} - PowAPS_{cor}) \cdot -1 \cdot P_{E,Hub}$ for each of these hours. Figure 42 shows that opportunity revenue (for each year during the project) (mean and standard deviation of 10000 runs). One can see that the maximum opportunity to absorb volatility at the hub is ~$25 to ~55 million in 27 years. This corresponds to less than 5 to 10% of the total APS revenue from electricity sales.

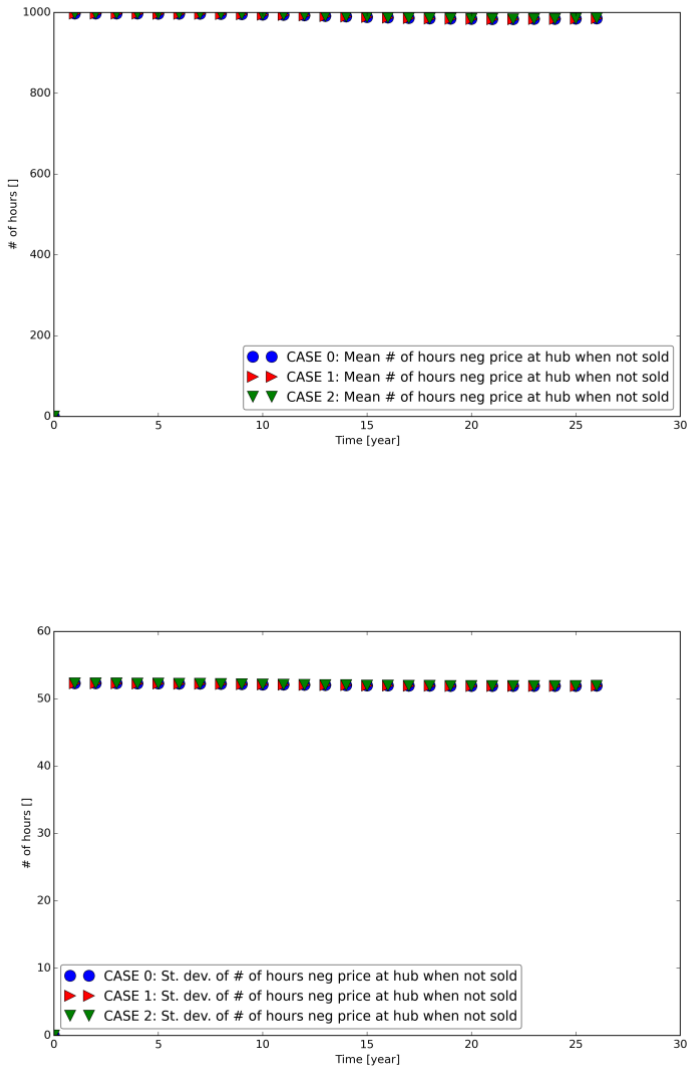

Figure 41: Results for 10^4 runs: Mean and standard deviation for yearly number of hours when $ED_{Net} > PowAPS_{cor}$ and the hub price is negative at the same time.

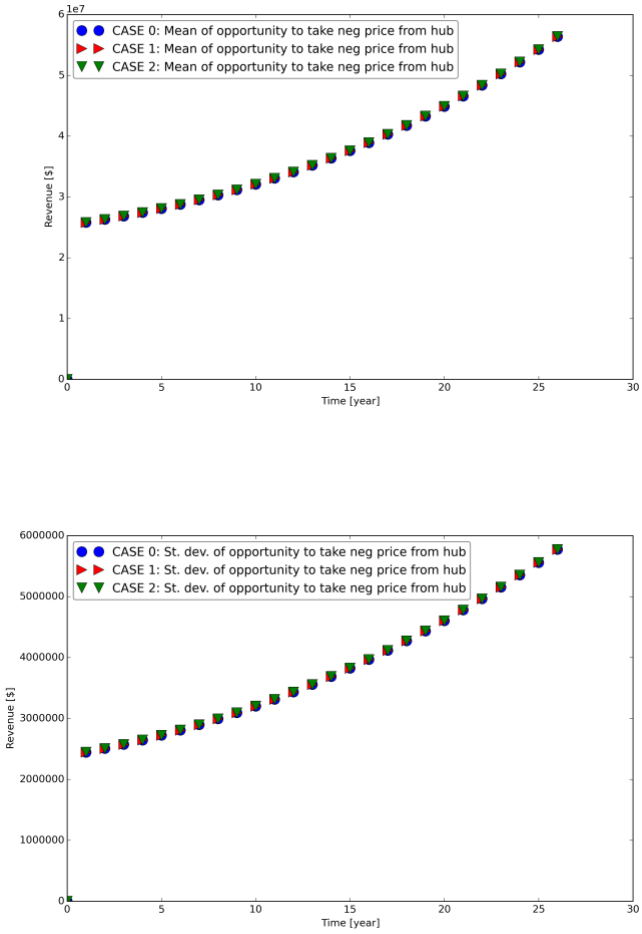

Figure 42: Results for 10^4 runs: Mean and standard deviation for yearly possible opportunity revenue during hours when $ED_{Net} > PowAPS_{cor}$ and the hub price is negative at the same time.

In conclusion, one can say that the maximum opportunity to absorb volatility at the hub by simply add baseload is less that 10% of the total revenue of APS electricity sales. On the other hand, the actual gain from this effect by adding RO1 and RO2 is negligible. These findings don't seem to be in line with APS internal findings and need to be confirmed. In particular, hub price projection models should be investigated and added to this APS case study.

Overall economic results for reference cases

After presenting the physics results of the model as well as the detailed economics, we can look at the overall economic results for the reference cases.

For the overall plots, the monthly results presented previously for RO1_split 20% and 80% are both shown for one year, supplemented by more results for other values of RO1_split. Results are then presented as a function of RO1_split. For better readability, the x-axis shows the RO1 capacity instead of RO1_split (which are directly proportional). Figure 43 shows the delta NPV between CASE 1 and CASE 0 as well as the LCOW that offsets the difference in water acquisition cost between CASE 0 and CASE 2 (capex and O&M of RO1 and 2, difference in O&M of WRF, etc.) for CASE 2, as discussed in Section 3.2.5. One can see that, for a fixed amount of brackish water purchased, the delta NPV becomes more and more negative

the as the size of RO1 increases. One can see that for a very small RO1, the delta NPV is positive, which means that this size of RO1 is economically viable. For CASE 2, one can see that the LCOW increases for increasing RO1 capacity. This can be explained, since the LCOW has to offset the increased expenses associated with RO1 for a fixed size of RO2. The size of RO2 is set by the amount of brackish water acquired which is always the same, independent of RO1 size, i.e. the amount of purified brackish water sold is always the same for the different sizes of RO1. A sensitivity to the amount of brackish water pumped is show later in Section 4.2.2.

A review of Figure 43 suggests that the smallest possible RO1 should be built. To determine this minimum RO1 size consider Figure 44, which shows the constraint that the reservoir water must have a chloride concentration < 450 ppm. As one can see, to satisfy that condition, an RO1 with a capacity greater than ~500 kg/s should be built. On the other hand, a larger RO1 is not needed, since there is no benefit from purer water. Finally, Figure 45 shows the second constraint on the system, which is the water flow to the evaporation ponds.

In conclusion, we can say that for the reference case:

- CASE 1
    - An RO1 of ~500 kg/s capacity is needed to satisfy the maximum chloride concentration in the reservoir ponds.
    - For that size of RO1, the delta NPV between CASE 1 and CASE 0 is negative, i.e. it is economically beneficial to keep buying 100% effluent water rather than to build the RO1.
- CASE 2
    - The size of RO1 needed in CASE 2 to satisfy the needed chloride concentration is comparable to CASE 1, i.e. ~500 kg/s.
    - The LCOW that offsets the cost in that case is ~0.15 cents/liter (1.5 $/m^3). This amount is on the expensive side, but one has to keep in mind that for the reference case, only 5000 acre-foot (~6.2 million m^3) of brackish water are purified per year.

Finally, it is worth reminding the reader that the needed size of RO1 for this case is based in the maximum chloride concentration in the reservoir ponds. As discussed, a more realistic model of these ponds will reduce the necessary RO1 size and may push it in the economically viable space.

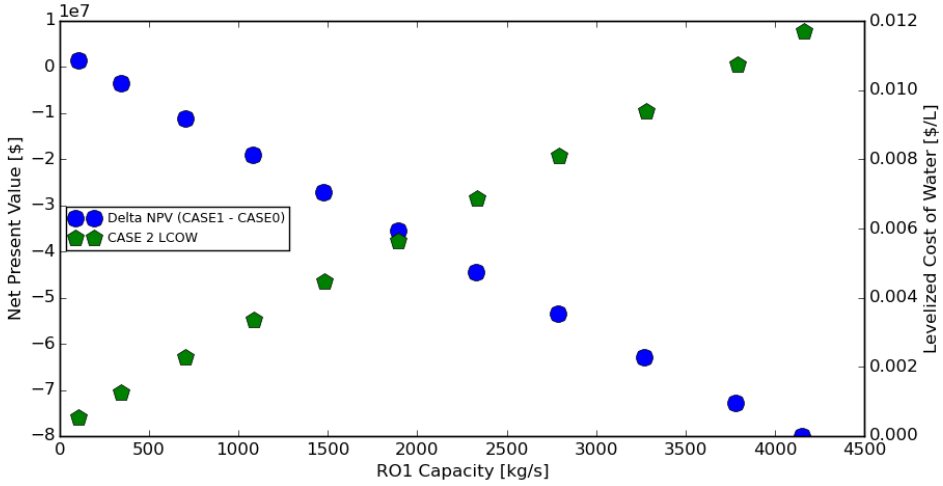

Figure 43: Reference case: Delta NPV for CASE 1 and LCOW for CASE 2 as a function of RO1 capacity.

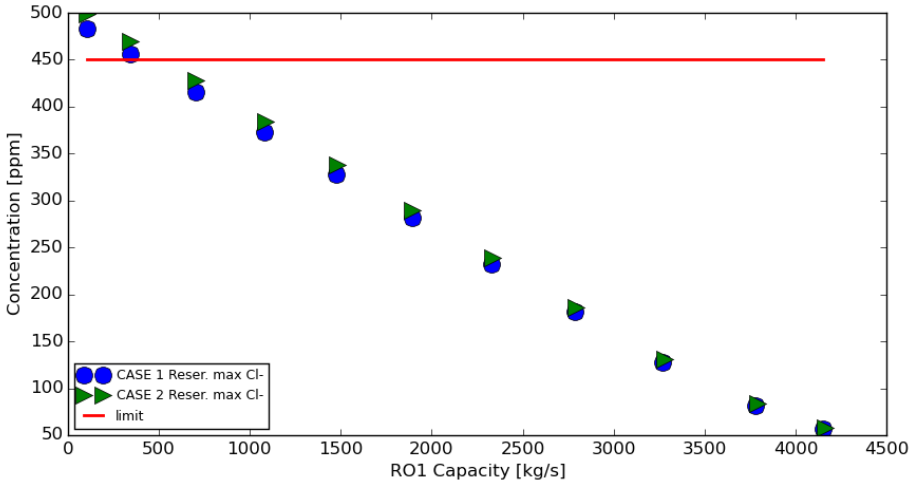

Figure 44: Reference case: Maximum chloride concentration in the reservoir ponds for CASE 1 and CASE 2 as a function of RO1 capacity.

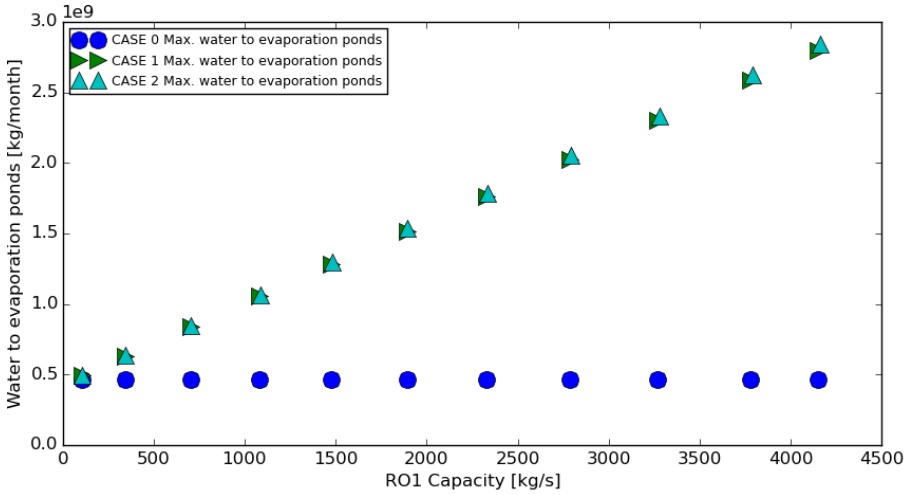

Figure 45: Reference case: Maximum water flow to the evaporation ponds for CASE 1 and CASE 2 as a function of RO1 capacity.

4.2.2 Sensitivity studies

A variety of sensitivity studies were performed to assess the effect of important input parameters on the economic results. Table 15 summarizes the sensitivity studies performed. The plots shown for the sensitivity studies further collapse the plots shown in the overall economic results for the reference case above. Only the values (delta NPV, LCOW, etc.) at the optimum RO1 capacity are reported as a function of the sensitivity variable (discount rate, wholesale price, etc.), i.e. at the minimum RO1 capacity that still satisfies the chloride concentration constraint.

Table 15: Sensitivity studies performed (reference in **red**).

Discount rate	**5, 10, 15 %**
Wholesale electricity price	**30.0, 35.0, 40.0 $/MWh**
Project lifetime	**27, 47 years**
Net demand projection model	**- Demand scales exponentially with 3.3% while the rPV grows linearly, adding 200 MW/year.** - Both the demand and rPV grow exponentially 3.3% per year.
Amount of brackish water	**400, 1200, 2400, 4000 AF/month**
Reservoir pond chloride concentration limit	**450.0, 500.0 ppm**

Discount rate

The first sensitivity analyzed is for the discount rate used to compute the NPV (see Section 3.2.5). Figure 46 shows the capacities for the RO1 (optimum only, as discussed above), RO2 (for the fixed amount of brackish water acquired) as well as the brackish water pump capacity as a function of the discount rate. Note that the optimum RO1 capacity is different for CASE 1 and CASE 2. Figure 47 shows the corresponding maximum water flows to the evaporation ponds. These results indicate that the capacities and water flows (i.e. the physics of the problem) are not affected by the discount rate. Finally, Figure 48 shows the delta NPV and LCOW as a function of the discount rate. Since the physics is not affected by the discount rate, but only the economics, the delta NPV becomes more negative while the LCOW for CASE 2 increases with growing discount rate, as expected.

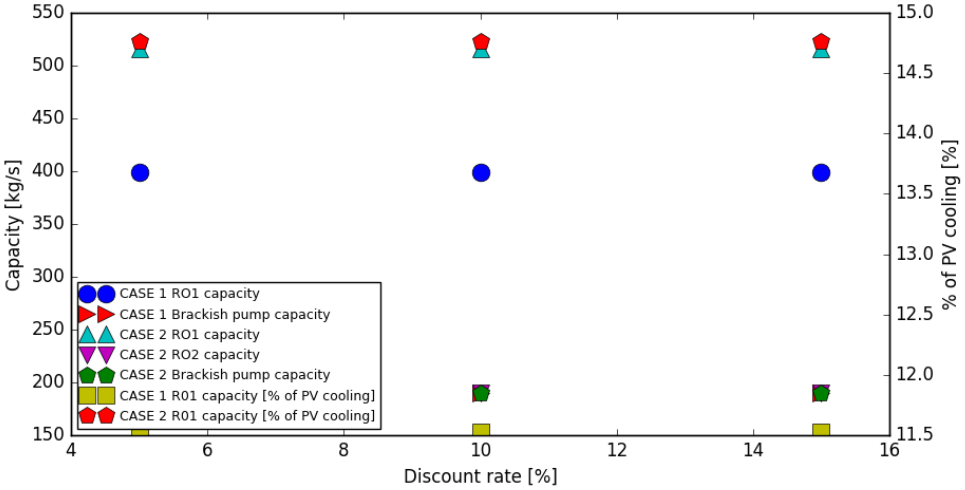

Figure 46: Sensitivity study: Discount rate. Optimum RO and pump capacities.

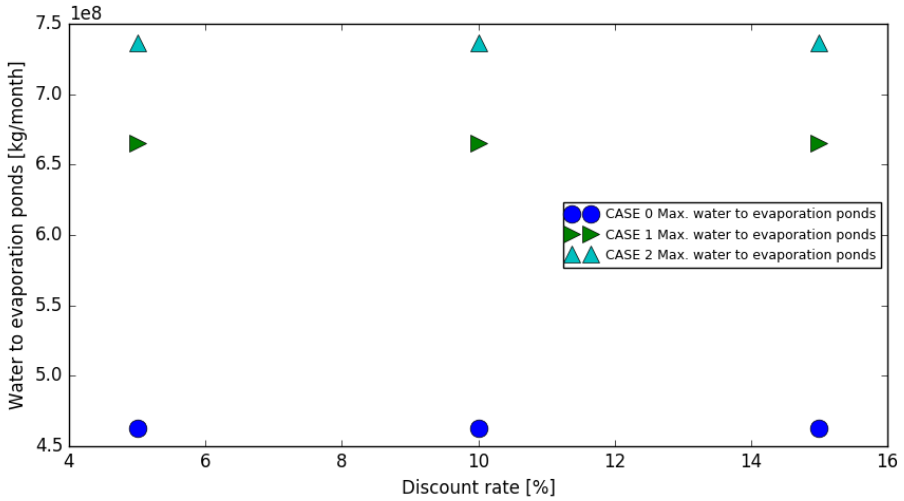

Figure 47: Sensitivity study: Discount rate. Maximum water flows to evaporation ponds.

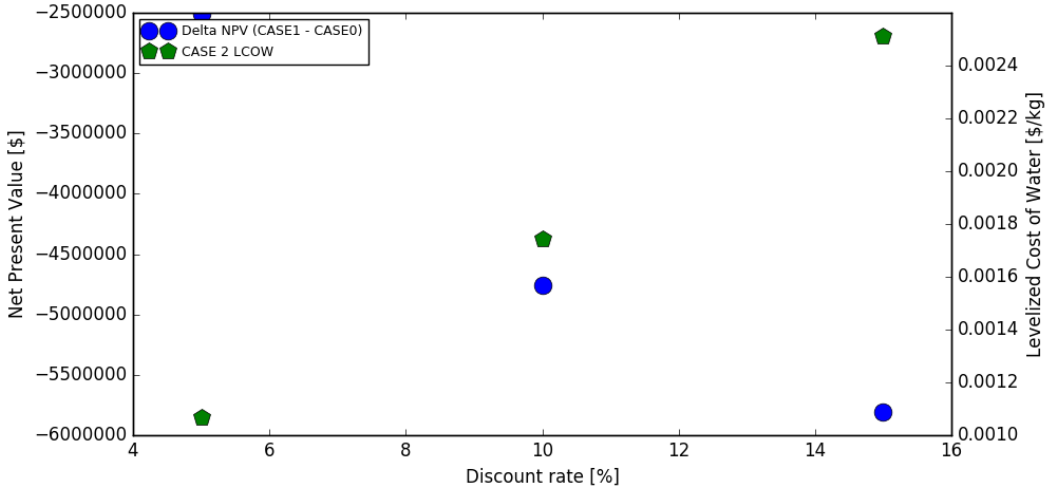

Figure 48: Sensitivity study: Discount rate. Delta NPV (CASE 1) and LCOW (CASE 2).

Wholesale electricity price

In the same way as shown for the discount rate, the sensitivity for the wholesale electricity price is assessed. Figure 49 shows the capacities as a function of the wholesale price while Figure 50 shows the corresponding maximum water flows to the evaporation ponds. It can be seen that the capacities and water flows (i.e. the physical behavior of the system) are not affected by the wholesale price. Finally, Figure 51 shows the delta NPV and LCOW as a function of the wholesale price. Since the physical behavior of the system is not affected by the discount rate, but only the economics, the delta NPV becomes more negative while the LCOW for CASE 2 increases with increasing discount rate, as expected. It is worth mentioning that even for the lowest wholesale price of 30 $/MWh, CASE 1 is not economically viable (delta NPV negative) while the LCOW for CASE 2 is ~1.73 $/m^3 of purified water.

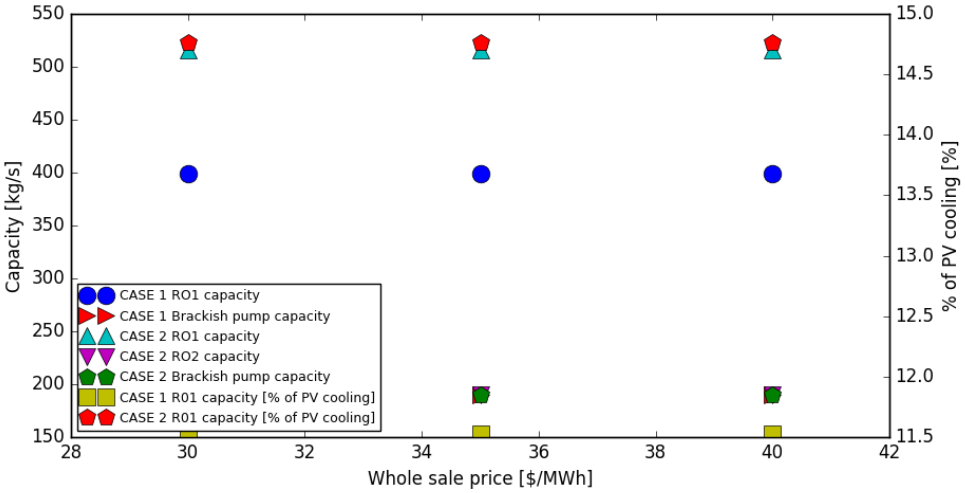

Figure 49: Sensitivity study: Wholesale electricity price. Optimum RO and pump capacities.

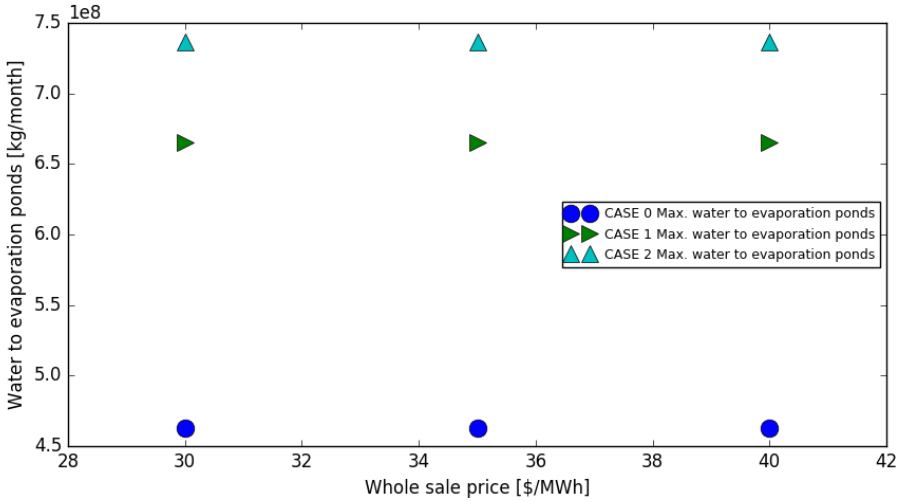

Figure 50: Sensitivity study: Wholesale electricity price. Maximum water flows to evaporation ponds.

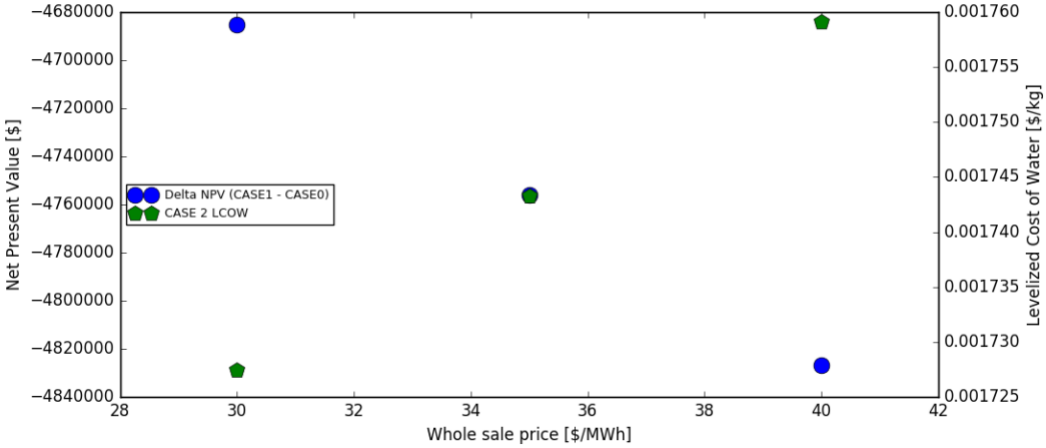

Figure 51: Sensitivity study: Wholesale electricity price. Delta NPV (CASE 1) and LCOW (CASE 2).

Project lifetime

The next parameter evaluated is the project lifetime. While the current PVGS license is valid for an additional 27 years, PVGS may consider seeking a license extension for another 20 years. Analogous to the other sensitivities, Figure 52 shows the optimum capacities, Figure 53 the water flows to the evaporation ponds and Figure 54 shows the delta NPV and LCOW as a function of the project lifetime. As expected, the delta NPV becomes less negative (CASE 1) and the LCOW is reduced for the longer project lifetime.

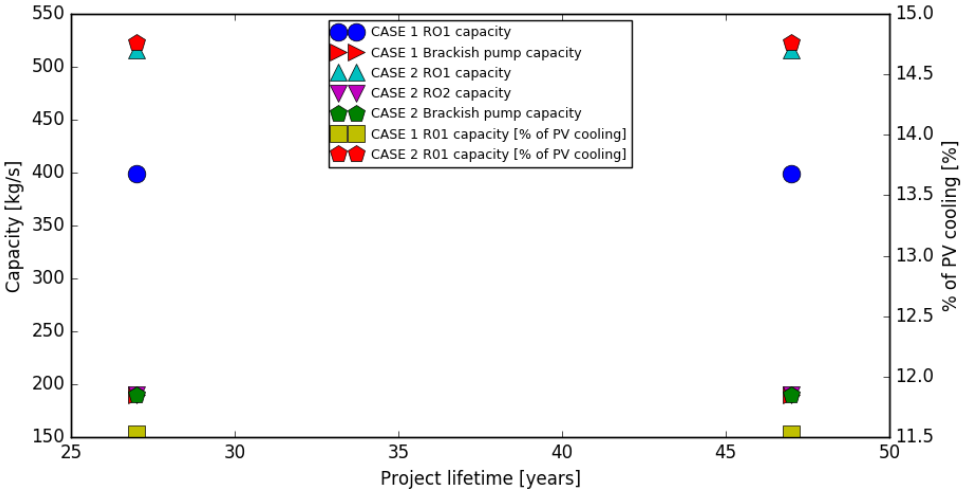

Figure 52: Sensitivity study: Project lifetime. Optimum RO and pump capacities.

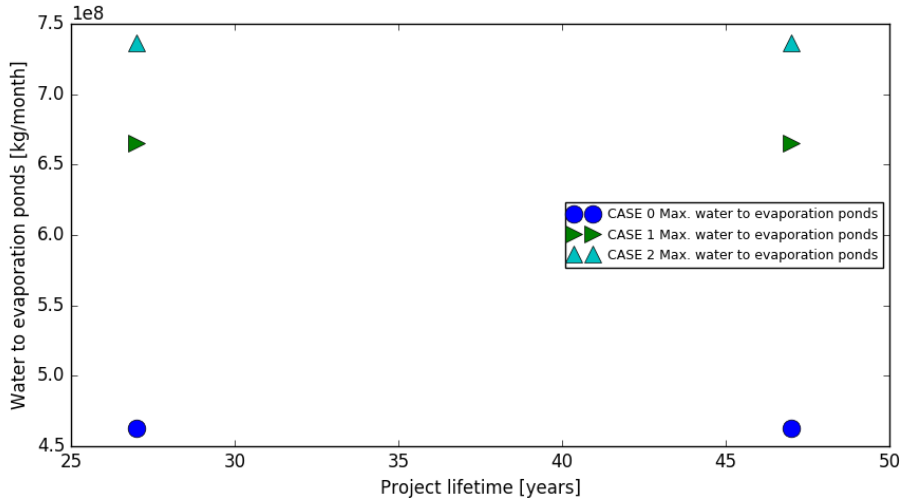

Figure 53: Sensitivity study: Project lifetime. Maximum water flows to evaporation ponds.

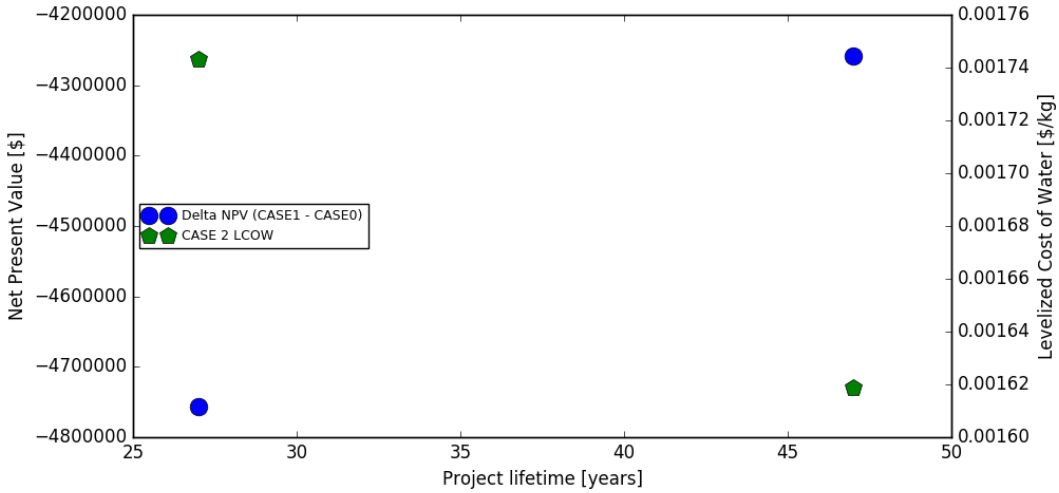

Figure 54: Sensitivity study: Project lifetime. Delta NPV (CASE 1) and LCOW (CASE 2).

Net demand projection model

As mentioned, two different net demand forecast models were investigated. Analogous to the other sensitivities, Figure 55 shows the optimum capacities, Figure 56 shows the water flows to the evaporation ponds and Figure 57 shows the delta NPV and LCOW for the two models. (Note that "exp/lin" on the x-axis represents the reference case where demand scales exponentially at 3.3% growth per year while the rPV grows linearly, adding 200 MW/year, and "exp/exp" represents the case where both the demand and rPV exponentially grow 3.3% per year.)

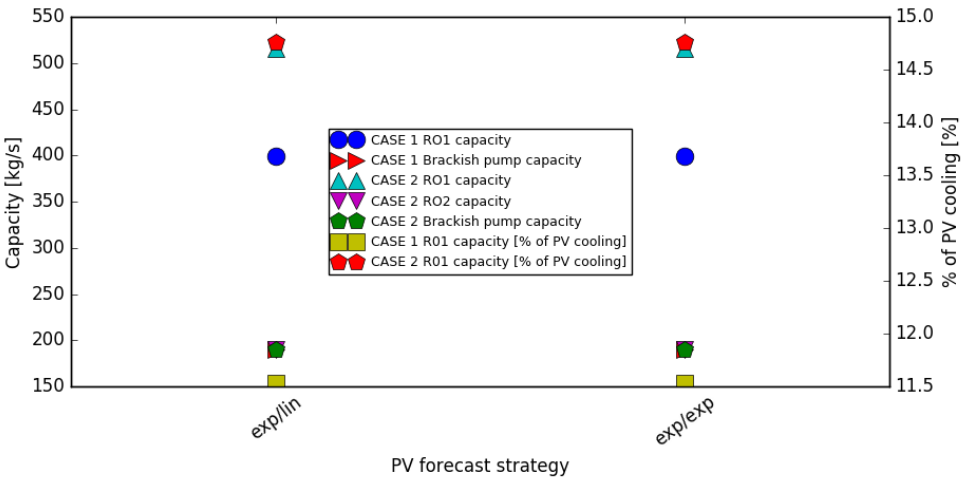

Figure 55: Sensitivity study: Net demand projection model. Optimum RO and pump capacities.

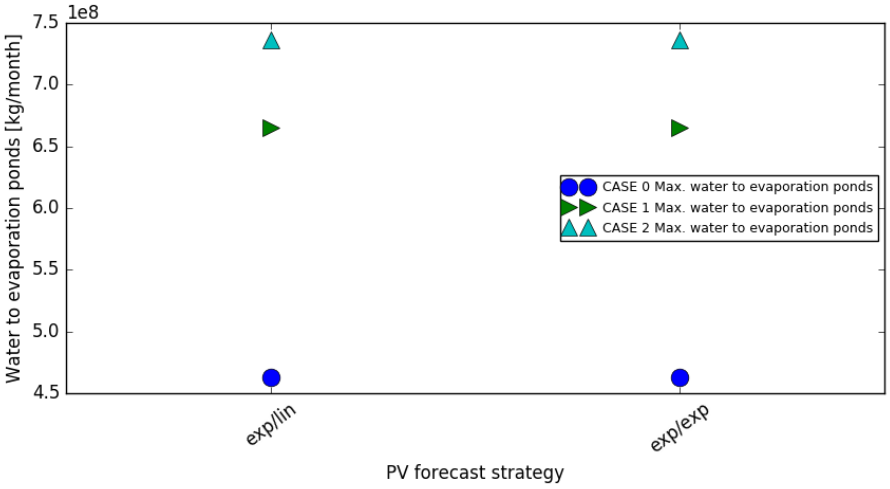

Figure 56: Sensitivity study: Net demand projection model. Maximum water flows to evaporation ponds.

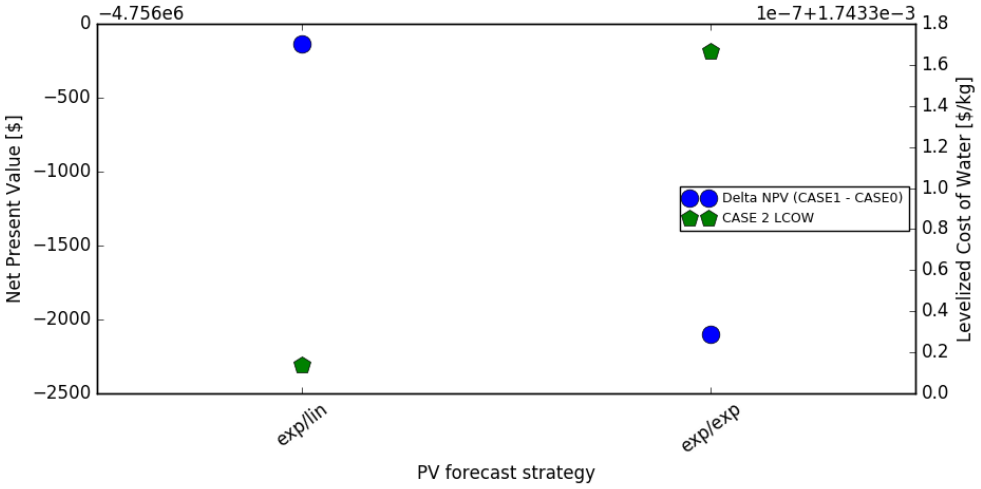

Figure 57: Sensitivity study: Net demand projection model. Delta NPV (CASE 1) and LCOW (CASE 2).

Amount of brackish water purchased and reservoir pond chloride concentration limit

For the last sensitivity study, a combination of the amount of brackish water acquired and allowed chloride level in the reservoir ponds are evaluated. First consider the case in which the chloride concentration is limited to 450 ppm as for the reference case. As for the other sensitivities, Figure 58 shows the optimum capacities, Figure 59 the water flows to the evaporation ponds and Figure 60 shows the delta NPV and LCOW as a function of the brackish water acquired. As one can see, in CASE 1 the size of RO1 grows linearly with the amount of brackish water acquired. For CASE 2, one can see that the optimum size of RO1 is increasing faster than the required size of RO2 for increasing amounts of brackish water. Looking at the delta NPV for CASE 1 (Figure 60), one can see that it is slightly decreasing with increasing brackish water intake. For the reference case, we have seen that the delta NPV varied from $0 to -$80 million for the RO1 size corresponding to 0 to 100% of the PVGS water treated. In the case where more brackish water is

purchased and processed through a larger RO1, the delta NPV is within ~$6 million of the base case. This result indicates that the savings realized by purchasing brackish water compared to effluent water are roughly offset by the increased RO1 cost; even purchasing more brackish water (vs. larger quantities of effluent) does not bring CASE 1 into the economically viable region. The same appears to be true for CASE 2. Although the LCOW for the purified water decreases with an increasing amount of brackish water purchased, the change is only 1.7 $/m^3 to 1.1 $/m^3 for an increase in brackish water purchased from 5000 acre-feet/year to 50000 acre-feet/year. These results suggest that the increasing sizes needed for RO2 and RO1 to process the increasing amounts of brackish water offset the revenue from the purified water sales.

The same sensitivity for the amount of brackish water acquired was performed, but allowing a chloride concentration of 500 ppm in the cooling water reservoirs. For that study the RO sizes were determined to allow for 500 ppm chloride and the amount of cooling water in the towers was adjusted for the increased blowdown (see Eq. 13). Figure 61 shows the optimum capacities, Figure 62 shows the water flows to the evaporation ponds and Figure 63 shows the delta NPV and LCOW as a function of the brackish water acquired (allowing 500 ppm maximum chloride concentration). Considering the necessary RO capacities (Figure 61), one can see that allowing 500 ppm chloride in the cooling water eliminates the need for RO1 needs to be built up to ~1e10 kg/year (~8000 acre-feet/year) of brackish water acquired. For larger amounts of brackish water the behavior is similar to the case where the chloride is limited to 450 ppm, i.e. delta NPV becomes more negative (CASE 1) and LCOW increases (CASE 2) for increasing amounts of brackish water purchased. Additionally, although less negative than the 450 ppm limit case, CASE 1 for the 500 ppm limit is still not economically viable for any amount of brackish water.

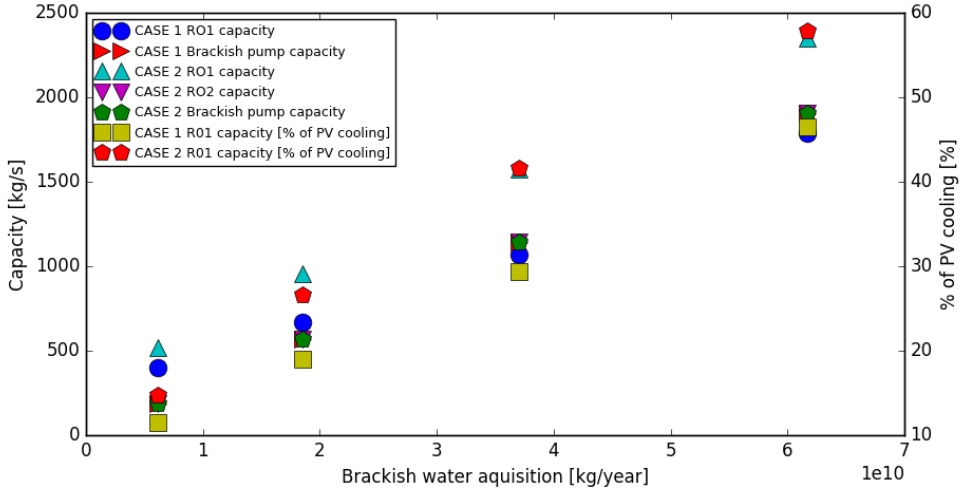

Figure 58: Sensitivity study: Brackish water, max Cl^- 450 ppm. Optimum RO and pump capacities.

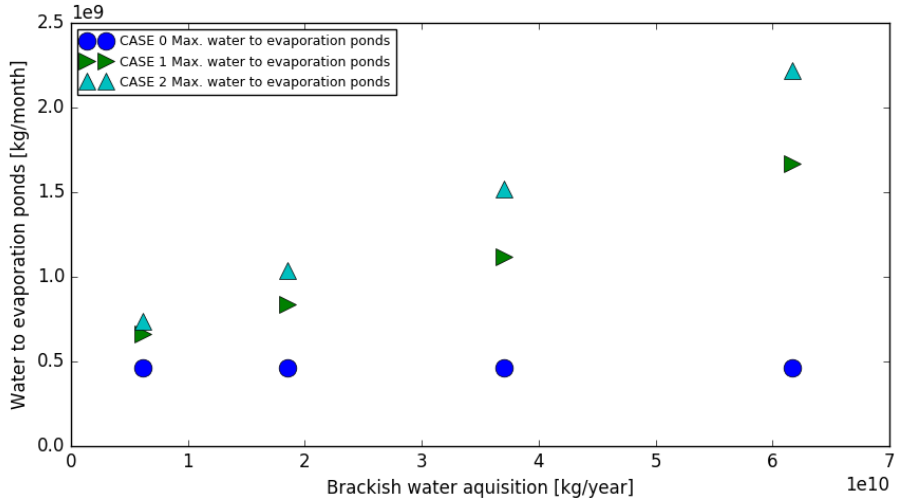

Figure 59: Sensitivity study: Brackish water, max Cl^- 450 ppm. Maximum water flows to evaporation ponds.

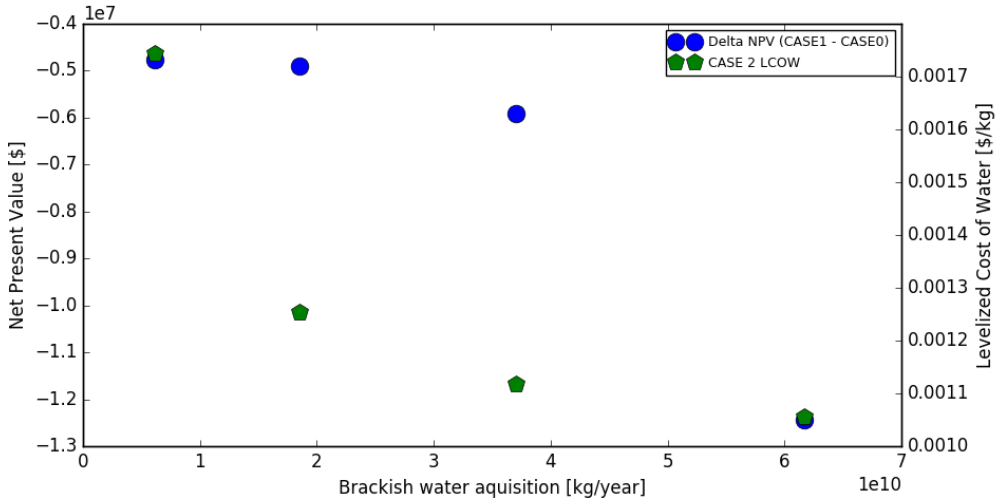

Figure 60: Sensitivity study: Brackish water, max Cl^- 450 ppm. Delta NPV (CASE 1) and LCOW (CASE 2).

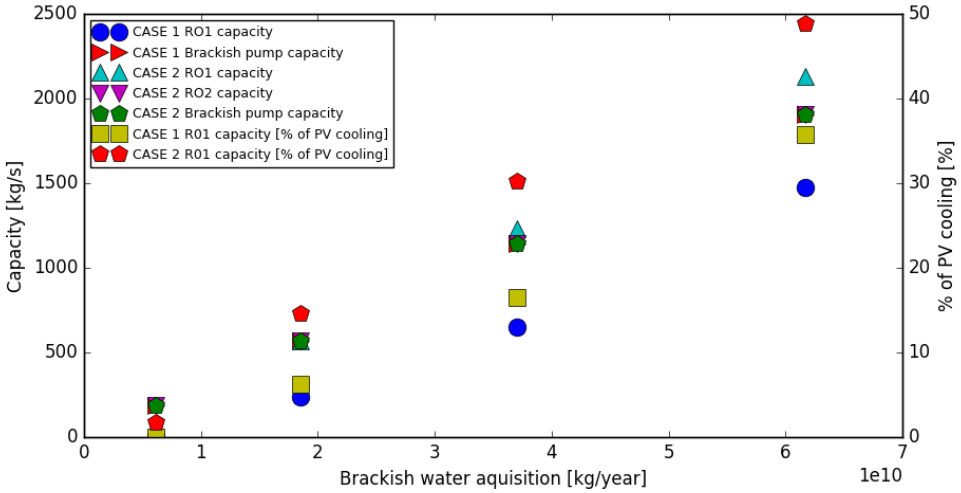

Figure 61: Sensitivity study: Brackish water, max Cl^- 500 ppm. Optimum RO and pump capacities.

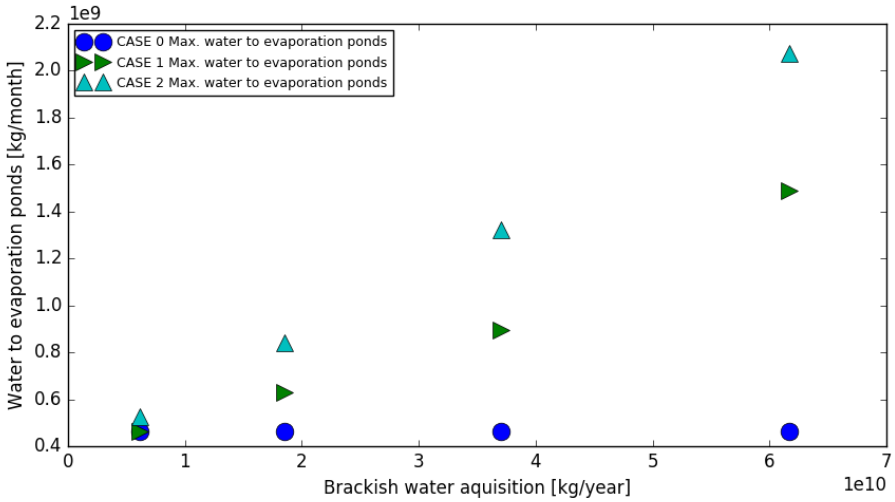

Figure 62: Sensitivity study: Brackish water, max Cl^- 500 ppm. Maximum water flows to evaporation ponds.

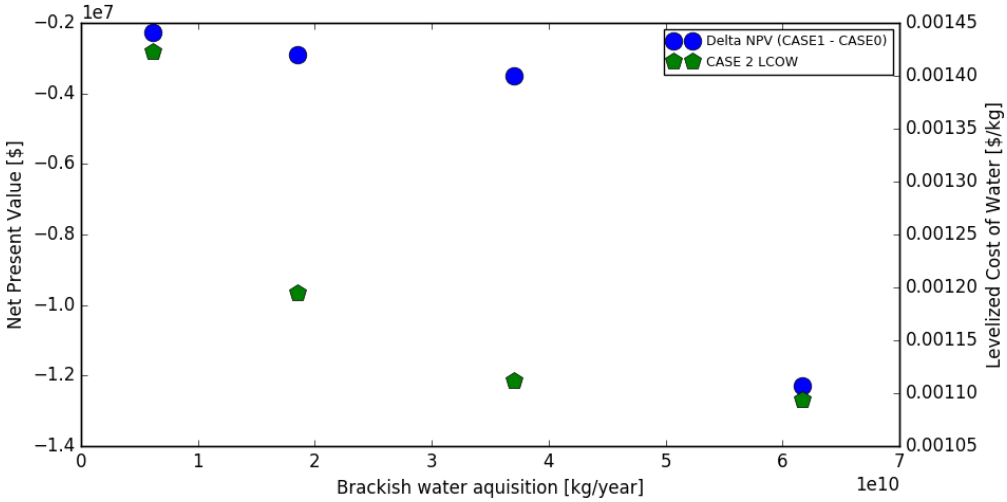

Figure 63: Sensitivity study: Brackish water, max Cl^- 500 ppm. Delta NPV (CASE 1) and LCOW (CASE 2).

As a final investigation, instead of scaling the ROs for the maximum chloride concentration (which is the most conservative case), the economics analysis was performed by limiting the volume weighted yearly average chloride concentration to 450 ppm. This is the least conservative case, as it can allow for the chloride concentration to exceed 450 ppm at some moments in time. The true reservoir chloride concentration lies somewhere between the two extreme cases. As mentioned, a more detailed reservoir model that considers the pool water mixing with the incoming water from the WRF and RO1 is needed to make a more detailed assessment of the actual time dependent chloride concentration seen by the PVGS cooling towers. As one can see, considering the average chloride concentration instead of the maximum means that no RO1 is needed in CASE 1 up to ~ 2e10 kg/year (~ 16000 acre-feet/year) of brackish water acquired. Furthermore, one can see that CASE 1 becomes economically viable for all amounts of brackish water acquired (delta NPV > 0), while LCOW is ~1 $\$/m^3$ of purified water.

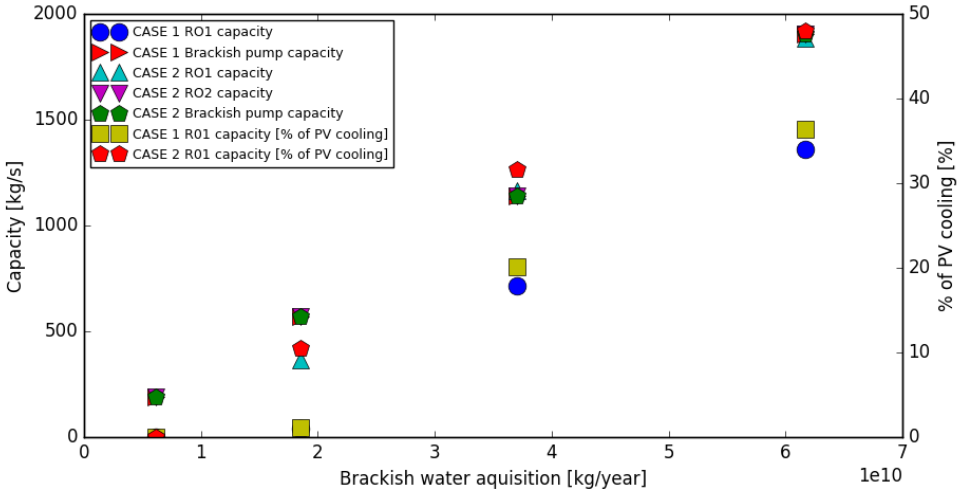

Figure 64: Sensitivity study: Brackish water, average Cl^- 450 ppm. Optimum RO and pump capacities.

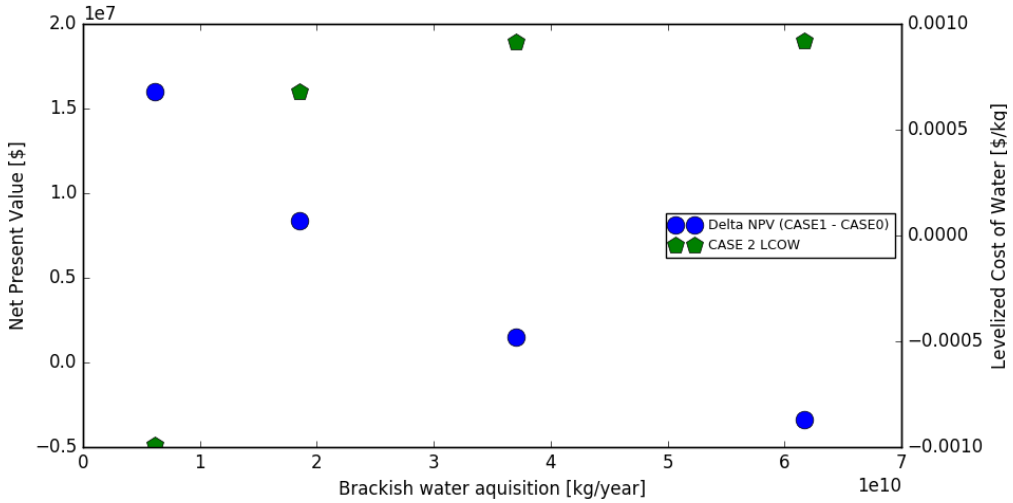

Figure 65: Sensitivity study: Brackish water, average Cl^- 450 ppm. Delta NPV (CASE 1) and LCOW (CASE 2).

5. CONCLUSIONS AND FUTURE WORK

This section provides a summary of the conclusions drawn from the analysis results and provides recommendations for possible future work. First, these conclusions identify where more detailed data is required and more accurate model assumptions are necessary to reproduce all of the driving physical and economic phenomena in order to capture sufficient complexity such that APS can apply these results to strategic decisions. Second, areas for possible extension of the cases evaluated in this report are presented.

5.1 Conclusion

Considering the stochastic data demand, rPV and electricity price at the PV Hub, it has been shown that:

- Statistically meaningful demand, rPV and hub price data can be reproduced with the recently implemented FVARMA model when 2 month blocks are trained individually versus training using the full year. It is suggested for future work that the "arbitrary" 2 month blocks be replaced by a cluster analysis, i.e. so that FVARMAs can be trained on groups of similar weeks or days throughout the year. It is believed that this will increase the quality of the synthetic data even further.
- The FVARMA can reproduce capped signals like the rPV generation with the help of the "zero filter" capability developed for the FVARMA module. However, it is suggested that additional signal treatment methods (in addition to Fourier) that are capable of capturing capped data like spikes are assessed for use in the FVARMA model.
- It has been shown that the correlated FVARMA capability is working as intended. However, no correlation could be found between the demand and the rPV or the demand and the hub price, although it is suspected that correlation exists and is an important driver for the economic analysis. Concerning the rPV data, higher resolution data is needed to support a correlation analysis. For the

hub price it is assumed that there is no actual correlation or it is so weak or delayed that it cannot be captured.

- Depending on the net demand forecast model, the variance of the net demand changes considerably. Future work is necessary to understand which forecast model (in general, not just out of the two presented here) is best for this type of analysis.
- There is no forecast for the hub price. In addition, PVGS is considered a price taker at the hub and cannot influence its price. A better market model is needed.

Considering the effect of adding an RO load to mitigate the effect of negative prices at the Palo Verde Hub due to increasing VRE penetration, it has been shown that:

- The number of hours when APS has to sell excess electricity at the hub is negligible. Recall that only rooftop solar is considered, but no (curtailable) industrial solar. The future projection of the net demand and the hub prices show that APS could curtail its internal production to take advantage of negative electricity prices at the Palo Verde Hub. This could add up to an additional 10% of the APS revenue. While in principle adding more internal baseload (i.e. RO electricity consumption) enhances such capability, the size of the RO in this study is such that the effect is negligible. These findings do not seem to be in line with APS internal findings and need to be confirmed. In particular, hub price projection models should be investigated and added to this APS case study.
- The economic benefits of installing an RO are realized via savings in the water acquisition costs, not in mitigating VRE penetration.

For the reference cases studied, it has been shown that:

- **CASE 1**: An RO1 of ~500 kg/s capacity is needed to satisfy the maximum chloride concentration in the reservoir ponds. For that size of RO1, the delta NPV between CASE 1 and CASE 0 is negative, i.e. it is economically beneficial to keep buying 100% effluent water rather than build the RO1.
- **CASE 2**: The size of RO1 needed in CASE 2 is comparable to CASE 1, i.e. ~500 kg/s. The LCOW that offsets the cost in that case is ~0.15 cents/liter (1.5 $\$/m^3$). This amount appears expensive, but one has to keep in mind that for the reference case, only 5000 acre-feet of brackish water are purified per year.

The following conclusions are drawn from the sensitivity studies on the input parameters:

- Sensitivities on the Discount Rate, Wholesale Electricity Price and Project Lifetime change the delta NPV for CASE 1 and the LCOW for CASE 2, but these studies do not change the conclusions drawn from the reference case.
- When keeping the chloride limit at 450 ppm and purchasing more brackish water, analyses indicate that the savings made by buying brackish water compared to effluent water are roughly offset by the increased RO1 cost. Buying more brackish water does not bring CASE1 into the economically viable region. The same conclusion seems to be true for CASE 2. It looks as though the increasing sizes needed for RO2 and RO1 to process increasing amounts of brackish water purchased offset the revenue from the purified water sales.
- Allowing up to 500 ppm chloride in the cooling water removes the need to build RO1 for up to ~1e10 kg/year (~ 8000 acre-feet/year) of brackish water acquired.
- Considering the average chloride concentration instead of the maximum means that no RO1 is needed in CASE 1 up to ~2e10 kg/year (~16000 acre-feet/year) of brackish water acquired. Furthermore, CASE 1 becomes economically viable for all amounts of brackish water acquired (delta NPV > 0), while LCOW is ~1 $\$/m^3$ of purified water. A more realistic model of the reservoir ponds is needed to refine the results.

5.2 Future Work

The above-mentioned conclusions suggest several further investigation directions. The first step needed would be to improve the representation of the condition under which APS operates. In particular:

- Better data are needed to generate a more reliable model of the net demand and Palo Verde Hub prices. In particular, it will be necessary to have higher resolution rPV data to better correlate electricity demand and hub prices to the rPV production.
- The above-mentioned increase in data resolution should be paired with an improved projection model for scaling the APS internal demand and rPV production over the lifetime of the project.
- A projection model for the lifetime of the project and possibly an elasticity curve of the price at the PV Hub would be necessary to define a strategy that optimizes the utilization of the PV Hub imbalance market.

Once a higher fidelity scenario is available via the above-mentioned improvements in data and prediction models, several strategies can be considered to increase the economic performance of PVGS for APS. These strategies include the following:

- Consider the possibility of using the reservoir pond as a means to smooth out the salinity peak (average salinity limited case).
- Consider the possibility of using the reservoir pond as a battery, which would make the RO1 and the WRF a variable load without jeopardizing the water supply to PVGS.
- If net demand falls below the PVGS capacity examine the financial implications of performing "economical dispatch" (i.e. load following) versus increasing the base load via a large desalination plant.

6. REFERENCES

1. C. Rabiti, H. E. Garcia, R. Hovsapian, R. A. Kinoshita, G. L. Mesina, S. M. Bragg-Sitton, R. D. Boardman, "Strategy and Gaps for Modeling, Simulation, and Control of Hybrid Systems", Idaho National Laboratory, April 2015, INL/EXT-15-34877.
2. A. S. Epiney, J. Chen, C. Rabiti, "Status on the Development of a Modeling and Simulation Framework for the Economic Assessment of Nuclear Hybrid Energy Systems (FY 16)", Idaho National Laboratory, September 2016, INL/EXT-16-39832.
3. A. S. Epiney, R. A. Kinoshita, J. S. Kim, C. Rabiti, M. S. Greenwood, "Software development infrastructure for the HYBRID modeling and simulation project", INL report INL/EXT-16-40004, September 2016.
4. A. S. Epiney, C. Rabiti, A. Alfonsi, P. Talbot, F. Ganda, "Report on the Economic Optimization of a Demonstration Case for a Static N-R HES Configuration using RAVEN," Idaho National Laboratory, April 2017, INL/EXT-17-41915.
5. C. Rabiti, A. S. Epiney, P. Talbot, J. S. Kim, S. Bragg-Sitton, A. Alfonsi, A. Yigitoglu, S. Greenwood, S. M. Cetiner, F. Ganda, G. Maronati, "Status Report on Modeling and Simulation Capabilities for Nuclear-Renewable Hybrid Energy Systems," Idaho National Laboratory, September 2017, INL/EXT-17-43441.
6. R. Ponciroli and R. B. Vilim "Testing of Strategies for the Acceleration of the Cost Optimization," Argonne National Laboratory August 2017, ANL/NE-17/21.
7. M.S. Greenwood, S.M. Cetiner, T.J. Harrison, D. L. Fugate, "A Templated Approach for Multi-Physics Modeling of Hybrid Energy Systems in Modelica." (In Press)
8. C. Rabiti, A. Alfonsi, J. Cogliati, D. Mandelli, R. Kinoshita, S. Sen, C. Wang, J. Chen, "RAVEN User Manual," INL/EXT-15-34123, Printed March 2017.
9. A. Alfonsi, C. Rabiti, D. Mandelli, J. Cogliati, R. Kinoshita, and A. Naviglio,"RAVEN and Dynamic Probabilistic Risk Assessment: Software Overview,"Proceedings of European Safety and Reliability Conference (ESREL), Wroklaw (Poland), 2014.
10. A. Alfonsi, C. Rabiti, D. Mandelli, "Raven Facing the Problem of assembling Multiple Models to Speed up the Uncertainty Quantification and Probabilistic Risk Assessment Analyses", Proceedings of *13th Iternational Conference on Probabilistic Safety Assessment and Management (PSAM 13)*, 2~7 October 2016, Seoul, South Korea.
11. J. S. Kim, H. E. Garcia "Nuclear-Renewable Hybrid Energy System for Reverse Osmosis Desalination Process," Transactions of the American Nuclear Society. 2015;112:121-4.
12. J. S. Kim, J. Chen J, H. E. Garcia. "Modeling, control, and dynamic performance analysis of a reverse osmosis desalination plant integrated within hybrid energy systems," Energy. 2016;112:52-66.
13. J. S. Kim, K. Frick. "Status Report on the Component Models Developed in the Modelica Framework: Reverse Osmosis Desalination Plant & Thermal Energy Storage," Idaho National Laboratory, October 2016, INL/EXT-18-45505.
14. L. F. Greenlee, D. F. Lawler, B. D. Freeman, B. Marrot, P. Moulin "Reverse osmosis desalination: Water sources, technology, and today's challenges," Water Research. 2009;43:2317-48.
15. H. E. Garcia, J. Chen, J. S. Kim, M. G. McKellar, W. R. Deason, R. B. Vilim et al., "Nuclear Hybrid Energy Systems – Regional Studies: West Texas & Northeastern Arizona," Idaho National Laboratory, April 2015, INL/EXT-15-34503.
16. H. E. Garcia, J. Chen, J. S. Kim, R. B. Vilim, W. R. Binder, S. M. Bragg Sitton et al. "Dynamic performance analysis of two regional Nuclear Hybrid Energy Systems," Energy. 2016;107:234-58.
17. P. Fritzson. Principles of Object-Oriented Modeling and Simulation with Modelica 3.3: A Cyber-Physical Approach: 2nd ed. New Jersey: Wiley; 2014.

18. Dassault Systems. DYMOLA Systems Engineering, available at https://www.3ds.com/products-services/catia/products/dymola/, accessed on September 2018.
19. J. Chen, C. Rabiti, “Synthetic wind speed scenarios generation for probabilistic analysis of hybrid energy systems”, Energy 120, 2017, p. 507-517.
20. P. W. Talbot, C. Rabiti, A. Alfonsi, C. Krome, M. R. Kunz, A. S. Epimey, C. Wang, D. Mandelli, “Correlated Synthetic Time Series Generation for Energy System Simulations using Fourier and ARMA Signal Processing,” NURER 2018, Sept 30 – Oct 3, 2018, Jeju, Korea.
21. R. P. Brent, "Chapter 4: An Algorithm with Guaranteed Convergence for Finding a Zero of a Function," Algorithms for Minimization without Derivatives, Englewood Cliffs, NJ: Prentice-Hall, 1973.
22. “2017 Monthly Chemisty.xlsx,” APS private communication, June 2018.
23. “Cooling Demand and Cost.xlsx,” APS private communication, June 2018.
24. “Cost Function for the Palo Verde Water Reclamation Facility_v2,” APS private communication, August 2018.
25. G. Noreddine, T. M. Missimer, G. L. Amy, “technical review and evaluation of the economics of water desalination: current and future challenges for better water supply sustainability,” Desalination 309 (2013): 197-207.
26. “160411 WRSS-Buckeye canal connection-JAB-R1.xlsx,” APS private communication, May 2018.
27. “Tertiary PPM.xlsx,” APS private communication, June 2018.
28. “Model Data - 1_SEND.XLSX,” APS private communication, June 2018.
29. “Palovrde_asr_apnd_010116_123116_v1091917.xlsx,” APS private communication, June 2018.
30. “2017 - 1.1 to 8.31 LMP 5 min at PV Hub.xlsx,” APS private communication, June 2018.
31. “18D2686 Sample2COC Rev FINAL 05 07 18 1535.pdf,” APS private communication, June 2018.
32. “4 season rep for Justin.xlsx,” APS private communication, June 2018.
33. http://oasis.caiso.com/mrioasis/logon (Prices>LMP Market:DAM Node:PALOVRDE_5_N101)